Alma Mater Studiorum · Università di Bologna

Scuola di Scienze
Dipartimento di Fisica e Astronomia
Corso di Laurea Magistrale in Fisica

Primordial Dark Matter Halos from Fifth-Forces

Relatore:
Prof. Lauro Moscardini

Presentata da:
Stefano Savastano

Correlatori:
Prof. Luca Amendola
Dr. Javier Rubio

Anno Accademico 2017/2018

Abstract

In this thesis we investigate a possible formation mechanism of non-linear structures, such as primordial black holes or similar screened objects, within a modified gravity framework. In particular, these structures can form during radiation era and provide the current dark matter component of the Universe. We refer to a model consisting of a long range attractive fifth-force stronger than gravity, mediated by a light scalar field ϕ - which could be in principle dynamical dark energy of Coupled Quintessence - interacting with a non-relativistic ψ-particle. The latter is coupled to radiation and matter species only via usual gravity.

By means of a dynamical system approach, we select the unique stable scaling solution of the phase space providing a radiation dominated era. Besides, after the introduction of the cosmological perturbation theory, we study the non-linear growth of the ψ field density fluctuations in this epoch. The latter, being enhanced by the fifth interaction, in view of a field theory screening mechanisms that suppress the additional interaction, eventually collapse in stable and virialized structures, namely dark matter halos. We compare the theoretical predictions on the radius and the mass of the halos with experimental constraints on primordial black holes abundances, with an emphasis on their lensing signature in the solar mass window. In conclusion, we outline a viable scenario where the missing dark matter component of the universe might be completely supplied in form of dark halos.

Sommario

In questo lavoro di tesi studiamo un possibile meccanismo che prevede la formazione di strutture non lineari, come Primordial Black Holes o oggetti egualmente schermati, all'interno di un contesto di gravità modificata. Queste strutture possono formarsi nei primi istanti dell'universo e potrebbero spiegare la preponderante componente di materia oscura che osserviamo oggi. Tale meccanismo si basa sull'esistenza in epoca primordiale di un'ulteriore forza di tipo gravitazionale, cioè attrattiva e a lungo raggio, ma potenzialmente molto più intensa di quella usuale. Questa forza è mediata da un campo scalare leggero ϕ - in linea di principio potrebbe essere un campo di energia oscura dinamica - che interagisce con una particella non relativistica ψ, accoppiata con le altre specie solo attaverso la gravità.

Introdotta la teoria dei sistemi dinamici, mostriamo quale sia il punto fisso dello spazio delle fasi che indica l'evoluzione di questo sistema durante l'era radiativa. Inoltre, grazie alla teoria della perturbazioni, valutiamo la crescita delle fluttuazioni di densità nel campo ψ in regime non lineare. Queste, per mezzo di un meccanismo che sopprime l'interazione primordiale aggiuntiva, conducono eventualmente al collasso di regioni sovra-dense dell'universo primordiale in oggetti stabili e virializzati, ovvero aloni di materia oscura. A seguire, compariamo le previsioni teoriche del modello riguardo la massa e il raggio degli aloni con i vincoli osservativi nella finestra della massa solare, soffermandoci sul segnale che potrebbero produrre queste strutture in fenomeni di microlensing. Infine, concludiamo delineando un possibile scenario in cui gli aloni sarebbero in grado di indicare in che forma si presenta la sfuggente componente di materia oscura dell'universo.

Nello spazio vuoto
tra ogni sassolino e l'altro
ho creduto di vederere anch'io
qualcosa che non c'è.

Niccolò Contessa

Contents

Acknowledgements

I would like to express my deep gratitude equally to each one of my three supervisors. Thanks to Prof. Lauro Moscardini, who let me pursue my interests and addressed me to Heidelberg to work at this thesis, nonetheless supporting me from Bologna in each and every moment. Thanks to Prof. Luca Amendola who accepted me in his research group at the Institut für Theoretische Physik and treated me like one of his collaborator more than a student. I will keep in my mind our pleasant last discussions on the project in the sunny garden of Philosophenweg 16. Thanks to Javier, whose assistance, encouragement, suggestions and friendship were crucial to the success of this work.

I wish to thank my family for their support to my choices, their encouragement throughout my study and their constant presence. But also those friends from Italy who, in spite of the distance, constantly cheer my days. Moreover, I extend my thanks to the cosmology group, to the boulderhaus folks and to all the people who made my staying in Heidelberg an unforgettable experience.

A special thanks goes to Amalia, my travelling companion. Words are not enough to say why.

Final remark. My personal story would not be the same even if I removed just a tiny fragment of joy or pain. Thus, many people and many events met in my life deserve my gratitude: thanks to you as well.

Introduction

In 1933, the Swiss astronomer Fritz Zwicky, investigating the Coma cluster of galaxies, found a discrepancy from its average mass inferred from the velocity dispersion and the value deduced from observed visible matter [1]. He figured out that the outer components of the cluster were moving too fast to be just experiencing the gravitational potential of the observed matter and was the first to suggest the introduction of a new matter component to explain these astronomical evidences; he referred it as *dunkle materie*, in English, *dark matter*. Nowadays, the dark matter is an essential ingredient of modern cosmology and the puzzle on its fundamental nature is still one of the biggest open enigma in physics. Among the many candidates that have been proposed, primordial black holes (PBHs) have gain a renewed interest in the last few years since they could in principle source gravitational wave signals observed by the LIGO/VIRGO collaborations. Most of the models providing this type of compact dark objects rely on very particular features of the post-inflationary power spectrum, which is very weakly constrained if one strays from the cosmic microwave background (CMB) scale. However, the PLANCK collaboration results [2] suggest that this spectrum might be nearly scale invariant, that means inflation does not select a preferred scale, in accordance with the Harrison-Zel'dovich scale invariant prescription. This work is based on a recently introduced mechanism for compact dark matter formation which does not depend on inflationary physics. Its main feature is to allow the growth of non-interacting matter fluctuations even during a radiation dominated era of the cosmological evolution, through an additional gravity-like interaction, whereas the standard scenario inhibits it.

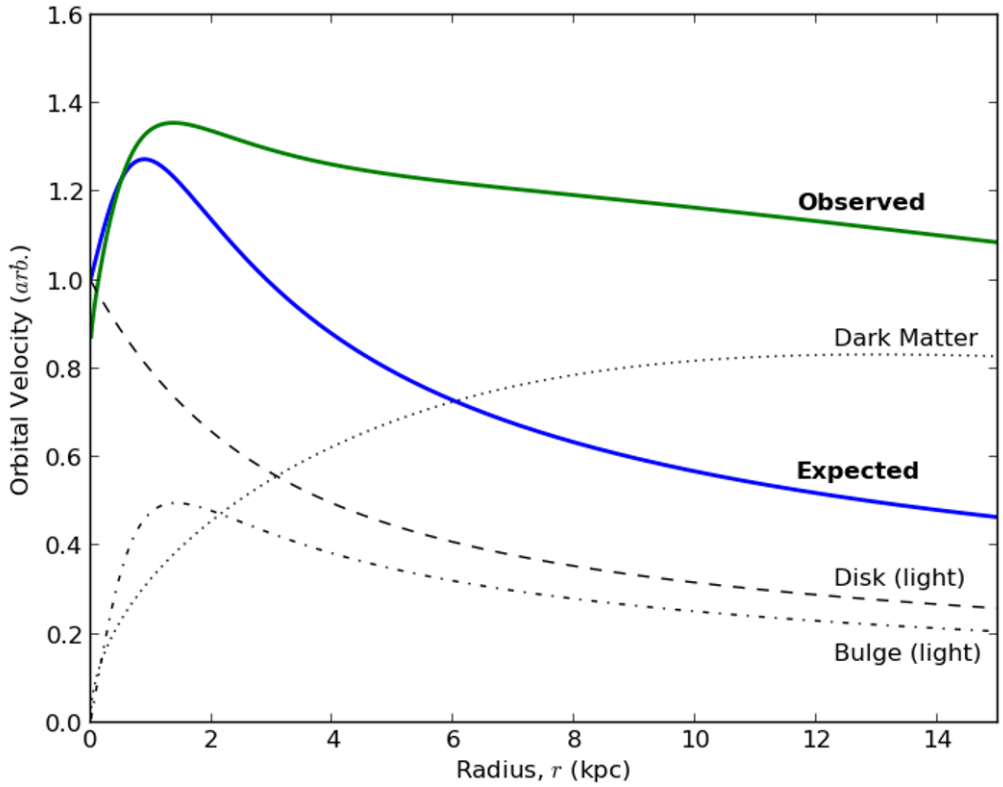

Figure 1. A galaxy rotation curve: the first hint of missing matter in the universe.
Credits to: Matthew Newby, Milkyway@home.

The thesis work is organised as follows:

◇ In Chapter 1 we briefly introduce the standard theory of general relativity and provide the basic cosmological tools which are used throughout this work.

◇ In Chapter 2 we review the novel primordial modified gravity framework mentioned above and illustrate how the cosmological evolution of the different matter species in the universe can be followed through a dynamical system approach. Lastly, we discuss how a field theory screening mechanism suppresses the fifth force with the formation of highly non-linear structures and make it nowadays ineffective.

◇ In Chapter 3 we present the cosmological perturbation theory, that is an essential tool to study the evolution of the post-inflationary initial density perturbations. We extend the standard picture to our modified gravity scenario and investigate the evolution of matter fluctuations and their subsequent collapse in virialized stable dark lumps, or rather Primordial Dark Matter Halos (PDMHs). In the end, we outline two possible scenarios resulting from our analysis.

◇ In Chapter 4 we explore the possibility to provide all the missing dark matter in the universe in the form of PDMHs within the solar mass window. In this range the halos turn not to be black holes and therefore the existing constraints on PBHs do not directly apply to them. After an introduction on gravitational lensing theory, we discuss how the tight lensing constraints apply to the halos and show that escaping these constraints is possible within one of the two outlined scenarios.

Chapter 1

Fundamentals in Cosmology

In this chapter we review the basics on both general relativity and cosmology with the aim this can provide a self-contained handbook section for the reader. For the sake of brevity, we will focus only on the key concepts that will be used or discussed throughout the thesis work.

Conventions: Metric signature $(-,+,+,+)$; Natural units $c = \hbar = 1$.

1.1 General Relativity in a nutshell

This section is devoted to present the elegant theory of general relativity within the action formalism and, in order to preserve the fluency of the following discussion, to set forthwith some basic definitions will be used through this chapter.

Given a $1+3$-dimensional Riemannian manifold $\mathcal{M}$ equipped with a metric tensor $g_{\mu\nu}$ and local chart of coordinates x^μ, it is possible to express the Christoffel symbols as

$$\Gamma^\sigma_{\mu\nu} = \frac{1}{2} g^{\sigma\rho} \left(g_{\nu\rho,\mu} + g_{\rho\mu,\nu} - g_{\mu\nu,\rho} \right) ,$$

where the comma indicates a partial derivative with respect to the specified coordinate. Those quantities, which are not tensors, define a rule for the parallel transport of vectors on the manifold. Indeed, given a generic vector V^ν, if its covariant derivative

$$\nabla_\mu V^\nu = \partial_\mu V^\nu + \Gamma^\nu_{\mu\lambda} V^\lambda = V^\nu_{;\mu}$$

is null, the vector is said to be transported parallel along the μ direction. A very fundamental tensor can be constructed out of the Christoffel's symbols, namely the Riemann tensor

$$R^{\rho}{}_{\mu\lambda\nu} = \partial_\lambda \Gamma^{\lambda}_{\nu\mu} + \Gamma^{\rho}_{\lambda\mu}\Gamma^{\sigma}_{\nu\mu} - (\lambda \leftrightarrow \nu) \ .$$

Loosely speaking, it measures the non-commutativity of the covariant derivative, or rather how the result of the parallel transport rule depends on the followed path. Furthermore, summing up the upper and the lower middle indexes of this tensor, one obtains the Ricci tensor

$$R_{\mu\nu} = R^{\lambda}{}_{\mu\lambda\nu} \, .$$

Finally, contracting the remaining indexes, a scalar quantity arises: the Ricci scalar or *scalar curvature*

$$R = g^{\mu\nu} R_{\mu\nu} \, ,$$

which is the only independent scalar can be constructed from the metric tensor with no higher than second-order derivatives. In general relativity the gravitational interaction is related to the evolution of the spacetime manifold, such that the components of the metric tensor represents the gravitational potentials, and are indeed the dynamical variables of the theory. Its equation of motions, namely Einstein's equations, can be inferred from the action formalism through the least action principle. Indeed, Hilbert realised that the simplest possible[1] action matching the principles of general relativity is

$$S_H = \frac{M_P^2}{2} \int_{\mathcal{M}} \sqrt{-g} R \, d^4x \, , \tag{1.1}$$

where $\sqrt{-g}\, d^4x$ is the natural invariant volume form of the manifold $\mathcal{M}$. The trajectories of the dynamical space which minimise the Einstein-Hilbert action are the solutions to Einstein's equations in vacuum

$$\frac{1}{\sqrt{-g}} \frac{\delta S_H}{\delta g^{\mu\nu}} = R_{\mu\nu} - \frac{1}{2} R g_{\mu\nu} = 0 \, . \tag{1.2}$$

[1] **Pill:** Occam's razor principle states *"Entia non sunt multiplicanda praeter necessitatem"*, which translates into *"More things should not be used than are necessary"*. Applied to physics, it suggests that among a set of equally working theories, the simplest is probably the correct one.

For the sake of completeness, one has to sum up to the Einstein-Hilbert action also the *Gibbons–Hawking–York* boundary term

$$S_{\rm GHY} = M_P^2 \int_{\partial\mathcal{M}} \mathrm{d}^3x \sqrt{|h|}\mathcal{K}\,, \tag{1.3}$$

where h is the determinant of the induced metric on the boundary $\partial\mathcal{M}$ and $\mathcal{K}$ is the trace of its *extrinsic curvature*. That is necessary when the underlying spacetime manifold has a boundary, in order to get rid of the non-trivial boundary terms that involves second-order derivatives of the metric when one varies the Hilbert-Einstein action. In order to recover the full equations, we need to consider a source of gravity in the previous action, that is $S = S_H + S_M$. As a result, the previous equations becomes

$$\frac{1}{\sqrt{-g}}\frac{\delta S}{\delta g^{\mu\nu}} = \frac{1}{16\pi G}\left(R_{\mu\nu} - \frac{1}{2}Rg_{\mu\nu}\right) + \frac{1}{\sqrt{-g}}\frac{\delta S_M}{\delta g^{\mu\nu}} = 0\,. \tag{1.4}$$

Defining the matter *energy-momentum tensor*, or *stress tensor*, to be

$$T_{\mu\nu} = -2\frac{1}{\sqrt{-g}}\frac{\delta S_M}{\delta g^{\mu\nu}}\,, \tag{1.5}$$

we finally recover the very well known complete Einstein's equations

$$G_{\mu\nu} = R_{\mu\nu} - \frac{1}{2}Rg_{\mu\nu} = 8\pi G T_{\mu\nu}\,, \tag{1.6}$$

where $G_{\mu\nu}$ is referred as Einstein's tensor. These are ten indipendent equations for the ten unknown functions of the metric components - which is a symmetric tensor. However, the Bianchi identities $\nabla^\mu G_{\mu\nu} = 0$ add four additional constraints on Ricci tensor, so there are only six truly independent equations. This is not surprising. Indeed, if a certain metric is a solution to Einstein's equations in one coordinate system x_μ, this should also hold true in any other coordinate system x'_μ. That implies we already expect four unphysical degrees in the metric, therefore Einstein's equations only constrains the six coordinate-independent degrees of freedom. In addition, the Bianchi identities entail the conservation of the energy-momentum tensor on the right hand side of Einstein's equations, namely $\nabla^\mu T_{\mu\nu} = 0$.

1.2 Friedmann–Lemaître–Robertson–Walker metric

A variety of observations, as most remarkably the temperature map of the cosmic microwave background (CMB), concluded that the universe where we live is homogeneous and isotropic on large scales. These two proprieties can be stated mathematically if one requires the manifold of the physical spacetime to respect some symmetries; we can think of isotropy as its invariance under rotations while homogeneity as invariance under translations of the spacetime metric tensor. Isotropy applies at some specific point in the space, and states that the space looks the same towards all directions. Observations point out a wide accordance on an isotropic universe and, if we assume not to be in a special favoured place in the universe, this turns into an any point isotropic spacetime, that is homogeneous. This is the content of the *Cosmological Principle* which is adopted to set the mathematical theory beyond our universe. It is also equivalent of stating that the spacetime have a maximally symmetric spatial sector, or rather, the maximum number of Killing vectors. This propriety allows to foil it in time independent spatial surfaces Σ such that the metric can be reduced to

$$ds^2 = -\mathrm{d}t^2 + A^2(t)\gamma_{ij}(w)\mathrm{d}w^i\mathrm{d}w^j\,, \tag{1.7}$$

where t is a time-like coordinate, and w is the set of global spatial coordinates. The latter do not change with time but rather *co-move* with the shrinking or the expansion of the spatial manifold specified by $A(t)$. For this reason, the set of coordinates $\{t, w\}$ is called co-moving and an ideal observer that moves along them experiences an isotropic universe.

A maximally symmetric space is also a constant curvature space, that means the spatial Ricci tensor takes the form

$$R_{ijkl} = K(\gamma_{ik}\gamma_{jl} - \gamma_{jk}\gamma_{il})\,, \tag{1.8}$$

where K is a constant that can assume any real value, and the latin indexes run only over the spatial coordinates. Engaging this condition and modelling the isotropy through a spatial spherically symmetric manifold, we can recast the metric above as

$$ds^2 = -\mathrm{d}t^2 + A^2(t)\left[\frac{\mathrm{d}r^2}{1-Kr^2} + r^2(\mathrm{d}\theta^2 + \sin^2\theta\,\mathrm{d}\varphi^2)\right]. \tag{1.9}$$

This metric is invariant by a re-scaling of the coordinates and the scale factor by means of some constant, thus it can be re-parametrised as a function of $k = K/|K|$ to cast the very well-known Friedmann–Lemaître–Robertson–Walker (FLRW) metric:

$$ds^2 = -\mathrm{d}t^2 + a^2(t)\left[\frac{\mathrm{d}r^2}{1-kr^2} + r^2(\mathrm{d}\theta^2 + \sin^2\theta\,\mathrm{d}\varphi^2)\right], \tag{1.10}$$

with $a(t)$ the so-called *scale factor*. The constant $k = K/|K|$ can assume only one of the 3 values among 1,0, −1, which corresponds to different shaped universes. The $k = -1$ case, to be named *open* universe, is the case where the spatial manifold represents a hyperbolic 3-dimensional surface. The $k = 1$ case, to be called *close* universe, corresponds to a 3-dimensional sphere. Lastly, the $k = 0$ case describes a spatially *flat* universe and will be throughout this work. Eventually, one can re-arrange the FLRW metric also as a function of the *conformal time* η as

$$ds^2 = a^2(\eta)\left(-\mathrm{d}\eta^2 + \left[\frac{\mathrm{d}r^2}{1-kr^2} + r^2(\mathrm{d}\theta^2 + \sin^2\theta\,\mathrm{d}\varphi^2)\right]\right), \tag{1.11}$$

where $\mathrm{d}\eta \equiv \mathrm{d}t/a(t)$. Note that the conformal time has not really a physical meaning, and is not the proper time of the co-moving observer, but nevertheless it is often useful to simplify some calculations.

Symmetry principles give us the shape of the spacetime manifold, but cannot return its dynamical evolution, which is encoded in the scale factor $a(t)$. As shown in the previous section, the evolution of the metric components is indeed ruled by Einstein equation

$$R_{\mu\nu} - \frac{1}{2}Rg_{\mu\nu} = 8\pi G T_{\mu\nu}\,. \tag{1.12}$$

Cosmology usually models the energy-momentum tensor of the Universe by a perfect fluid, that is shear-less and without any flow between energy and momentum in the rest frame. Accordingly,

$$T_{\mu\nu} = (p+\rho)U_\mu U_\nu + p g_{\mu\nu}\,, \tag{1.13}$$

where ρ is the density, p is the pression and U_μ is the mean velocity of the fluid. This extends trivially to a multi-fluids universe. In the co-moving frame the velocity

reduces to $U_\mu = (1,0,0,0)$, and the energy-momentum becomes diagonal

$$T^\mu{}_\nu = \mathrm{diag}(-\rho, p, p, p) \quad T = -\rho + 3p\,, \tag{1.14}$$

where $T = T^\mu_\nu$ is its trace. For almost all perfect fluids met in cosmology it in possible to postulate an equation of state

$$p = w\rho\,, \tag{1.15}$$

where the parameter w is a constant such that $|w| \leq 1$. If $w = 0, 1/3$ we retrieve, respectively, the equation of state for pressureless and radiation fluids; different values have been explored in cosmology with $w = -1$ associated to the cosmological constant - we shall see it later.

Once that the energy-momentum on the right hand side of Einstein equations is set, due to its isotropy, only the equations indexed by $\mu\nu = 00$ and $\mu\nu = ij$ differ and lead to the well-known *Friedmann equations*. The first reads as

$$\frac{\ddot{a}}{a} = -\frac{4\pi G}{3}\left(\rho + 3p\right) = -\frac{4\pi G}{3}\left(1 + 3w\right)\rho\,, \tag{1.16}$$

where the dot indicates a derivative with respect to the cosmic time t. It describes a decelerated expansion stage of the Universe for any $w > -1/3$, as turns to be for radiation and matter dominated universes. The second equation

$$\left(\frac{\dot{a}}{a}\right)^2 = \frac{8\pi G}{3}\rho - \frac{k}{a^2}\,, \tag{1.17}$$

allows us to introduce some terminology of common use in cosmology. On the left hand side, there is the so-called *Hubble parameter* $H \equiv \dot{a}/a$, which measures the expansion rate of the Universe. If one divides both sides of the equation by H^2, it yields

$$1 = \frac{8\pi G}{3H^2}\rho - \frac{k}{a^2H^2} = \frac{\rho}{\rho_{cr}} - \frac{k}{H^2a^2}\,, \tag{1.18}$$

or, alternatively,

$$1 - \Omega = \frac{k}{a^2H^2}\,, \tag{1.19}$$

where $\rho_{cr} \equiv 3H^2/8\pi G$ is the *critical density*, which is completely fixed by the Hubble rate, while $\Omega \equiv \rho/\rho_{cr}$ is the *density parameter*. The critical density, in dependence

if its smaller, larger or equal to the fluid density, discriminates between an open, closed or flat universe, respectively.

Since the Einstein tensor is divergence-free, the energy-momentum tensor obeys a conservation equation, whose 0-component reads as

$$\nabla_\mu T^\mu{}_0 = \partial_\mu T^\mu{}_0 + \Gamma^\mu_{\mu 0} T^0{}_0 = 0\,, \tag{1.20}$$

or, equivalently,

$$\frac{\dot\rho}{\rho} = -3\,(1+w)\,\frac{\dot a}{a}\,. \tag{1.21}$$

This equation can be easily integrated to express the density evolution as a function of the scale factor

$$\rho \propto a^{-3(1+w)}\,. \tag{1.22}$$

According to the Friedmann equations, $a(t)$ is an increasing function of time both for a matter and a radiation dominated universe. Therefore, we expect in general the fluids density to decrease through the cosmological history, with the exception of the cosmological constant $w = -1$. In particular, in case of a matter fluid $\rho \propto a^{-3}$, while for a radiation fluid $\rho \propto a^{-4}$.

For many purposes it is useful to recast the second Friedmann equation in (1.19) as a function of the Hubble and density parameters today values. Since k is constant, the left hand side must be a constant too and its generic time value can be set equal to the one it assumes nowadays. Developing the calculation this yields to

$$\dot a = a_0 H_0 \left[1 - \Omega_0 + \Omega_0 \left(\frac{a_0}{a}\right)^{1+3w}\right]^{1/2}\,. \tag{1.23}$$

Time evolution of the scale factor

Consider the second Friedman equation in (1.17) for a flat space, that is $k = 0$, and substitute therein the density relation (1.22), it yields

$$\dot a \propto a^{-(1+3w)/2}\,. \tag{1.24}$$

This equation can be integrated on both side to gather the dependence on cosmic time of the scale factor in a flat, or Einstein-de Sitter (EdS), universe:

$$t \propto a^{3(1+w)/2}\,. \tag{1.25}$$

It predicts for a radiation dominated universe $t \propto a^2$, while for a matter dominated $t \propto a^{3/2}$. Accordingly, the Hubble parameter during the radiation era scales as $H(a) \propto a^{-2}$, while during the matter era $H \propto a^{-3/2}$. These behaviours are essential to recover the cosmological evolution of physical quantities.

1.2.1 Horizons in cosmology

The correlation between events in the spacetime manifold is described by causality, which is a crucial concept in cosmology. It tells whether or not interactions other than gravity have taken place through the cosmological evolution, and therefore influences the big picture of the standard cosmological model. To encode the concept of causality we define *horizons*, namely particular distance scales that evolve in time and are meant to describe different type of causal connection between events.

The *cosmological horizon*, also called particle horizon, is the maximum distance particles could have covered to arrive at the observer from the initial time of the Universe. From the physical point of view it delimits the observable Universe: nothing from further distances can reach or be in causal contact with the observer. In a flat but accelerating spacetime the distance the light rays cover is not just given by the product between the speed of light and the age of the Universe, but rather it is inferred considering the null radial directions of the FLRW metric, that is $\mathrm{d}s^2 = 0 = \mathrm{d}t^2 + a^2(t)\mathrm{d}r^2$. Accordingly, the cosmological horizon is

$$R_{\mathrm{H}}(t) = a(t) r_{\mathrm{H}}(t) = a(t) \int_0^t \frac{\mathrm{d}t'}{a(t')} \,, \tag{1.26}$$

where r_{H} is its co-moving counterpart. To elaborate this expression further, we make use of equation (1.23) and integrate with respect to the scale factor rather than the cosmic time. Accordingly it can be recast as

$$R_{\mathrm{H}}(t) = \frac{a(t)}{a_0 H_0} \int_0^{a(t)} \frac{\mathrm{d}\bar{a}}{\bar{a}\left[(1-\Omega_0) + \Omega_0 \left(\frac{a_0}{\bar{a}}\right)^{1+3w}\right]^{1/2}} \,. \tag{1.27}$$

In the primordial Universe, that is when $a \to 0$, the first term in the square bracket

is negligible, thus

$$R_{\rm H} \simeq \frac{1}{H_0 \Omega_0^{1/2}} \frac{2}{1+3w} \left(\frac{a}{a_0}\right)^{3(1+w)/2} . \tag{1.28}$$

This shows that during a radiation dominated era $R_{\rm H} \simeq 2ct$ and the causal connected region seems to grow faster than the speed of light because of the expansion of the Universe - the physical units have been employed for the sake of clarity. The expression for the Hubble horizon we have found is very useful in the context of early cosmology and perhaps it resembles another type of cosmological horizon: the *Hubble horizon*

$$\mathcal{R}_{\mathcal{H}}(t) \equiv \frac{c}{H(t)} . \tag{1.29}$$

It defines the boundary between particles that are moving slower and faster than the speed of light relative to an observer at one given time. The two horizons differ only by a factor of 2 in early universe and therefore, even if conceptually different, we will no more distinguish them throughout this work.

1.2.2 Cosmological constant and Quintessence

According to different results of observations, the present epoch is an accelerated expansion stage of the Universe. We have shown that in order to provide such a feature, according to the Friedmann equations, the Universe must be dominated by a fluid with $w < -1/3$, the so-called *dark energy* fluid. It could arise from an additional constant term Λ, the cosmological constant, in the Einstein equations (1.6), that turns into

$$R_{\mu\nu} - \frac{1}{2} R g_{\mu\nu} + \Lambda g_{\mu\nu} = 8\pi G T_{\mu\nu} . \tag{1.30}$$

This term represents an additional density within the Universe, it keeps constant through its evolution while the matter and radiation components dilute, and dominates at present time. To have such features, namely constancy and acceleration, its equation of state must be specified by $w_\Lambda = -1$. The main problems of this model are essentially two: first, the extremely fine-tuning needs to set a Λ value compatible with observations, second, the so-called *coincidence problem*. The latter wonders why just right now the cosmological constant started to dominate and

accelerate the Universe, that is equivalent of saying why the time of dark-matter/Λ equality its so close to the present time.

The simplest extension of the cosmological constant model consists in requiring a *dynamical* dark energy components. The first proposals trace back to 1987, when Christof Wetterich, followed later by Ratra, Bharat and Peebles, presented the idea of a *quintessence*[2] [3, 4]. They notice that instead of adding a cosmological constant term, the same effects might be mimicked by introducing a new scalar degree of freedom in the Einstein's theory. This framework, in a sort of sense, *alleviates* the problem of coincidence by relating it to some feature of the field evolution - we show how in Section 2.2.3. Nonetheless, it also reduces the fine-tuning problem to the choice of a suitable parametrization for the scalar field. Let us briefly describe it. The quintessence scalar field action is given by

$$S_M^{(\phi)} = \int d^4x\sqrt{-g}\left[-\frac{1}{2}\nabla_\mu\phi\nabla^\mu\phi - V(\phi)\right], \tag{1.31}$$

where in the kinetic term we could have used as well the standard partial derivative ∂_μ rather than the covariant version ∇_μ seeing that they coincide when acting on scalars. The corresponding energy-momentum tensor, according to (1.5), reads as

$$\begin{aligned} T_{\mu\nu}^{(\phi)} &= -2\frac{1}{\sqrt{-g}}\frac{\delta S_\phi}{\delta g^{\mu\nu}} \\ &= \nabla_\mu\phi\nabla_\nu\phi - g_{\mu\nu}\left[\frac{1}{2}\nabla_\rho\phi\nabla^\rho\phi + V(\phi)\right]. \end{aligned} \tag{1.32}$$

The equations (1.6) describe both the effect of the field on the spacetime geometry and the effect of spacetime geometry on the field evolution, which, in this case, is ruled by the Klein-Gordon equation

$$\Box\phi - \frac{dV}{d\phi} = 0\,. \tag{1.33}$$

[2] **Pill:** The name "Quintessence" comes from ancient Greece. The Earth was though to be embedded in a "fifth element", "quinta essentia" in Latin, such as the aether. Likewise, in addition to the known four components of mass–energy content of the Universe, namely baryons, neutrinos, dark matter and radiation, quintessence would be the fifth known dynamical, time-dependent and spatially inhomogeneous contribution.

In particular, gravity is embodied into the d'Alembert operator $\Box = \nabla_\mu \nabla^\mu$ whereas the covariant derivative encodes the information on the spacetime geometry. For instance, with a FLRW metric the Klein-Gordon equation reads as

$$\ddot{\phi} + 3H\dot{\phi} + \frac{dV}{d\phi} = 0\,, \tag{1.34}$$

and it shows that the expansion of the Universe shapes the evolution of the scalar field. In cosmology we work with a maximally symmetrical 1+3 dimensional space and we assume the relevant fields to be completely homogeneous and isotropic through space, meaning that any their spatial derivative is discarded. As a consequence, fields energy-momentum tensors are isotropic in the local rest frame - no off-diagonal terms, and can be mapped into perfect fluid stress tensors with the conditions

$$\begin{aligned} \rho_\phi &= T_{00} = \frac{\dot{\phi}^2}{2} + V(\phi) \\ p_\phi &= T_{0k} = \frac{\dot{\phi}^2}{2} - V(\phi)\,, \end{aligned} \tag{1.35}$$

where the dot stands for time derivatives and (ρ_ϕ, p_ϕ) are the density and pressure of the fluid, respectively. With these two quantities, it is possible to compute the parameter w_ψ that specifies the equation of state of the scalar field fluid, namely

$$w_\phi = \frac{p_\phi}{\rho_\phi} = \frac{T - V}{T + V}\,, \tag{1.36}$$

where $T = \dot{\phi}^2/2$ is the kinetic energy of the quintessence field. Whenever during the evolution of the field its potential term overwhelms the kinetic contribution - the so-called *slow-roll* condition - then $w_\phi = -1$ and the scalar field behaves like a cosmological constant term which can dynamically provide the Universe acceleration.

Chapter 2

Primordial modified gravity

The standard model of cosmology predicts the growth of fluctuations via gravity to be inhibited in a primordial era of the cosmological history for all the matter species. This is due to the fast expansion of the universe, driven by the background radiation fluid, that overwhelms the bounding action of gravity. For this reason, the tiny over-densities in the matter fluid are not able to grow and dig a deep enough gravitational well that set the way for a collapse stage. This can be eventually regarded as a problem of time scales: the time necessary for matter to free fall under the effect of usual gravity is too large if compared to the time scale of universe expansion. However, in the early universe, gravity could have been different from the scenario we presently observe and one can imagine a *modified* theory of gravity capable to provide structure formations by very intense gravitational coupling among matter fields.

Theories of gravity constructed from the metric tensor alone are constrained by the Lovelock's theorem. It states that if we try to create any gravitational theory in a four-dimensional Riemannian space from an action principle involving just the metric tensor and its derivatives, then the only field equations that are second order or less are Einstein's equations, with an eventual cosmological constant term. As a consequence, in general, if we aim to build up a metric theory of gravity alternative to general relativity, one or more of the following options must be taken into account [5].

- ◇ Introduce other degrees of freedom, such as additional fields beyond the metric tensor.

- ◇ Accept higher than second derivatives of the metric in the field equations.
- ◇ Work in a space with dimension different from four, as in string theories.
- ◇ Give up on: rank two tensor field equations, or symmetry of the field equations under exchange of indices, or divergence-free field equations.
- ◇ Give up locality.

In this chapter we present and investigate a novel theory of modified gravity which will be used throughout this work. In the following chapters we will illustrate that this model does actually provide a mechanism for non-linear structures formation during radiation dominated era. It matches the first option of the above list, and its main assumption is the presence in the early universe of a long-range fifth interaction stronger than gravity, mediates by an additional light scalar field, and acting on a matter heavy field. A coherent presentation of the main set of alternative modified gravity scenarios can be found, for instance, in Ref. [6].

2.1 Fifth-force interaction

For a matter field collapse during primordial era, we require it to interact with the other contents of the universe only via gravity, since a non zero electromagnetic coupling would not allow over-densities to grow, while a weak-interaction coupling can be disregarded. Therefore, we can think of it as an extra degrees of freedom ψ beyond the set of elementary particles. In the Standard Model framework, each fundamental interaction is associated with the exchange of some bosons between the interacting fields. Thus, if we aim to model a fifth-force among the ψ field particles, the simplest option is to introduce also an additional scalar field ϕ that mediates this interaction.

As already mentioned in the previous chapter, the inverse of the Hubble parameter H is related to the horizon of causality; therefore, if we want the fifth-force to be a long-range interaction, the wave-lenght of the mediating particle has to be large, at least, as the scale set by horizon. For this to happen, we need to assume that during some epoch of the universe evolution the mass of this scalar field is lighter than

the Hubble parameter. On the contrary, to prevent it from behaving like radiation and inhibit the growth of fluctuations, the interacting particle ψ is required to be a non-relativistic fermionic field and, consequently, its mass is expected to be larger than H before the eventual collapse can take place. These requirements set the theory of an attractive and long range fifth-force similar to gravity, but potentially even more intense.

Within the action and fields formalism, the physical picture just outlined translates into set the action

$$S = \int d^4x\sqrt{-g}\left[\frac{M_P^2}{2}R + \mathcal{L}_{sm} + \mathcal{L}(\phi) + \mathcal{L}(\phi,\psi)\right], \tag{2.1}$$

with $M_P = (8\pi G)^{-1/2} = 2.435 \times 10^{18}\,\mathrm{GeV}$ the reduced Planck mass and $\mathcal{L}_{sm}$ is the Lagrangian of the Standard Model content. As pointed out, at early times, the radiative fluid dominates over the other components, and therefore we will replace henceforth $\mathcal{L}_{sm}$ with the radiation contribute $\mathcal{L}_r$. The third term in the action S is the Lagrangian density related to the scalar field ϕ

$$\mathcal{L}(\phi) = -\frac{1}{2}\partial^\mu\phi\partial_\mu\phi - V(\phi)\,, \tag{2.2}$$

where $V(\phi)$ is its potential energy, which can be neglected or not further specified since we supposed the mass of ϕ to be smaller than H. The fifth-force interaction arise from the last addendum of the action (2.1), which reads as

$$\mathcal{L}(\phi,\psi) = i\bar{\psi}\left(\gamma^\mu\nabla_\mu - m(\phi)\right)\psi\,, \tag{2.3}$$

$m(\phi)$ being a coupled mass term consisting, for instance, of a Yukawa-like coupling

$$m(\phi) \sim g\phi\bar{\psi}\psi\,. \tag{2.4}$$

As anticipated, both the light scalar ϕ and the heavy fermion ψ do not interact electromagnetically with the Standard Model sector, to whom they are indeed uncoupled or the coupling being close to zero. Taking the fifth-force aside, they only experience the usual gravity by a *minimal coupling*[1] to the metric.

[1]**Definition:** A field is *minimally coupled* to gravity if it has no direct coupling to the scalar curvature R.

The just outlined action, as many other fifth-force models, have been very widely studied in the literature of alternative dark energy scenarios. Indeed, the pressure component of the scalar field, under specific assumptions, can be made negative enough to counteract gravity contraction effect, providing the accelerated expansion of the universe. Moreover, such theories are *conformally equivalent*[2] to *scalar-tensor* Lagrangians. These are the most natural extensions of General Relativity, in which the metric tensor interacts with a scalar field via an explicit coupling to the Ricci scalar or, rather, where the gravitational interaction is mediated by an additional scalar field more than the graviton. Their equivalence entails that the effect of introducing a dark energy field, namely the accelerated expansion of the universe, can me mimicked by a modified theory of gravity, or viceversa. More on the topic can be found in the very exhaustive monography in Ref. [7].

However, in these work we will not study implications the dark energy sector of these models, but rather we will refer to the propose presented by L. Amendola, J. Rubio and C. Wetterich in Ref. [8], where the action (2.1) has been stated for a novel purpose: providing the formation of dark matter non-linear structures, such as primordial black holes or similar screened objects, even during radiation era, as a result of the strong attractive coupling.

Who are the players?

When we have introduced the additional ϕ and ψ fields, we have not further characterised them, neither discussed their possible origin. One could perhaps wonder *who* are these new degrees of freedoms and how do we justify their presence in the universe after inflation. Here below we follow the intriguing discussion in Ref. [8].

Incidentally, the existence of long-range attractive forces stronger than gravity is

[2]**Definition:** A *conformal* or *Weyl trasfmormation* is a rescaling of the metric tensor between the spacetimes $(M,\, g_{\mu\nu})$ and $(M,\, \tilde{g}_{\mu\nu})$ of the form

$$g_{\mu\nu} = \Omega^2(x)\, \tilde{g}_{\mu\nu}\,,$$

with $\Omega(x)$ being a regular function. It affects the norm of vectors in the spacetimes but leaving invariant the causal structure. Two theories are said to be *conformally invariant* if there exists a conformal trasformation mapping their actions.

a natural expectation in particle physics models containing scalar fields. A straightaway example is the interaction via Higgs exchange among Standard Model fermion, which originates an attractive interaction that is much stronger than gravity and long range, since in the early Universe the mass of this particle was smaller than the Hubble parameter. However, the gravitational collapse of matter at early times is precluded in this picture; in fact, in case of equally charged fermions, the electromagnetic repulsion counteracts the effect of the Higgs interaction, while for opposite charged particles it leads to their annihilation.

Nevertheless, there is a plenty of physical theories justifying this scenario, and the ϕ and ψ fields could be associated alternatively to Grand Unified t Theories (GUTs) frameworks. For instance, we can think the ψ field as a scalar triplet predicted by GUT interacting with an heavy neutrino, with the collapsing stage, in this case, occurring nearly after inflation. Indeed, the point of the timeline cosmic evolution when the matter clustering occurs depends on the properties of the participating particles and, in principle, it could also take place after nucleosynthesis without violating its tight constraints - we will show it later. In this case, if not all the heavy particles ψ end in clustered structures, those remaining might decay after the moment of formation and be unobservable today. Correspondingly, the scalar field, enhancing the collapse of matter, could relax after the structures form to a minimum of effective potential with mass eventually exceeding the decreasing Hubble parameter. That means the field ϕ would not be observable at the present time either. On the other hand, ϕ could be an additional dark matter candidate, or be associated with dynamical dark energy, such as in *Coupled Quintessence* [9] models.

2.1.1 Equations of motion

The equation of motion of the fields can be inferred from the variational principle, that is taking a variation of the action with respect to the metric tensor, analogously to the case of the Einstein-Hilbert action of section 1.1 section. The result resembles Einstein equations with non-null energy momentum tensor:

$$G_{\mu\nu} \equiv R_{\mu\nu} - \frac{1}{2} R\, g_{\mu\nu} = 8\pi G \left(T_{\mu\nu(r)} + T_{\mu\nu(\phi)} + T_{\mu\nu(\psi)} \right) , \tag{2.5}$$

where the energy-momentum tensors are defined accordingly to equation (1.5). Henceforth we will assume the field equations derived from the action (2.1) to admit a perfect fluid description and consider a FLRW background. Since the covariant derivative of the tensor $G_{\mu\nu}$ is null, taking the covariant derivative on both sides of the previous equation, we infer the conservation of the *total* energy-momentum tensor

$$T^{tot}_{\mu\nu;\mu} = \left(T_{\mu\nu(r)} + T_{\mu\nu(\phi)} + T_{\mu\nu(\psi)}\right)_{;\mu} = 0\,. \tag{2.6}$$

Notice that this relation does already hold true separately for the radiation energy-tensor $T_{\mu\nu(r)}$ whereas it is not coupled to the other species. For this reason, the previous equations can be recast as

$$T_{\mu\nu(\phi);\mu} + T_{\mu\nu(\psi);\mu} = 0 \qquad \rightarrow \qquad T_{\mu\nu(\phi);\mu} = -T_{\mu\nu(\psi);\mu}\,. \tag{2.7}$$

The coupling encoded by $m(\phi)$ must satisfy the above conditions, which limit the set of viable coupling functions. A particular option among them is

$$T^{\mu}_{\nu(\phi);\mu} = + \;\; CT_{(\psi)}\phi_{;\nu}\,, \tag{2.8}$$

$$T^{\mu}_{\nu(\psi);\mu} = - \;\; CT_{(\psi)}\phi_{;\nu}\,, \tag{2.9}$$

with C a coupling constant and $T_{(\psi)}$ the trace of energy-momentum tensor related to the ψ field. This kind of coupling was already explored in early works on the topic [9], and has been widely investigated in the literature .

Now, let us elaborate the non-relativistic limit for the ψ field, that is $\rho_\psi \gg p_\psi$. Then, the spatial components of the equation (2.8) can be expressed as

$$\vec{F}_{5^{th}} = -Cm_\psi \vec{\nabla}\phi\,.$$

where m_ψ is the rest mass of the ψ field in this limit. We have showed that this kind of model does actually correspond, in the Newtonian framework, to an additional force acting on the ψ-particles originated from the scalar field ϕ, which can be regarded as a classical potential energy. On the contrary, in case the matter fluid ψ is relativistic, its trace $T_{(\psi)} = 0$, and the coupling is null and no more effective.

Since the scalar field drives this coupling, it is interesting to investigate its dynamical evolution too. The variational principle, applied to the action (2.1), shows that the usual Klein-Gordon equation (1.34), in this case, gains an extra source term and reads as

$$\Box\phi - V_{,\phi} = \ddot{\phi} + 3H\dot{\phi} + V_{,\phi} = \frac{\beta(\phi)}{M_P}\rho_\psi \,, \tag{2.10}$$

where $V_{,\phi}$ is a functional derivative with respect to the field and in the first equality we have used Christoffel's symbols of the FLRW metric. To derive this equation we employied the fermionic field number operator $n(\bar{\psi}\psi) \propto \bar{\psi}\psi$, which if multiplied by the mass function $m(\phi)$, yields the field density ρ_ψ. In addition, the function $\beta(\phi)$ is defined as

$$\beta(\phi) = -M_P \frac{\partial \ln m(\phi)}{\partial \phi} \,. \tag{2.11}$$

and it measures the dependence of the effective mass $m(\phi)$ on the scalar field ϕ. Because of it is physical meaning, the factor C in equation (2.7) can be suitably choose to match the coupling experienced by the scalar field evolution, and therefore hereafter we will adopt $C = \beta/M_P$.

The normalization of $\beta(\phi)$ involving M_P has been chosen such that for $\beta^2 = 1/2$ the attraction mediated by the scalar field has the same strength as gravity. Indeed, in Section 3.5, in the context of perturbation theory, we will prove that the combined strength of the fifth force and gravity is proportional to

$$Y \equiv 1 + 2\beta^2 \,. \tag{2.12}$$

A given model is specified by a choice of $\beta(\phi)$, and we expect its value to be rather large. Let us elaborate more on this point. Consider for instance a renormalizable interaction term of the form

$$m(\phi)\bar{\psi}\psi = m_0\bar{\psi}\psi + g\phi\bar{\psi}\psi$$

with m_0 a constant mass parameter and g a dimensionless coupling. For this particular example, we can rewrite the definition in (2.11) as $\beta(\phi) = -g\, M_P/m(\phi)$, which leads to

$$|\beta| \gg 1 \quad \text{if} \quad m(\phi)/M_P \ll g \,. \tag{2.13}$$

Since the ratio $m(\phi)/M_P$ is expected to be reasonably small because of the presence of the Planck mass scale at the denominator, even a very tiny Yukawa coupling g easily satisfies this relation. The higher it is, the more intense is the fifth force, that is the factor $2\beta^2$ can be naturally rather large. However, throughout this work we will assume $\beta(\phi)$ to assume a constant value over the radiation era, that is equivalent to say we are choosing an exponential coupling

$$m(\phi) \sim e^{-\frac{\beta\phi}{M_P}} \,. \tag{2.14}$$

Notice that the case of a Yukawa coupling we just discussed is recover expanding this mass function at the first order.

Lastly, we derive the background evolution equations for the average ϕ and ψ fluid energy densities that arise from (2.7). Basically, they differ from the uncoupled case we showed in Section (3.1) by the trace term on the right hand side, which is readily computed for a perfect fluid as $T(\psi) = \rho_\psi - 3p_\psi$. They follow straight off

$$\dot{\rho}_\phi + 3H(\rho_\phi + p_\phi) = + \frac{\beta}{M_P} (\rho_\psi - 3p_\psi)\, \dot{\phi} \,, \tag{2.15}$$

$$\dot{\rho}_\psi + 3H\,(\rho_\psi + p_\psi) = - \frac{\beta}{M_P} (\rho_\psi - 3p_\psi)\, \dot{\phi} \,, \tag{2.16}$$

with $H^2 = \rho/(3M_P^2)$. Again, the ϕ and ψ fluids are coupled whenever the ψ particles are non-relativistic, that is whenever $\rho_\psi \neq 3p_\psi$. On the contrary, the radiation fluid will not be affected by the extra interaction, and its evolution will therefore remain unchanged:

$$\dot{\rho}_r + 4H(\rho_r + p_r) = 0 \,. \tag{2.17}$$

2.2 Dynamical system approach

The evolution of a certain environment can be often described by a first set of first order differential equations, and whenever an analytical solution cannot be obtained in full generality, one needs a qualitative approach to elaborate the dynamical evolution of the system. The theory of dynamical systems is an extremely useful

mathematical tool to analyse such cases, with its applications regarding almost all circumstances where dynamical equations must be investigated. In addition, it also a powerful method when implemented by numerical analysis since, by means of it, the dynamical evolution in a geometrical space can easily be drawn and the physical picture of the system be inferred. Its first implementation in the context of cosmological dynamics date back to the 1970s by C. B. Collins and J. M. Stewart. in Ref. [10], and so far it has been widely employed in several branches of cosmology, especially in alternative dark energy models and modified gravity theories. The broad subject of cosmological dynamical systems is introduced below, but for further references and for a comprehensive, general and complete review we address to Ref. [11, 12, 7].

In this section we adapt this framework to the specific case of our model, which has already been extensively studied under this prospective, especially when referred as coupled quintessence. Instead of dealing with *quantitative* solutions, usually required to predict accurate experimental results, we will deal with *qualitative* analyses and global properties of the space of solutions, which are equally capable to yield a great physical insight.

Why do we need it?

The presence of a quintessence-like scalar field, with a suitably chosen potential, can alter the expansion rate of the universe at a certain time or temperature of the history. That means its evolution can in principle modify the relation between the abundance of light elements and the expansion rate in the radiation dominated era. This statement holds particularly for the Big Bang nucleosynthesis epoch - at a temperature $T_{nucl} \sim 1\,\mathrm{MeV}$ - when the weak interactions freeze out and are no more able to keep the equilibrium between protons and neutrons, allowing the formation by means of recombination of light elements. The tight constraints inferred from the known abundances of the latter, together with the observationally allowed range of the expansion rate at this temperature, lead to a bound on the maximum energy density of the scalar field: $\Omega_\phi(T \sim 1\,\mathrm{MeV}) < 0.045$. Any model involving a scalar field must be in agreement with this constraint at the time of nucleosynthesis in order to preserve its successful prediction.

The reader shall notice that we have not specified any equation of state for the scalar field, and $w(\phi)$ is basically left as free parameter of the theory. Therefore, the dependence on this degree of freedom affects the evolution of our cosmological model, which in consequence has to be investigated within the framework of dynamical systems, such that we can select, among all the possibilities, those trajectories of the phase space that turn to be compatible with aims and observations.

For instance, in the case of a coupled quintessence scenario, this approach translates into outline the set of possible configurations of the scalar field phase space allowing to provide an accelerated universe. Indeed, the existence of attractor-like solutions, in which the field energy tracks the background fluid density for a wide range of initial conditions, is of remarkable importance to alleviate the coincidence problem of dark energy.

In the following, we will point out why these kind of solutions turn to be useful also for our purposes.

2.2.1 Basics

Practically speaking, a *dynamical system* can be defined as any abstract system consisting of:

1. a space (state space or phase space);

2. a mathematical rule describing the evolution of points in that space.

In order to characterise the system, we need a set $\mathbf{x} = (x_1, x_2, ...)$ of quantities describing its state. We call the *state space* X the set of all possible values of these quantities. The rule describing a dynamical system is generally written in the form

$$\dot{\mathbf{x}} = \mathbf{f}(\mathbf{x}) \,, \tag{2.18}$$

where $\mathbf{f}$ is a differentiable map $\mathbf{f} : X \to X$ and the dot stands for the derivative with respect to a suitable time parameter $t \in \mathbb{R}$. Any solution $\mathbf{x}(t)$ of the system is commonly called an *orbit* or a *trajectory* of the phase space.

Moreover, a dynamical system is said to be *autonomous* if the map $\mathbf{f}$ does not contain explicit time-dependent terms. To this category belong the systems that

arise studying most of the dynamical dark energy scenarios, therefore henceforth we will restrict our analysis within this assumption. For this kind of dynamical systems there is a significant class of points of the phase space: the *fixed* or *critical* points, defined as the set of values $\mathbf{x}_c$ satisfying the relation

$$\mathbf{f}(\mathbf{x}_c) = 0\,. \tag{2.19}$$

The physics intuition beyond it is that the system, once placed at one of these points, could in principle remain in this steady state indefinitely. However, one needs to clarify whether or not the system can actually reach this state during its evolution, and, as well, if this state is stable when moderately perturbed. Therefore, we introduce two more definitions to identify two relevant cases among many.

A fixed point is called *stable* if any solution $\mathbf{x}(t)$ contained in a generic neighbourhood of this point at a time t_0 will be thereafter included in the same neighbourhood. In addition, it takes the name *asymptotically stable*, or *attractor* point, if at later times the solution approaches to it, namely $\mathbf{x}(t) \to \mathbf{x}_0$ for $t \to \infty$. The subtle difference between these two definitions is that trajectories near a simple stable point could never reach it and just circling around. However, almost every fixed points within the context of cosmology which are stable are also asymptotically stable, therefore, if not further specified, we will refer in the following without distinction to both of them as stable points.

The previous set of definitions has already exhibit a remarkable feature of the attractor-like points: they force different initial conditions to converge towards a unique solution. As a consequence, studying the critical or fixed points of a dynamical system is of the utmost importance, since it allows to almost completely understand the key features of a model under investigation and make qualitative considerations about all the possible evolutionary pictures.

Once introduced the concept of stability, we have everything we need to present a method that can be used to study and identify stable points of cosmological dynamical systems. The so-called *linear stability theory* is the most commonly employed technique and, for most cosmological applications, it is able to grant a good insight on physical properties. Beyond this method, the subject extend much farther as discussed in Ref. [11] .

2.2.2 Linear stability theory

The basic idea is to linearise the trajectories near a fixed point to infer the proprieties and to understand the dynamics of the entire system from this domain.

Let us consider a generic dimension dynamical system specified by the vector map $\mathbf{f}(\mathbf{x}) = (f_1(\mathbf{x}), f_2(\mathbf{x}), ...)$, its fixed point being $\mathbf{x}_c$. A Taylor expansion in a neighbourhood of this point yields to

$$\begin{aligned} f_i(\mathbf{x}) &= f_i(\mathbf{x}_c) \\ &+ \sum_j \frac{\partial f_i}{\partial x_j}(x^j - x_c^j) + \frac{1}{2}\sum_{j,k} \frac{\partial^2 f_i}{\partial x_j \partial x_k}(x^j - x_c^j)(x^k - x_c^k) + \mathcal{O}(\delta x^3)\,. \end{aligned} \tag{2.20}$$

The first term of the sum is null by definition of critical point and thus we will focus on the second one, which is linear with respect to the deviation term $\delta x^j = (x^j - x_c^j)$. A particular relevance in this relation is assumed by the object $\partial f_i/\partial x_j$, it being a generic element of the Jacobian matrix $\mathbf{J}$, also called the *stability matrix*. Indeed, by means of equation (2.20), the dynamical system rule (2.18) can be recast as

$$\frac{\mathrm{d}\delta\mathbf{x}}{\mathrm{d}t} = \mathbf{J}|_{\mathbf{x}_c} \cdot \delta\mathbf{x}\,. \tag{2.21}$$

This formula tell us that the eigenvalues of $\mathbf{J}$, once evaluated at $\mathbf{x}_c$, contain the information about the evolution of the dynamical system orbit and describe the stability conditions at the fixed point.

In addition, the analysis of the stability matrix eigenvalues lead us to distinguish three further broad cases to classify fixed points. Firstly, if all eigenvalues of the Jacobian matrix at the fixed point have positive real parts, trajectories are repelled from the fixed point; in this case we name it an *unstable point* or a *repelling node*. Secondly, if all eigenvalues at the fixed point have negative real parts and the determinant is positive, the point would attract all nearby trajectories and, as already stated, it is regarded as stable or as an attractor node[3]. In this case, the imaginary

[3]**Notice:** there exist also attractor-like solutions, which are particular trajectories of the phase space that, in a similar manner of stable points, attract the nearby trajectories to converge towards them.

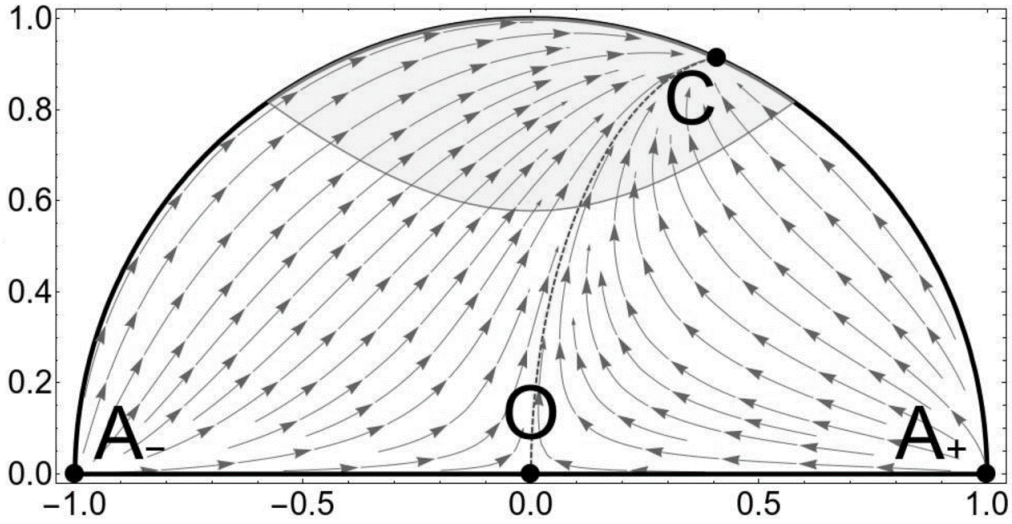

Figure 2.1. Schematic evolution of a 2-dimensional phase space, The points A_- and A_+ are two repelling nodes, the point O is a saddle point, while the point C is the only attractor node for the system evolution. Picture from Ref. [11].

parts of the eigenvalues can eventually give rise to spiral orbits - an example in cosmology is the solution to the graceful exit problem of inflationary models proposed by A. Linde [13]. Lastly, if at least two eigenvalues at the fixed point have real parts with opposite signs, then the corresponding fixed point is called a saddle point, that means it attracts trajectories in some directions but repels them along the others. In 2 and 3 dimensional one can classify all possible critical points of a system, however, in more than 3 dimensions this becomes difficult and very laborious. Anyway, for all practical applications to cosmology, the above classification is sufficient for the majority of models.

For illustrative purposes, we briefly show how these three possibilities are realised in case of a dynamical system described by a 2-dimensional phase space. Consider the dynamical system specified by the rules

$$\dot{x_1} = f_1(x_1, x_2)\,, \qquad \dot{x_2} = f_2(x_1, x_2)\,, \tag{2.22}$$

let $(\bar{x}_1, \bar{x}_2)$ be a critical point of its phase space and $\delta x_1, \delta x_2$ to be small deviations from it. Reducing the Jacobian to a diagonal matrix, and by means of equation

(2.21), we get

$$\begin{pmatrix} \dot{\delta x_1} \\ \dot{\delta x_2} \end{pmatrix} = \begin{pmatrix} \mu_1 & 0 \\ 0 & \mu_2 \end{pmatrix} \begin{pmatrix} \delta x_1 \\ \delta x_2 \end{pmatrix} \tag{2.23}$$

where μ_1 and μ_2 are the complex eigenvalues - their expression in the general case can be found in [7, 11]. The class of solutions to this linear system of differential equations can be generically written as

$$\delta x_1 \quad = C_1 e^{\mu_1 t} + C_2 e^{\mu_2 t} \tag{2.24}$$

$$\delta x_2 \quad = C_3 e^{\mu_1 t} + C_4 e^{-\mu_2 t}\,, \tag{2.25}$$

where $\{C_i\}$ are integration constants. As already anticipated, these show that the eigenvalues of the Jacobian matrix determine the behaviour of the system near the fixed point. Accordingly, we recover the previous classification for the latter:

- **stable** when $\Re(\mu_1) < 0$ and $\Re(\mu_2) < 0$. As the time flows, the distances δx_1, δx_2 approach to 0;

- **unstable** when $\Re(\mu_1) > 0$ and $\Re(\mu_2) > 0$. As the time flows, the distances δx_1, δx_2 increase while the linear approximation breaks down at some point;

- **saddle** when $\Re(\mu_1) > 0$ and $\Re(\mu_2) < 0$ or viceversa. As the time flows, one of the δx increases while the other approaches to 0, that indicates a convergence only towards one direction.

Moreover, if the determinant of the Jacobian is null, then the matrix is singular and the systems reduce to a 1-dimensional phase space around the fixed point.

2.2.3 Scaling solutions

As discussed earlier, the coupled quintessence and our fifth-force model rely on the very same action, and the former has been broadly studied in the literature within the context of dynamical systems approach. Even though the aim of our work differs from providing an alternative dark energy scenarios, this literature can be transposed directly to our context to outline viable phase space solutions that provide the growth of matter perturbation during the radiative era.

The earliest studies on this specific topic were carried out by L. Amendola in Ref. [9, 14] and in the following, we will illustrate and further explain some of these results. The reader should be careful in comparing this work with the aforementioned, since the coupling adopted there is $\sqrt{2/3}$ times the one we introduced in section 2.1.1.

If we neglect the baryonic matter content of the Standard Model - which is a reasonable assumption since it is subdominant during radiation era - it is possible to model the universe at early times as made of three fluid components: radiation, ϕ particles and ψ particles. Implementing the pressure-less assumption for the ψ-matter fluid, and let the scalar field ϕ have a generic state equation, the energy densities evolution equations turn into

$$\begin{aligned} \dot{\rho}_\phi + 3H(\rho_\phi + p_\phi) &= +\frac{\beta}{M_P}\rho_\psi\dot{\phi}\,, \\ \dot{\rho}_\psi + 3H\rho_\psi &= -\frac{\beta}{M_P}\rho_\psi\dot{\phi}\,, \\ \dot{\rho}_r + 4H\rho_r &= 0\,. \end{aligned} \tag{2.26}$$

The last equation can be quickly integrated and leads to the familiar behaviour for relativistic fluids $\rho_\gamma \propto a^{-4}$, while the second one has the intuitive solution

$$\rho_\psi \propto a^{-3}\, e^{-\frac{\beta\phi}{M_P}}\,, \tag{2.27}$$

which differs from the standard behaviour of matter components $\rho_\psi \propto a^{-3}$ that has been outlined in Chapter 1. Finally, we raise the discussion on the first equation. Since the state equation for the ϕ fluid is not fixed, the solution (2.27) consists of an infinite set of possibilities. In this case, the dynamical system approach might come in handy to classify and to understand the qualitative possible evolution of the cosmological model. The 3-dimensional[4] phase space of this dynamical system

[4]**Note:** in principle the dynamical system could be described out of the six couples of variables (ρ_i, p_i), namely by a 6-dimensional phase space. However, the constraining state equations for matter and radiation fluids, together with the Friedmann equation, lower the space dimensions to 3.

can be parametrized through the following set of variables:

$$x = \frac{\kappa}{H}\frac{\dot{\phi}}{\sqrt{6}}, \quad y = \frac{\kappa}{H}\sqrt{\frac{U}{3}}, \quad = \frac{\kappa}{H}\sqrt{\frac{\rho_\gamma}{3}}\,, \tag{2.28}$$

where $\kappa = M_P^{-1}$ is the inverse of the Planck mass. Notice that x^2, y^2 and z^2 are proportional, respectively, to the fraction of total energy density carried by the field kinetic energy, the field potential energy, and the radiation. Moreover, it holds

$$\Omega_\phi = x^2 + y^2\,, \quad \Omega_\gamma = z^2\,, \quad \Omega_\psi = 1 - x^2 - y^2 - z^2\,, \tag{2.29}$$

where the last is nothing more than Friedmann equations for a flat universe, that is a fair assumption during the radiation epoch. In order to proceed with the analysis it is necessary to fix the potential term of the scalar field, therefore, following Ref. [9], we adopt the exponential potential

$$V(\phi) = A\, e^{\sqrt{\frac{2}{3}}\kappa\mu\phi}\,, \tag{2.30}$$

with μ and A two suitable parameter. According to the definition of dynamical system in 2.2.1, we also need to specify a rule, or rather a system of differential equation, that drives its time evolution, that is

$$\begin{aligned} x' &= \left(\frac{z'}{z} - 1\right) - \mu y^2 + \sqrt{\frac{2}{3}}(1 - x^2 - y^2 - z^2)\,, \\ y' &= \mu x y + y\left(2 + \frac{z'}{z}\right)\,, \\ z' &= -\frac{z}{2}\left(1 - 3x^2 + 3y^2 - z^2\right)\,, \end{aligned} \tag{2.31}$$

where the prime here denotes differentiation with respect to the e-fold parameter $N = \ln a$. These are derived combining the ϕ field equation of motion (2.10) and the Friedman equations recast as in equation (2.29). Notice that this set of ordinary differential equation is invariant under the change of sign of $y\,, z$ and N. Moreover, it is also limited by the positiveness of the total density to the circle $x^2+y^2+z^2 \leq 1$, thus we can restrict the analysis of the solutions to the quarter of the unitary sphere with $y\,, z > 0$.

The result consists of eight viable fixed points, identified by the conditions $x' = y' = z' = 0$, and belonging to the phase space of the system; we have listed them in Tab. 2.1 , while their existence and stability domains are summarised in Tab. 2.2. The effective parameter w_{eff}, defined as

$$w_{eff} = (p_\phi + p_r)/(\rho_\phi + \rho_r + \rho_\psi)\,, \tag{2.32}$$

encodes the behaviour of the system in a fluid which has the average pressure and density of its components. For our purpose, we need a critical point that work as attractor node for the trajectories of the phase space during the radiation dominated era, such that, for any initial conditions, we ensure those always converge to it. According to Tab. 2.1, the unique point meeting our aims is the one labelled as c_{RM}. It describes a universe having an effective $w_{eff} = 1/3$, as expected from a radiation dominated era, nonetheless still allowing a tiny amount of matter to be present. We remark that, despite it results from the choice of the exponential potential, this fixed point pops up also with other functional forms [12], therefore, hereafter, we shall consider the discussion as independent from this choice. Now, a question arise: how does the matter density evolve at this phase space point?

To elaborate the answer, we first have to observe that all these critical points have the remarkable feature to be *scaling solutions*. Those are defined to be orbits of the dynamical system in which the energy density of the scalar field mimics the energy density of background fluid. This tracking feature is crucial. For instance, in alternative dark energy scenarios it allows to explain dynamically why the density of dark energy is similar to the present dark matter density just by assuming that nowadays the universe lays on such attractor-like solution.

Going back to our case, in the limit of $\beta \gg 1$, we can realise a stage where all the density parameters evolve as a constant

$$\Omega_\psi = \frac{1}{3\beta^2}\,, \qquad \Omega_\phi = \frac{1}{6\beta^2}\,, \qquad \Omega_\gamma = 1 - \frac{1}{2\beta^2}\,, \tag{2.33}$$

that means every single matter species density parameter scale as radiation $\rho_\gamma \propto a^{-4}$. By virtue of equation (2.27) , imposing this condition, we infer

$$\phi' = M_P/\beta\,. \tag{2.34}$$

The physical picture beyond this scaling solution is an unceasing leakage of energy between the ψ and ϕ fields that dilutes their energy densities.

From the point of view of the cosmological evolution, after the exit from the inflationary era, the system begins to fall towards this attractor point and can reach it straightaway, or at later times, depending on the initial conditions for the energy densities ρ_ψ and ρ_ϕ, which are typically set at the end of inflation, after reheating. During this falling, the fifth force plays then no role for the evolution of the background and the matter field density behaves as usual non-relativistic matter $\rho_\psi \sim a^{-3}$. This means that the density parameter Ω_ψ increases with time till it reaches and seats on the scaling solution $\Omega_\psi = 1/(3\beta^2)$ at some time $t_{\rm in}$. This stage could eventually extend later than nucleosynthesis, because the strong coupling β would allow the scalar field density parameter Ω_ϕ to easily pass the constraints we have previously outlined. We will see in the next chapter that from the moment the system ends up at the scaling solutions, the fluctuations on the ψ field start inevitably to grow.

Lastly, let us add a further comment. From Tab. 2.2 we realise that this solution

Point	x	y	z	Ω_ϕ	Ω_ϕ	w_{eff}	w_ϕ
a	$-\frac{\mu}{3}$	$\left(1-\frac{\mu^2}{9}\right)^{1/2}$	0	1	0	$\frac{2\mu^2}{9}-1$	$\frac{2\mu^2}{9}-1$
b_R	$-\frac{2}{\mu}$	$\frac{\sqrt{2}}{\mu}$	$\left(1-\frac{6}{\mu^2}\right)^{1/2}$	$\frac{1}{2}$	$1-\frac{6}{\mu^2\kappa^2}$	$\frac{1}{3}$	$\frac{1}{3}$
b_M	$\frac{-3}{2\left(\mu+\beta\sqrt{3/2}\right)}$	$\frac{(g-9)^{1/2}}{2\left\lvert\mu+\beta\sqrt{3/2}\right\rvert}$	0	$\frac{g}{4\left(\mu+\beta\sqrt{3/2}\right)^2}$	0	$\frac{\mu}{\mu+\beta\sqrt{3/2}}$	$\frac{18}{g}-1$
c_R	0	0	1	0	1	$1/3$	–
c_{RM}	$\frac{1}{\sqrt{6}\beta}$	0	$\left(1-\frac{1}{2\beta^2}\right)^{1/2}$	$\frac{1}{6\beta^2}$	$1-\frac{1}{2\beta^2}$	$\frac{1}{3}$	1
c_M	$\sqrt{\frac{2}{3}}\beta$	0	0	$\frac{4}{9}\beta^2$	0	$\frac{2\beta^2}{3}$	1
d	-1	0	0	1	0	1	1
e	$+1$	0	0	1	0	1	1

Table 2.1. Critical points for coupled quintessence models [9]. They are labelled by a subscript indicating whether, other than the scalar field, are components as matter (M), radiation (R) or both (RM) are allowed. Moreover, we have defined $g = 6\beta^2 + 4\beta\lambda/\kappa + 18$.

Point	Existence	Stability	Acceleration
a	$\frac{\mu}{\kappa} < \sqrt{6}$	$\sqrt{\frac{3}{2}}\frac{\mu}{\kappa} < \mu_+, \quad \frac{\mu}{\kappa} < \sqrt{4}$	$\frac{\mu}{\kappa} < \sqrt{2}$
b_R	$\frac{\mu}{\kappa} > \sqrt{4}$	$0 < \frac{\mu}{\kappa} < -4\beta$	never
b_M	$\left\|\frac{\mu}{\kappa} + \beta\right\| > \sqrt{\frac{3}{2}}, \sqrt{\frac{3}{2}}\frac{\mu}{\kappa} > \mu_0$	$\sqrt{\frac{3}{2}}\frac{\mu}{\kappa} > \mu_+ \quad \frac{\mu}{\kappa} > -4\beta$	$\frac{\mu}{\kappa} < 2\beta$
c_R	$\forall \mu, \beta$	unstable $\forall \mu, \beta$	never
c_{RM}	$\lvert\beta\rvert > 1$	$\frac{\mu}{\kappa} > -4\beta$	never
c_M	$\lvert\beta\rvert < \sqrt{3/2}$	$\lvert\beta\rvert < 1/\sqrt{2}, \sqrt{\frac{3}{2}}\frac{\mu}{\kappa} < \mu_0$	never
d	$\forall \mu, \beta$	unstable $\forall \mu, \beta$	never
e	$\forall \mu, \beta$	unstable $\forall \mu, \beta$	never

Table 2.2. Properties of critical points, where $\mu_0 = -\sqrt{3/2}\beta - 3\sqrt{3}/\sqrt{2}\beta$, $\mu_+ = 1/2\left(-\sqrt{3/2}\beta + \sqrt{18 + 3\beta^2/2}\right)$.

could never provide for the universe accelerated expansion and, in principle, rules out the hypothesis of the scalar field as dynamical dark energy. Anyway, non-linear over-densities trigger a screening mechanism - see the next section - that kill the strong coupling after structure formation. After that, the system is no more in a coupled scenario, the validity of the scaling solution drops and the dynamical system evolves turning away from the critical point c_{RM}. But, if in the future another scaling solution during matter era is met, the scalar field is eventually able to provide the acceleration of the universe. Lastly, we remark that further crossover effects might be able to move the system out from the scaling solution, as pointed out in [15].

2.3 Screening effects

Modified gravity models that suggest an additional gravity-like interaction with respect to the standard scenario - potentially involving baryonic matter too - lead to the question of how such modifications can be made compatible with the stringent solar system tests. As matter of fact, there are no evidence in observations of any fifth-force acting on solar system scale and, on the other hand, General Relativity

theory has faced several observational tests: from Eddington's pioneering measurement of light bending by the Sun in 1919, to the first detection of gravitational waves by the LIGO/VIRGO collaboration, its predictions have always been outstandingly validated. This would in principle close the doors to this class of theories, but the introduction in the last decade of *screening mechanisms* allowed these models to evade classical fifth-force searches. This has, in turn, originated an intense effort to design new experiments able to find probes of a fifth interaction - for a detailed review see Ref. [16]. Screening mechanisms lay on the fact that there can be orders of magnitude in distance and density scales between different environments, for instance say the terrestrial and the cosmological scales, and, as a consequence, the properties of the scalar field mediating the additional force can vary wildly among them.

With regard to our fifth-force model, we have to face the problem that an additional interaction, which we wish to be effective at early times of the universe, if not counteracted, would be somehow still effective nowadays. Therefore this theoretical machinery can very helpful for our purposes, because a screening mechanism could kill this interaction at some point in the past. More specifically, we aim that, once some particular feature of the scalar field fluid is met and a screening mechanism is triggered off, the ψ-particles inside the over-dense region stop interacting mutually, and as well with those outside, via fifth-force. Otherwise, the consequence in a lack of such mechanism would be that the ψ fluid density fluctuations would probably over-close the universe.

In order to illustrate the possible ways to achieve a fade off in the coupling function β, we adopt the example of a spherical spatial over-dense region with mass M, radius R and density ρ, embedded in an homogeneous matter fluid background with density ρ_0. As stated in equation (2.10), the field ϕ behaves like a potential energy and originates a fifth-force among the matter particles. Therefore, it is interesting to study the profile this field assumes as a consequence of the presence of this over-density in the matter fluid. Whence the scalar field ϕ is coupled to matter, its evolution is ruled by equation (2.10), and this result can be further manipulated

as

$$\Box\phi = +\frac{\beta}{M_P}\rho - V_{,\phi} \equiv V^{\rm eff}_{,\phi}\,. \tag{2.35}$$

where $V^{\rm eff}_{,\phi}$ is defined by last equality. This entails that the very responsible for the dynamic of the scalar field is the effective potential

$$V_{\rm eff} = V(\phi) + m(\phi)\bar{\psi}\psi = V(\phi) + \rho_\psi(\phi)\,, \tag{2.36}$$

which embodies either the effects of the potential energy and the coupling Let us consider it to have a minimum, and name $\phi_0 = \phi_{min}(\rho_0)$ the value the scalar field assumes in correspondence of this minimum for the background environment. Thus, taking a small time-independent deviation $\phi_0 + \delta\phi(r)$ to trace the shift induced by the static over-density, the previous equation can be expanded on both side around the minimum ϕ_0 and it turns into

$$\Delta\delta\phi(r) - m^2_{\rm eff}(\phi_0)\delta\phi(r) = \frac{\beta(\phi_0)}{M_P}\rho\,, \tag{2.37}$$

where Δ is the Laplace operator, $m_{\rm eff}(\phi_0) = V^{\rm eff}_{,\phi\phi}\big|_{\phi_0}$ is the mass of small fluctuations about the minimum of the effective potential and r is the distance from the centre of the source. The equation (2.37) is a second order differential equation, thus we must impose two boundary conditions. The first is that the solution must be regular at the origin $d\,\delta\phi/dr = 0$, while the second is that the field approach its ambient-density minimum at very large distances $\delta\phi(r \to \infty) = 0$. Then, the scalar field profile outside around the source reads as

$$\delta\phi = \frac{\beta(\phi_0)}{4\pi M_P}\frac{f(M,R)}{r-R}e^{-m_{\rm eff}(\phi_0)(r-R)}\,, \tag{2.38}$$

where the undetermined function f depends on the model of the sourcing object, for instance, $f(M,R) = M$ in the point-like case. Since a non-vanishing gradient of the scalar field translates into an effective fifth-force on matter fields, the previous equation suggests three ways to suppress this interaction:

1. if the mass $m_{\rm eff}(\phi_0) \gg 1$, the force is short ranged;

2. if the coupling to matter $\beta(\phi_0) \ll 1$, the force is scarcely effective;

3. if not all the mass of the fluctuations ϕ sources the scalar field, but just part of it, the potential energy drops right outside the structure.

With the help of some suitable fine-tuned parameters, it is always possible to satisfy the first two conditions and alter the background values of m_{eff} and β. Of course, from this option, only trivial models arise, with trivial specifying that their deviation from standard gravity is negligible on all scales. In spite of that, if we construct theories that satisfy these two conditions only locally, or in other words that are equipped with a screening effect which is environment dependent, it is possible to realise a coherent non trivial modify gravity framework. The *chameleon* mechanism uses an environment dependent scalar field mass to provide the screening, while the *dilaton* mechanism suppose a varying matter coupling. In the following section, we shall analyse also the possibility to implement the third option we have listed above, which has not been discussed yet. For the sake of completeness, another possibility to realise screening arises in the context of conformally equivalent scalar-tensor theories, where the kinetic term of the scalar field could also involve its derivative self-interactions. These are encoded in a functional pre-factor $Z(\phi, \delta\phi, ...)$, that turns to appear in the denominator of the solution (2.41), and therefore is able to suppress the interaction as well. To this category belongs the well known *Vainshtein* screening.

Among them, the chameleon mechanism is the most suitable for our purposes, since it can be switched on or off depending on the density of the environment, and therefore can be triggered off by the eventual non-linearity in the matter fluid. We discuss this possibility in the following, while, for complete review of the aforementioned screening mechanisms, we remand to Ref. [16, 5].

2.3.1 Chameleon screening

The chameleon mechanism was first introduced by Khoury & Weltman in 2003 [17] and is one of the earliest successful attempts to produce screening mechanism in field theory. In the previous section, we have shown through a simple example that an environment dependent scalar field mass can produce a suppression in the gradient of the scalar potential profile. Now, we address the discussion on how such a feature

can be realised, namely how the mass of the scalar can be properly related to the energy density that the matter field acquire in a certain environment, and what are the necessary conditions for this to work.

If $V(\phi)$ is neither constant, linear nor quadratic in ϕ, the mass $m_{\text{eff}} = V^{\text{eff}}_{,\phi\phi}|_{\phi_0}$ will depend on ϕ_0. Moreover, it minimises V_{eff} at the background level and, from the definition in (2.36), it manifestly depends on the matter density ρ_0. Therefore, the scalar field in the background domain acquire an effective mass that can be large enough to suppress the fifth-force in the surroundings of the compact object.

One should notice that it is not necessary for either $V(\phi)$ or the term $\beta\rho_\psi/M_P$ to have any minima themselves in order to have any minimum in the effective potential V_{eff}. They could in principle have also a runaway behaviour as, for instance, the exponentially decreasing scalar potential we adopt to compute the fixed points of our cosmological model in (2.30). However, in order to have interesting effects, we want to balance the two contributions to the effective potential $V_{\text{eff}} = V(\phi) + \rho_\psi(\phi)$, thus, without any loss of generality, $\rho_\psi(\phi)$ can be assumed to be monotonically increasing with respect to ϕ, while $V(\phi)$ as monotonically decreasing, or vice-versa. The above assumptions allow a minimum in the effective potential curve, just as we postulated in the previous example and as illustrated in Figure 2.2. Anyway, in this work we will not fix any particular choice of the parameters in the scalar field potential in (2.30), leaving the model as independent as possible from ad-hoc model building or fine-tuning characterisations.

So far, we have discussed only what happen in the outer space to a compact object a chameleon field is set up ; the next step is to further work out the previous example to illustrate the possible internal solutions for the scalar field profile.

Thin-shell effect

Accordingly to the previous notation, we denote by ϕ_c and ϕ_0, the minima of the effective potential at the object and ambient density, respectively. To readily visualise the physical meaning of the considerations in what follows, it is useful to think of r as a time coordinate and ϕ as the position of a particle of a standard dynamical problem in classical mechanics. Within this picture, the effect of the fifth

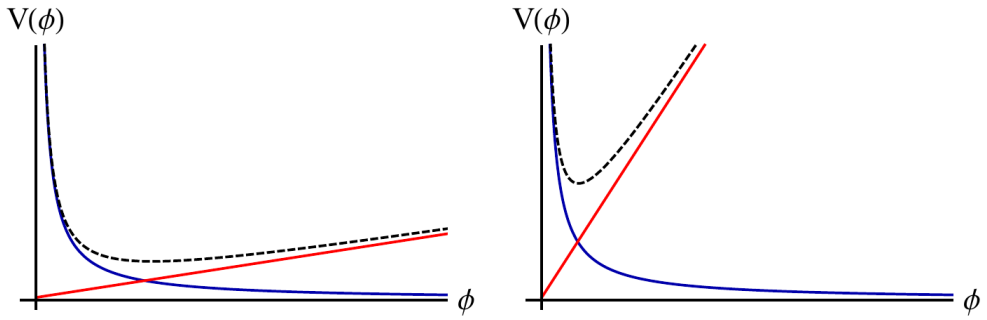

Figure 2.2. Example of Chameleon effective potential. The left and right panels depict the low and high density cases, respectively. The blue lines specify the potential while the red one the coupling of the chameleon field to to matter. The black dashed lines indicate the resulting effective potential, which is the sum of the two contribution, and drives the dynamics of the scalar field. Picture from Ref. [16]

force, originated by the scalar field gradient, is represented by the speeding up of the particle. Since the model has spherical symmetry, we can expand the Laplace operator in equation (2.35) as

$$\begin{aligned} \frac{d^2\phi}{dr^2} + \frac{2}{r}\frac{d\phi}{dr} &= +\frac{\beta}{M_P}\rho(r) - V_{,\phi}\,, \\ &= V^{\rm eff}_{,\phi}\,. \end{aligned} \tag{2.39}$$

The imaginary particle moves along the potential $V_{\rm eff}$, its motion being counteracted by the second term on the left-hand side of the previous equation, proportional to $1/r$, that is recognised as a damping term. For small r, this friction term dominates over the potential, and thus the particle is essentially frozen at $\phi = \phi_c$. It will not move until the damping becomes sufficiently small that the driving term $V^{\rm eff}_{,\phi}$ turns to be effective, only afterwards the particle begins to roll down the potential. In other words, the amount of "time" the particle remains frozen near $\phi = \phi_c$ depends just on the slope of its potential.

We consider here two possible regimes. If $|\phi_0 - \phi_c| \ll \phi_c$, namely if the initial slope of the potential is almost negligible, the field remains frozen at its initial value $\phi = \phi_c$ for a long time, since the friction do not allow the particle to roll. We shall denote by R_s the radius at which this occurs, that is the so-called *screening radius*. Therefore, there is no fifth-force for $r < R_s$, while afterwards the particle begins to

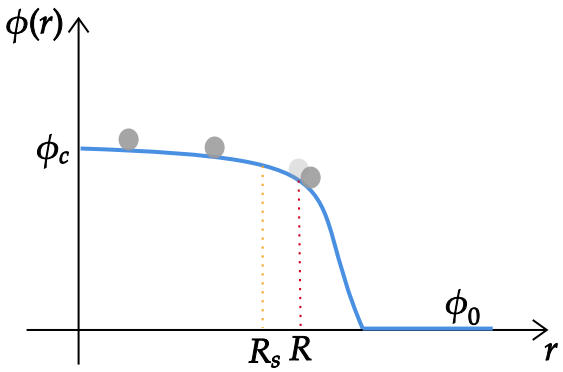

Figure 2.3. The picture depicts the potential energy experienced by an imaginary particle rolling down its profile. When the curve is flat, the particle is not accelerated, meaning that the fifth interaction is negligible in this region, while, when the curve becomes steep at the screening radius R_s, the particle moves due to the large gradient of the potential energy.

roll down the curve. Since the two minima of the effective potential only slightly differ from the inside to the outside, the region between the screening radius and the object boundary is very thin, that entails during this stage the potential energy term in (2.39) is negligible as it cannot develop a large steepness - see Figure 2.3. The solution for the scalar field potential is very straightforward and can be found in Ref. [17]. Notice that the limit $R_s = R$ is not possible because the solution wouldn't be regular at the boundary of the object $r = R$ where the energy density undergoes a jump from ρ_c to ρ_0. When $r > R$ the particle speeds up rolling down the curve under the action of the fifth force, which is originated by the large gradient of the scalar field, and we can disregard the curvature of the effective potential since the kinetic term of the imaginary particle is initially large compared to it, namely

$$\frac{d^2\phi}{dr^2} + \frac{2}{r}\frac{d\phi}{dr} \approx 0\,. \tag{2.40}$$

Integrating this equation, and matching the conditions forϕ and $\mathrm{d}\,\delta\phi/\mathrm{d}r$ at $r = R$, we infer the shape of scalar field outside the compact object

$$\delta\phi = M\frac{\beta(\phi_0)}{4\pi M_P}\frac{3\Delta R}{R}\frac{e^{-m_{\rm eff}(\phi_0)(r-R_c)}}{r}\,. \tag{2.41}$$

with $\Delta R = (R - R_s)$. Only a thin shell beneath the surface contributes significantly to the exterior field profile, or, loosely speaking, the chameleon field effectively couples only to a thin shell beneath the surface of an object. This is in analogy with electrostatics, indeed the body acts as a conducting sphere where any chameleon charge is confined to a thin shell of thickness ΔR near the surface. Therefore, the fifth force is screened both inside and outside the object, with the exception of a region nearby its border. This is properly what we do want: stable structures, out of the matter field over-densities, that inhibit the effects of the fifth force among the ψ particles after their formation both inside and outside them. Only a tiny remnant interaction between the outer shells of these structures would be possible, even though that is hardly detectable.

On the other hand, when $\phi_c \gg \phi_0$, that is the field is initially sufficiently displaced from ϕ_0 and it begins to roll as soon as it is released at $r = 0$. Hence, there is no friction-dominated regime in this case, and the interior solution for ϕ is most easily obtained by taking the screening radius $R_s \to 0$. In the latter case, since the gradient of the scalar field potential is no more negligible, the matter fluid inside the object is not screened anymore by the fifth-force interaction, although the value the effective mass acquire outside can still be adjusted to suppress the fifth interaction. A middle way to this case and the previous one is possible, and it would lead to a

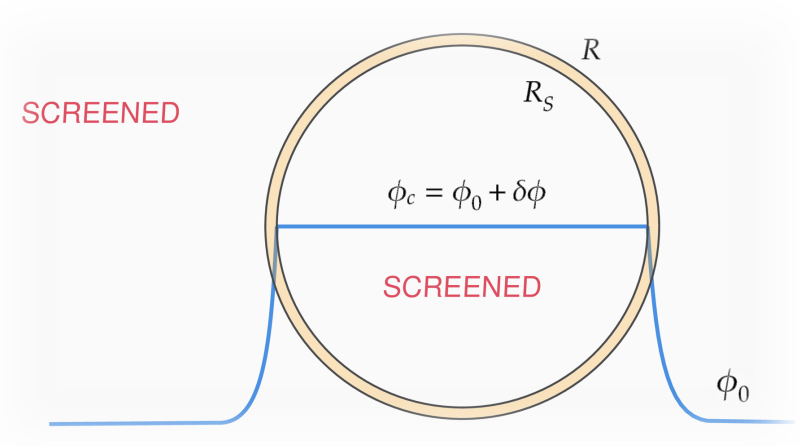

Figure 2.4. The thin shell effect. The ψ-field particles are screened both outside and inside the object and the fifth force interaction is suppressed.

non negligible non screened shell inside the object.

What is next? The discussion we developed so far set the necessary tools and the basic ideas of this novel mechanism that aims to provide the growth of fluctuations during radiation era. The next chapter will focus on the study of the inhomogeneities evolution when enhanced by a fifth gravity-like interaction.

Chapter 3

Cosmological Perturbation Theory

The usage of the Friedmann-Lemaitre-Robertson-Walker metric to describe our universe is very productive when considering scales at whom the homogeneous and isotropic assumptions for the universe hold true, namely of the order $100Mpc$. Our purpose is rather to investigate inhomogeneities on very small scales, let say comparable to the size of the Hubble horizon when perturbations re-enter after the inflationary era. Clearly the FLRW metric is not able to give any physical insight for them, and therefore, to describe how they couple to the spacetime manifold, we need to employ *perturbation theory*. Within this framework, the real spacetime manifold is regarded as a deviation from the homogeneous and isotropic background encoding the effects of spatial inhomogeneities.

In this chapter, we review the relativistic cosmological perturbation theory, presenting both the linear and non-linear discussion for a flat universe, and recovering the non relativistic Newtonian regime for sub-horizon perturbations. This discussion is further extended to our modified gravity framework, and its key features are pointed out. In particular, it predicts that the growth of the density fluctuations in a radiation dominated era is enhanced by the strong attractive fifth force such that the non-linear regime can be achieved. Lastly, we explore the eventual collapse of the ψ matter fluid over-densities in screened matter halos.

3.1 Relativistic perturbation theory

The full metric $g^p_{\mu\nu}$ of the physical spacetime manifold can be approximate with a first order expansion about some suitable background metric $g^b_{\mu\nu}$, that is

$$g^p_{\mu\nu} = g^b_{\mu\nu} + \delta g_{\mu\nu}\,, \tag{3.1}$$

where all the entries in δg are assumed to be small if compared to the unperturbed term $g^b_{\mu\nu}$. This statement, which is often employed in many context, is very ambiguous since the two metric tensors $g^p_{\mu\nu}$ and $g^b_{\mu\nu}$ are defined on two different manifolds, namely the physical and the background spacetimes, and therefore their sum has no meaning if we do not specify further what stands beyond this symbolic relation. This is achieved defining a map, namely a diffeomorphism, which identifies points of the background manifold to points of the physical manifold. This map is called *gauge*, is arbitrary, and allows us either to use a fixed coordinate system or to move back and forth between the background and the physical manifolds. For our purpose the most suitable choice is to work with the unperturbed background spacetime, and trace back through the gauge map the physical metric onto it; we will return on this in a while. Therefore, within this picture, the perturbation $\delta g_{\mu\nu}$ is a well defined difference difference between two tensor of the background manifold at the same point.

That explains why, for instance, scalar quantities on the perturbed manifold change under a gauge transformation but not under a simple general coordinate transformation. Indeed, these are two different kind of diffeomorphism: the first change the way we represent a physical picture, while the second can alter the physical picture itself. We remark that the class of general coordinate transformations is included in the broader set of gauge mappings, and engaging a certain coordinate system represents a gauge choice.

Let us elaborate more on this point following closely the discussion in Ref. [7]. If we fix a background spacetime, the physical picture can be described from a preferred coordinate system attached to the unperturbed manifold, for instance, the one that free-fall with particles. Nonetheless, we could also adopt a set of coordinates that instead free-fall according to gravitational fields in the perturbed manifolds, or even

adopt a totally different frame not related to the motion of matter particles. As an example, we can choose to or the observers to fixed points in the unperturbed frame or to the perturbed one. In the former case, to be called the *Newtonian or longitudinal* gauge, the observers will detect a velocity field of particles falling into the clumps of matter and will measure a gravitational potential. This choice is in fact the most intuitive one and reduces easily to the non relativistic Newtonian case. On the other hand, when the wavelengths of perturbations are larger than the horizon, since they grow exactly as the background fluid, is not a convenient choice to attach observers to an invisible background as done in the former case, but rather one employs the *synchronous gauge*. Within the latter, the observers are attached to the free-falling particles so they do not see any velocity field and, being always free falling, do not measure a gravitational potential. This gauge, on the contrary, does not have a straightforward Newtonian limit, but since we are above the horizon, we do not really need it. One can also define quantities that are gauge-invariant, as done to study inflationary perturbations, but this often makes the analysis more complicated and it is usually employed only if really necessary to disentangle non-physical effects. More on the topic of gauge choices can be found in Ref. [18].

3.1.1 Scalar, vector, tensor decomposition

Since we want to study the growth of sub-horizon perturbation in a cosmological context, we shall choose the Newtonian gauge an anchor the observer to a FLRW background frame. Let us see how to do it. In general, a metric has 10 independent components, and in consequence the most general tensor encoding the background perturbations is:

$$\delta g_{\mu\nu} = a^2 \begin{pmatrix} -2\Psi & w_i \\ w_i & 2\Phi\,\delta_{ij} + S_{ij} \end{pmatrix} \tag{3.2}$$

In this expression, we have just decomposed all the spatial scalars[1], w_i is a 3-vector, δ_{ij} is the spatial part of the FLRW metric, and S_{ij} is a traceless symmetric tensor

[1]**Definition:** A *spatial scalar* is a quantity invariant under a purely spatial transformation.

on a 3-dimensional space. An analogous decomposition can be done for any rank two tensor, for instance, the energy-momentum tensor. This result can be further simplified and the non-scalar entries of the decomposition can be related to some scalar quantity. With this purpose, let us recall Helmholtz's theorem: under certain conditions of regularity, a 3-dimensional vector w_i can be decomposed into the sum of an irrotational (longitudinal) and a solenoidal (trasverse) component, namely

$$w_i = w_i^{\parallel} + w_i^{\perp}\,, \tag{3.3}$$

with

$$\partial^i w_i^{\perp} = 0\,, \quad \epsilon^{ijk}\partial^j w_k^{\parallel} = 0\,, \tag{3.4}$$

where we use the metric δ_{ij} to raise and lower spatial indices, and ϵ^{ijk} is the Levi-Civita symbol normalised as $\epsilon^{123} = 1$. Of course, this decomposition is not unique and it is indeed defined up to a constant, but it always exists. Notice that since the longitudinal component is curl-free, it can be recast as the gradient of a scalar quantity, namely $w_i^{\parallel} = \nabla w_s$. This decomposition has a remarkable impact when studying Einstein equations. In fact, even though the $(0i)$ components will contain both the longitudinal and the transverse term, taking its curl or its divergence, the evolution of these two completely decouples. This is a very useful feature, because it entails that a scalar quantities, such as a cosmological fluid density, can have perturbations which are coupled only to the longitudinal term and directly related to w_s.

In 1946, Lifshitz introduced the scalar-vector-tensor decomposition (SVT), which is an extension of Helmoltz theorem to the context of tensors, see [19]. By the way, we can still make use of the vector case to figure out how the decomposition of a rank-two symmetric tensor S_{ij} works. The contraction of the divergence operator with one of its two indices defines, in effect, a vector $v_i = \partial^j S_{ij}$. This can be decomposed according to Helmholtz's theorem:

$$v_i = v_i^{\parallel} + v_i^{\perp} = (\partial^j S_{ij})^{\parallel} + (\partial^j S_{ij})^{\perp}\,, \tag{3.5}$$

where $(\partial^j S_{ij})^{\parallel}$ and $(\partial^j S_{ij})^{\perp}$ are the longitudinal and transverse components, such that

$$\epsilon_{ijk}\partial^j(\partial^l S_{kl})^{\perp} = 0\,, \qquad \partial^k(\partial^l S_{kl})^{\parallel} = 0\,, \tag{3.6}$$

and ϵ_{ijk} is the Levi-Civita symbol normalaized as $\epsilon_{123} = 1$. Clearly, if for both indexes the divergence is null, this reasoning fails; as a consequence, this possibility must be taken into account into a separate term. The previous arguments motivate the decompostion of S_{ij} as

$$S_{ij} = S_{ij}^{\parallel} + S_{ij}^{\perp} + S_{ij}^{T}\,, \tag{3.7}$$

with $\partial^j S_{ij}^T = 0$. It is possible to prove that, since $(\partial^j S_{ij})^\perp$ can be recast as gradient of a scalar function, $S_{ij}^\perp$ can be related to a scalar function B, that is

$$S_{ij}^{\perp} = \left(\partial_i\partial_j - \frac{1}{3}\delta_{ij}\Delta\right) \equiv D_{ij}B\,. \tag{3.8}$$

On the other hand, the relation $S_{ij}^\perp = \partial_i A_j + \partial_j A_i$, which is readily validate by a straightforward substitution in equation (3.6), shows that $S_{ij}^\perp$ can be instead related to a divergence-free vector A_i. Only the transverse part S_{ij}^T cannot be decomposed in any scalar or vector. Therefore, it constitutes a pure tensor perturbation.

The scalar-vector-tensor decomposition is a fundamental tool in first order perturbation theory since the three kind of metric deviations do not mix up, or rather any coupled term among them is second order and negligible. Therefore, these modes can be eventually employed separately, or disregarded, if one does not need to describe higher rank tensor effects. For instance, the vector and tensor modes both decouple from density perturbations; the first one giving rise to rotational velocity perturbations, while the second giving rise to gravitational waves which matters only for anisotropic perturbations. As a consequence, these two are unimportant for structure formation, although they do perturb the microwave background. Moreover, this dissociation proves that if initially the rotational, or vorticity, modes are zero they do not even arise at later times, while if they are present initially, they decrease as a^{-1} - if not enhanced by gravitational collapse.

Since we aim to study density perturbations, we shall consider only the terms of the metric which can be derived from a scalar, namely Φ, Ψ, $w_i^{\parallel}$, $S_{ij}^{\parallel}$. These quantities can be recast introducing two new scalar functions, $E(x)$ and $B(x)$, that produce the vector $E_{,i}$ and the tensor $D_{ij}B$, in analogy to the electromagnetic tensor.

Within this choice, the perturbation metric (3.2) reads as

$$\delta g_{\mu\nu} = a^2 \begin{pmatrix} -2\Psi & E_{,i} \\ E_{,i} & 2\Phi\,\delta_{ij} + D_{ij}B \end{pmatrix} \tag{3.9}$$

3.2 Perturbing the background

The complete metric we has just displayed $g^p_{\mu\nu} = g^b_{\mu\nu} + \delta g_{\mu\nu}$ has still 10 degrees of freedom, while we assert that a metric in general relativity is described by only 6 truly independent parameters. This is due to the intrinsic gauge invariance of the theory, and therefore we shall get rid of the non-physical degrees of free by fixing a gauge. This translates into impose up to four conditions on the metric coefficients which constraints four gauge coordinate transformations. It is worth to mention that an issue can arise. Due to this redundancy, some quantities, as the a matter density, may assume fictitious values after a gauge transformation, even if they are scalars. To avoid this problem, there are to way: work with gauge invariants, as pointed out by Bardeen [20], or fix and keep a gauge. The second choice is the most suitable for studying sub-horizon perturbations. Henceforth we fix $E_{,i} = 0$ and $B = 0$ - exactly $3+1$ conditions, that means we have selected a preferred perturbation tensor among the many possibilities. These option predicts the metric have null off-diagonal terms and thus represents the Newtonian gauge introduced previously. It is redundant to say that this gauge is not applicable in case vector and tensor components have to be taken into account, nonetheless it can be generalised to include them [20]. Finally, the *perturbed* FLRW metric can be recast as:

$$ds^2 = a^2(\eta)\left[-(1+2\Psi)d\eta^2 + (1+2\Phi)\delta_{ij}dx^i dx^j\right] . \tag{3.10}$$

The metric is now split in a background and a perturbed part, and Einstein equations will accordingly contain polynomial terms of various orders with respect to the perturbation quantities. The background cosmological evolution is obtained solving the 0-th order Einstein equation

$$G^{(0)}_{\mu\nu} = 8\pi G T^{(0)}_{\mu\nu} . \tag{3.11}$$

The additional gravitational effects due to the perturbed metric are instead expected to appear in the first or higher orders equations. To recover them, it is necessary to propagate the perturbation from the metric, through Ricci and Riemann tensors, to arrive at the perturbed Einstein tensor. Anyway, this is not the end of the story, indeed the right hand side of Einstein equation contains the energy-momentum tensor, which must be expanded too. In fact, the matter content evolution, which is subjected to gravity perturbations, can be depicted as a sum of an zero-order part, following the background gravity, and a perturbation term, encoding the additional gravitational physics. Thus, the perturbed Einstein equations

$$\delta G_{\mu\nu} = 8\pi G \delta T_{\mu\nu} \tag{3.12}$$

describe gravitational potentials originated by non-zero order terms and encodes the deviations from the background behaviour. In cosmology one usually assumes the matter content appearing in Einstein's equation to be described by a set of perfect fluids with given equations of state; for illustrative purpose, we first consider the single-fluid case. The quantities that source the perturbation of the energy-momentum tensor are essentially two: the fluctuation in the energy density field, which might differ spatially from the background value, and the fluctuations in fluid velocity field of free-falling particles, which can acquire a so-called *peculiar velocity* term. A very useful way to parameterise the fluid energy density fluctuation is by the definition of the *density contrast*

$$\delta = \frac{\delta\rho}{\rho} = \frac{\rho(x) - \rho_b}{\rho_b}\,, \tag{3.13}$$

where ρ_b is the background density. For sake of brevity, we shall not follow here the full derivation of the perturbed Einstein equations arising from density and velocity fluctuations; however the details can be found, for instance, in Ref. [7].

The background energy-momentum tensor $T^{(0)}_{\mu\nu}$ satisfies a continuity equation, and since an identical relation must hold also for the complete one $T_{\mu\nu} = T^{(0)}_{\mu\nu} + \delta T_{\mu\nu}$, we infer the conservation of the perturbed part as well, that is $\delta T^{\mu}_{\nu;\mu} = 0$. Notice the fluctuations propagate inside both the energy-momentum tensor and the covariant derivative. Assuming non-relativistic matter, The $\nu = 0$ component of the latter

equation entails the *continuity* or *mass conservation* equation

$$\delta' = -\theta - 3\Phi' \,, \tag{3.14}$$

where $\theta = \nabla \cdot v$ and, hereafter, the prime indicates a derivative with respect to the conformal time. Analogously, for $\nu = i$ we infer to the so-called *Euler equation*

$$(\nabla \cdot v)' + \mathcal{H}\nabla \cdot v = -\Delta\Psi - \Delta(c_s^2\delta) \,. \tag{3.15}$$

where c_s is the usual fluid sound speed and $\mathcal{H} = aH$ is the comoving Hubble rate.

In first order perturbation theory, owing to linearity, it is possible to move the discussion to the *Fourier space*, whereas all the perturbation variables can be decomposed in normal modes which mutually decouples. In this section, we assume to work on a generic component mode of the Fourier space and every perturbed quantity implicitly refers to it, namely $\delta = \delta_k$,$\Phi = \Phi_k$ and so on. Of course, when higher order non-linear terms are no more negligible, the Fourier representation drops and this treatment stops to be accurately predicting. Combining the different components of the perturbed Einstein equations, as illustrated in Ref. [7], it is possible to recover the *relativistic Poisson equation* within this framework, that is

$$k^2\Phi = 4\pi G a^2 \rho \left[\delta + 3\mathcal{H}(w+1)\theta/k^2\right] \,, \tag{3.16}$$

where $w = p/\rho$ as usual, and the perturbation Φ plays the role of Newtonian gravitational potential.

Remind that the causal horizon scale, which can be approximated by the Hubble scale $1/H$, identifies the region where interactions different from gravity can be active and affect perturbations. Thus the evolution of fluctuations on a certain scale depends, essentially, if that is larger or smaller than the horizon. We have indicate as $\lambda_c = (2\pi/k)$ the comoving wavelenght of the perturbation, which in physical coordinates translates into $\lambda_p = a\lambda_c$, a being the scale factor. On one hand, for super-horizon scales, namely $\lambda_p \gg 1/H$ or rather $k \ll \mathcal{H}$, the only active interaction remains gravity, and therefore perturbations can only follows the background universe expansion. On the other hand, deep inside the horizon, i.e

$k \gg \mathcal{H}$, the relativistic Poisson equation reduces to the usual non-relativistic linear version

$$k^2\Phi = 4\pi G a^2 \rho \delta \,, \tag{3.17}$$

while the continuity and the perturbation equations read as

$$\delta' = -\theta \tag{3.18}$$

$$\theta' = -\mathcal{H}\theta + c_s^2 k^2 \delta - k^2 \Phi \,. \tag{3.19}$$

The derivative of the continuity equation with respect to conformal time can be matched with Euler's one to get rid of velocity perturbations and to state the equation describing the density contrast evolution, that is

$$\delta'' + \mathcal{H}\delta' + \left(c_s^2 k^2 - \frac{3}{2}\mathcal{H}^2 \right) \delta = 0 \,. \tag{3.20}$$

Setting $\mathcal{H} \to 0$, that is for a steady universe, the latter reduces to the classical fluid wave equation $\delta'' + c_s^2 k^2 \delta = 0$, while the expansion of the universe has the effect to damp the growth of perturbations. Moreover, this equation shows that perturbations cannot grow if

$$c_s^2 k^2 - \frac{3}{2}\mathcal{H}^2 > 0 \,, \tag{3.21}$$

that is if the physical wavelenght $\lambda_p = a\, 2\pi/k$ is smaller than the *Jeans lenght*

$$\lambda_J = c_s \sqrt{\frac{\pi}{G\rho}} \,. \tag{3.22}$$

In case of a pressureless fluid, the velocity dispersion c_s is almost always negligible and $\lambda_J \simeq 0$, that means all the scales inside the horizon actually grow. On the contrary, `for radiation` $c_s \simeq c$, so that $\lambda_J \simeq H^{-1}$: `the growth of radiation fluid perturbations is prevented on all scales smaller than the horizon`.

3.3 Non-linear theory

As just shown, investigating sub-horizon scales at the linear order, one recovers the linearised equations of non-relativistic fluid dynamics, namely the Poisson, Euler and continuity equations. If perturbations enter into the non-linear regime, we can still make good use of this result. Indeed, for sub-horizon scales and small velocities, we can extend the linear Newtonian limit to the non-linear domain just tanking into account the full fluid dynamics equations in positions space.

Let us consider a pressureless perfect fluid with density ρ and moving with velocity $\mathbf{u}$ under the influence of a gravitational potential Φ_N that satisfies the Poisson equation

$$\Delta_r \Phi_N = 4\pi G \rho \,, \tag{3.23}$$

where r is the physical spatial coordinate. Its conservation of mass is described by the continuity equation, while the conservation of momentum is encoded in Euler equation; their complete form is

$$\partial_t \rho + \nabla_r \cdot (\rho \mathbf{u}) = 0 \tag{3.24}$$

$$\partial_t \mathbf{u} + (\mathbf{u} \cdot \nabla_r)\mathbf{u} = -\nabla_r \phi_N \,. \tag{3.25}$$

However, if one engage to the coordinates system which is comoving in the background model setting $\mathbf{x} = \mathbf{r}/a(t)$, the expansion of the universe can be taken out from the spatial coordinates. Then, the velocity $\mathbf{u} = \dot{r}$ must be decomposed in two contributes $\mathbf{u} = \dot{a}\mathbf{x} + \mathbf{v}(x,t)$, where $\mathbf{v} = a\dot{\mathbf{x}}$ is the peculiar velocity of the fluid, and is the one experienced in the comoving frame. The set of fluid dynamics equation can be recast within this frame and the time derivative can be transformed in a derivative with respect to the e-fold number $N = \ln a$. Recalling the definition of the density contrast $\delta(x,t)$ and using Friedmann equation , after some very straightforward manipulations, we arrive at

$$\mathcal{H}\delta' = \nabla^i[(1+\delta)v_i] \tag{3.26}$$

$$\mathcal{H}v_i' = -\mathcal{H}v_i - v_j \nabla^j v_i + \nabla_i \Phi \tag{3.27}$$

$$\Delta\Phi = -\frac{3}{2}\Omega_\psi \mathcal{H}^2 \delta \,, \tag{3.28}$$

where hereafter the prime indicates a derivation with respect to N, and we have introduced $\Phi = -(\Phi_N + a\ddot{a}\mathbf{x}^2/2)$. Notice that this set of equations have been derived under the assumption that any shear term in the Euler equation can be neglected, that is no the fluid has not viscosity. This propriety allows this system of relations to be closed and, on the physical side, implies that spherical perturbations at the initial stage remain spherical throughout. Therefore the transverse part of the peculiar velocity, if null initially, can be totally neglected, and an over-density modelled by a spherical homogeneous top-hat function, the infall remains purely radial.

However, the system of equations (3.27)-(3.28) can be compacted into a single equations as follows. First, take the spatial divergence of the Euler equation

$$\mathcal{H}\nabla^i v_i' = -\mathcal{H}\nabla_i v^i - \nabla^i v_j \nabla^j v_i + \Delta\Phi\,. \tag{3.29}$$

We can get rid of the $\Delta\Phi$ factor in the last equation by means of the Poisson equation (3.27), it yelds

$$\mathcal{H}\nabla_i v^{i'} = -\mathcal{H}\nabla_i v^i - \nabla^i(v_j\nabla^j v_i) - \frac{3}{2}\Omega_\psi \mathcal{H}^2\delta\,, \tag{3.30}$$

where, employing a spherically symmetrical density contrast, we can further expand

$$\nabla^i v_j \nabla^j v_i = (\nabla^i v_j)(\nabla^j v_i) + v_j\nabla^i\nabla^j v_i = \mathcal{H}^2(\nabla^i v_i^2)/3\,,$$

Furthermore, the continuity equation derived with respect to N gets

$$\mathcal{H}'\delta' + \mathcal{H}'\delta'' = \nabla^i v_i' + \delta\nabla^i v_i' + \delta'\nabla^i(v_i')\,, \tag{3.31}$$

which combined with the previous relations finally entails the non-linear equation for the evolution of density contrast:

$$\delta'' + \left(1 + \frac{\mathcal{H}'}{\mathcal{H}}\right)\delta' - \frac{3}{2}\Omega(1+\delta) - \frac{4}{3}\frac{\delta'^2}{(1+\delta)} = 0\,. \tag{3.32}$$

This equation is valid for sub-horizon perturbations of a pressureless matter fluid in a Einstein-de Sitter universe. In the following sections we will show how this relation can be generalised to our strongly coupled matter cosmologies, but first let us outline the key features of the standard picture,

3.3.1 The Meszaros effect

In the previous section we have claimed that the density perturbations related to the radiation fluid is prevented to grow due to the huge pressure component inhibiting the gravitational collapse. In addition, it can be easily proved that for the same reason the growth of any matter fluid over-density is inhibited if its particles are electromagnetically coupled and in thermal equilibrium with the radiation fluid. That is the reason why baryonic density perturbations starts to rise only after the recombination era, when matter decouples from radiation. On the other hand, the standard ΛCDM scenario predicts that the cold dark matter decouples much before than the baryonic matter from the radiative fluid, and neutrinos even earlier, therefore, in principle, its over-densities could start to grow in a former epoch. However it is well known that their growth is very moderate due to the so-called *Meszaros effect* [21] .

Before elaborating further this point, a clarification is needed. In the model presented in Chapter 2, we haven't identified the ψ-particles as cold dark matter but, rather, we have just assumed them to be particles affected by an intense gravity-like interaction and not coupled to the other matter species, if not via standard gravity. Analysing this effect, which is usually related to cold dark matter fluid, we aim to remark that such kind of non-interacting particles within the usual scenario, that is without the fifth-force, would not be allowed to produce non-linear over-densities during the radiation dominated era, even if they are not coupled directly to radiation.

Consider a universe made only two fluids, namely the radiation and the non-interacting matter fluids. The equation (3.32) at linear order can be easily extended to the two fluid case. Indeed, seeing that the two fluids are only coupled via gravity, their perturbations are described by two independent set of equations (3.27)-(3.28), while they share a single Poisson equation

$$\Delta\Phi = -\frac{3}{2}\mathcal{H}^2(\Omega_\psi\delta_\psi + \Omega_r\delta_r)\,. \tag{3.33}$$

Following the same steps carried out in the previous section, we can pack all these equations into the linear differential equation describing the non-interacting matter

over-densities

$$\delta_\psi'' + \left(1 + \frac{\mathcal{H}'}{\mathcal{H}}\right)\delta_\psi' - \frac{3}{2}(\Omega_\psi \delta_\psi + \Omega_r \delta_r) = 0\,. \tag{3.34}$$

Since the scale factor during radiation dominated era grows as $a(t) \propto t^{1/2}$, then $\mathcal{H} = \mathcal{H}'$ and the term inside the brackets in the previous equation is just zero. Moreover, switching from e-fold number to a proper time variable, we gather

$$\ddot{\delta}_\psi + H\dot{\delta}_\psi - \frac{3}{2}H^2(\Omega_\psi \delta_\psi + \Omega_r \delta_r) = 0\,, \tag{3.35}$$

where the dot here stands for time derivatives. Anyway, during radiative epoch Ω_ψ is subdominant, $\Omega_\psi \simeq 0$, thus this equation futher simplifies as

$$\ddot{\delta}_\psi + H\dot{\delta}_\psi + \frac{3}{2}H^2\Omega_r \delta_r \simeq 0\,. \tag{3.36}$$

Its solution is given by

$$\delta_\psi = C_1 + C_2 \int dt/a^2 = C_1 + C_2 \ln a\,,$$

where C_1, C_2 are constants. This expression predicts the aforementioned Meszaros effect, namely that density perturbations of the non-interacting matter fluid grows very mildly and cannot enter into the non-linear regime. Eventually, the physical insight beyond the above solution can be related to a competition between the necessary time for the non-interacting matter over-density to free-fall under the effect of its own gravitational potential, and the time scale of universe expansion, which is larger and overwhelms the perturbations growth. Indeed, even if the tiny perturbations in the radiation fluid density δ_r triggers inhomogeneities in the matter fluid, the Hubble flow $H\dot{\delta}_\psi$ acts as a damping term.

3.4 Genesis of perturbations

Before proceeding and extending perturbation theory to our framework, let us make a brief digression to discuss about the origin of small density fluctuations at early times of the universe. So far, we have assumed that after the inflationary era, that is the epoch of accelerated expansion of the universe, inhomogeneities in the matter

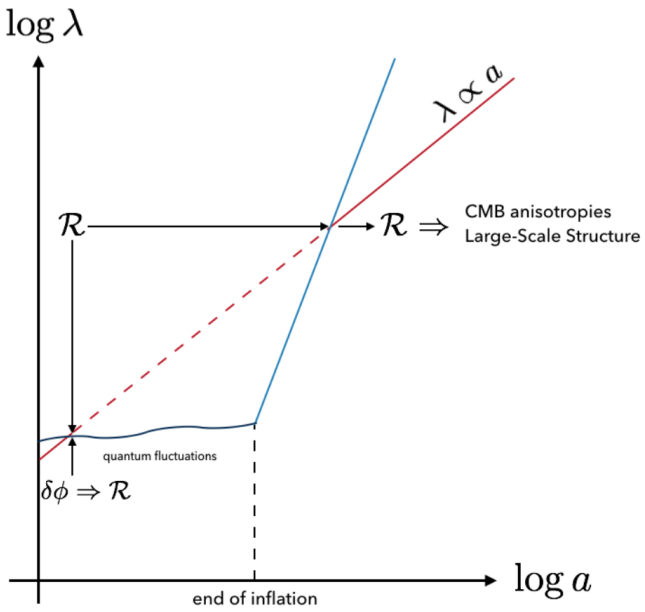

Figure 3.1. Representation of the genesis of quantum fluctuations during inflation. Notice that here $\delta\phi$ indicates the fluctuations of the inflaton field. Picture from Ref. [22].

fluid density pop up. The question on how these were originated naturally arise, therefore it is important to investigate this problem in order to figure out the proper initial conditions required by the structures formation machinery. Our best guess stems from quantum fluctuations of the scalar field driving the primordial acceleration of the universe, namely the *inflaton*. In facts, the capability to create these fluctuations is a native features of the inflation since a de Sitter expansion[2] of the universe originates quantum fluctuations for any scalar fields present at that time, as it results from quantum perturbations theory [22]. Of course that is in particular true for the inflaton which dominates the inflationary era. Any perturbation seed in the inflaton field translates into perturbations of its energy-momentum tensor and of the spacetime metric, in accordance with Einstein equations. In summary, small

[2]**Definition:** a de Sitter spacetime is a solution to Einstein equations that models a spatially flat universe dominated by a cosmological constant term, that could correspond to dark energy in our universe or the inflaton field in the early universe. The scale factor of this solution is commonly expressed as $a(t) = e^{Ht}$.

fluctuations of the inflaton field give rise to perturbations of the co-moving curvature $\mathcal{R}$ which can be thought as a gravitational potential, or more specifically, as a gauge invariant version of Newtonian potential in (3.9). The wavelenght λ of this quantum fluctuations, which grow as the scale factor $a(t)$, are stretched on larger scales because of the rapid super-luminal expansion of the universe. Once it slows down after inflation, the horizon starts to rise again, a given scale re-enters, and the curvature perturbations transfers to baryons and photons density fields via gravity, according to Poisson equation. In this manner, their initial conditions are set.The presence of primordial inflationary seeds is in great agreement with the detection of anisotropies in the temperature map of the *Cosmic Microwave Background* (CMB). Indeed, anisotropies on scales larger than 1 degree, that is angular size of the horizon at the time of last scattering, would be prevented by causality, but can properly explained if the inflaton quantum fluctuations were stretched up to that scale during the inflationary era.

It is often assumed, and supported by many models, that the post-inflationary spectrum on super-horizon scales is nearly scale invariant. If one defines the *density contrast* of a fluid having average background $\bar{\rho}$ as

$$\delta(x) = \frac{\rho(x) - \bar{\rho}}{\bar{\rho}}\,, \tag{3.37}$$

the previous assumption translates in requiring $n_s = 1$ into

$$\delta^2_{\mathrm{H}}(t_k) \simeq \left(\frac{10}{9}\right)^2 \delta^2_{\mathrm{H}}(t_{k^*}) \left(\frac{k}{k^*}\right)^{n_s - 1}\,, \tag{3.38}$$

where $\delta^2_{\mathrm{H}}(t_k)$ is the density contrast at the re-enter time of a scale k, k^* is a preferred reference scale and n_s is the so-called *spectral index*. We may say that the spectrum of perturbations is blue when $n_s > 1$ and has more power in the ultraviolet, while it is red when $n_s < 1$ and has more power in the infrared. If one allows a running of the spectral index, it takes the form

$$n_s(k) = n_s(k^*) + \left(\frac{dn_s}{d\ln k}\right)_{k=k^*} \ln\left(\frac{k}{k^*}\right)\,. \tag{3.39}$$

From CMB surveys is possible to infer the density contrast of the radiative fluid at the scales corresponding to the observed anisotropies at decoupling time, that

is $k_{\rm CMB} \simeq 0.05\ {\rm Mpc}^{-1}$, but also as well the spectral index and its running, that is $\mathrm{d}n_s/d\ln k$. The up to date values for these parameters have been elaborated by the Planck collaboration in 2018 [23] and are reported in the table below with one sigma confidence level (CL). According to the results, the primordial spectrum is not perfectly scale invariant but rather red, thus the smaller the scales the tinier the density perturbations.

Parameter	Value $\pm$ 68% CL
n_s	0.9649 ± 0.0042
$\mathrm{d}n_s/d\ln k$	0.0045 ± 0.0067

Now, it just remains to decide which are the relevant scales we want to investigate. For reasons that will be clarified in Chapter 3 and Chapter 4 we focus on scales containing an amount of matter equal to a solar mass unit. Let us consider the relation between the size of the horizon and the mass it contains M_H, that is

$$M_H = \frac{4\pi}{3}\frac{\rho_\psi(a)}{H^3} \simeq \frac{4\pi}{3\beta^2}\frac{M_P^2}{H}\,, \tag{3.40}$$

where in last equality we have employed the scaling solution (2.33) and the scale parameter a and the horizon H are intended to be computed at the same time instant. This result can be further manipulated and recast as

$$\frac{H_{\rm eq}}{H} = \frac{a_{\rm eq}^2}{a^2} = \frac{M_H}{M_\odot}\frac{3\beta^2}{m}\,, \qquad m \equiv \frac{M_{\rm eq}}{M_\odot} = 2.7\times 10^{17}\,, \tag{3.41}$$

with $M_{\rm eq} = 2GH_{\rm eq}^{-1}$ and $H_{\rm eq}$ is the Hubble constant at the matter-radiation equality. The latter can be easily estimated re-scaling the present Hubble constant at the equivalence, namely

$$H_{eq} = H_0\left(\frac{a_0}{a_{eq}}\right)^{3/2} = H_0\left(\frac{\Omega_{0,DM}}{\Omega_{0,rad}}\right)^{3/2} \simeq 3.8\cdot 10^{-13}\,{\rm s}^{-1}\,, \tag{3.42}$$

where the subscript 0 specify the quantities nowadays. If one assumes that all the ψ particles end up in screened structures, and those provide the whole amount of

dark matter of the universe, then

$$\Omega_\Psi(a_{\rm eq}) = \frac{a_{\rm eq}}{a_{\rm F}}\Omega_\Psi(a_{\rm F}) = \frac{1}{3\beta^2}\frac{a_{\rm eq}}{a_{\rm F}}\,. \tag{3.43}$$

where the subscript Ψ specifies these structures made out of the matter ψ particles, F identifies their formation instant, and $\Omega_\Psi(a_{\rm eq}) = 1/2$. This equation can be substituted in the horizon-mass expression (3.41) at formation, it yields

$$\frac{M_{\rm H,F}}{M_\odot} = \frac{m}{3\beta^2}\left(\frac{a_{\rm F}}{a_{\rm eq}}\right)^2 = \frac{m}{27\beta^6\Omega_\Psi^2(a_{\rm eq})}\,, \tag{3.44}$$

with $M_{\rm H,F}$ the mass contained in the horizon at formation. Therefore we found that β must obey to

$$\beta_c = 585\left(\frac{M_{\rm H,F}}{M_\odot}\right)^{-1/6}\,. \tag{3.45}$$

Of course the mass of the final structures would be just a part of the mass inside the horizon at formation, but its remarkable to observe that the latter depends solely on the value of the fifth-force coupling to the matter field. The coupling set the time after the inflationary era when screened structures eventually form. Anyway, we can roughly estimate the radius of these structures and its mass with the value of the horizon and the mass therein, that is

$$H_F^{-1} = m\cdot 10^{-17}\beta_c^2 H_{eq}^{-1}\cdot 10^7\left(\frac{M_{\rm H,F}}{M_\odot}\right)\,{\rm km} \tag{3.46}$$

$$= 2.7\cdot 10^7\left(\frac{M_{\rm H,F}}{M_\odot}\right)^{2/3}\,{\rm km}\,, \tag{3.47}$$

For a solar mass perturbation, in the momentum space, turns to be

$$k_\odot = 2\pi H \simeq 10^{13}\ {\rm Mpc}^{-1}\,.$$

Anyway, even if this is not really the first scale that re-enters the horizon, but rather the scale at formation time, the estimate is quite robust since those cannot differ as much to modify sensibly the nearly scale invariant post-inflationary fluctuations.

Now, we can finally compute $\delta^2_{\rm H}(t_\odot)$, and adopting the best fit value predicted by the Planck collaborations, one infers an initial seed $\delta_{in} \simeq \dot{1}0^{-7}$. Hereafter we will adopt this value to set the initial condition for perturbation theory, nonetheless we have displayed in Figure 3.2 how δ_{in} varies at different values of n_s and its running.

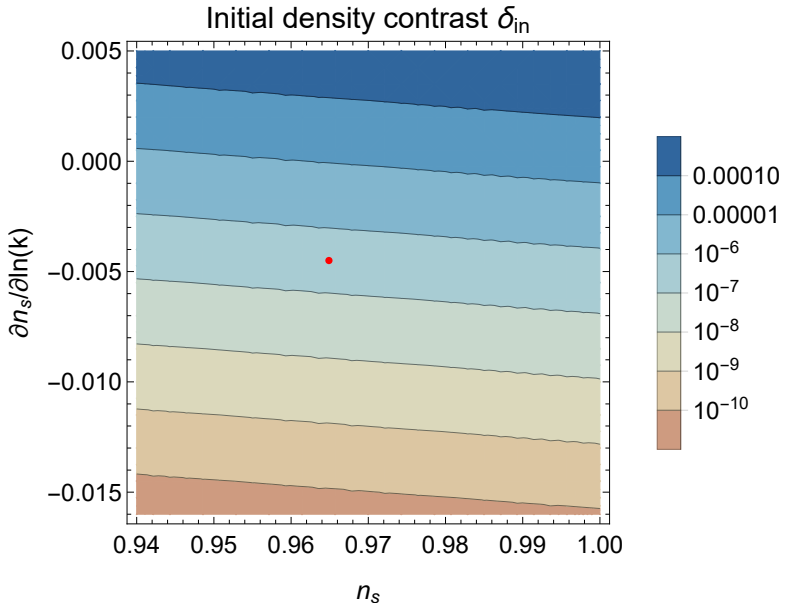

Figure 3.2. Dependence of the post-inflationary density power spectrum δ_{in} at solar mass scales on the spectral index n_s and it is running. The red point specifies the Plank collaboration best fit, that is the value employed through this work.

3.5 Perturbations in the fifth-force model

Now we illustrate how perturbation theory changes if the fifth interaction joins the picture. The discussion we carried out in section 3.1 about relativistic perturbation theory can be reconsidered starting from the modified Einstein equations we presented in equation (2.5). The only term of these equations differing from usual general relativity is the extended energy-momentum tensor on the their right hand side, while the Einstein tensor $G_{\mu\nu}$ remains indeed unchanged, and so its perturbative expansion. Hence, in order to take into account the fifth interaction effect, we just need to perturb the new terms arising from $T^{tot}_{\mu\nu}$ in equation (2.6) , namely the scalar and the spinor field contributions. Firstly, let us face the discussion at the linear level. Again, we will not report each step of the computation but, rather, we remand to Ref. [24] for a more detailed analysis.

3.5.1 Linear treatment

For the sake of coherency with the work mentioned above, let us re-define the perturbation variables as

$$\delta = \delta\rho/\rho, \quad \varphi = \kappa\delta\phi/\sqrt{6}, \quad \frac{a}{\mathcal{H}}\frac{\mathrm{d}x_i}{\mathrm{d}t}, \quad \nabla_i v_i = \theta \tag{3.48}$$

where $\kappa = M_P^{-1}$ is the inverse of the Planck mass, all the spatial derivatives are meant with respect of the co-moving coordinates and $\delta\phi$ is the scalar field perturbation; the old notation is simply recovered if one multiplies v_i and θ for $\mathcal{H}$. Notice that the scalar field induces fluctuations also in the ψ - matter field, to whom is indeed coupled. Accordingly, the Euler and continuity equations presented in equations (3.14)-(3.15) becomes, respectively,

$$\delta'_\psi = -\theta_\psi\,, \tag{3.49}$$

$$\theta'_\psi = -\left(1 + \frac{\mathcal{H}'}{\mathcal{H}} - \sqrt{6}\beta\right)\theta_\psi - \mathcal{H}^{-2}\Delta(\Phi - \sqrt{6}\beta\varphi)\,, \tag{3.50}$$

where the prime stands for a derivative with respect to $N = \ln a$. Taking the limit $\beta \to 0$, and restoring the old notation, one recovers the usual non-coupled scenario. We remark that the validity of these equation extends to the Newtonian domain only, that is for small sub-horizon scales and small peculiar velocities. On the other hand, on super-horizon scales the evolution of density perturbations is still driven only by gravity, and these grow accordingly to the dominating background fluid. The first order Poisson equation (3.17) remains unchanged, and for a radiation dominated universe populated by more than one fluid, it reads as

$$\Delta\Phi = \frac{3}{2}\mathcal{H}^2(\Omega_\psi\delta_\psi + \Omega_r\delta_r + \Omega_\phi\delta_\phi)\,. \tag{3.51}$$

There is an additional relation with respect to the standard case, that is the equation describing the scalar field fluctuations

$$\Delta\varphi = -\mathcal{H}^2\sqrt{\frac{3}{2}}\beta\,\Omega_\psi\delta_\psi, \tag{3.52}$$

which shows that the ψ matter perturbations source the scalar field potential. Eventually, if one defines $\hat{\Phi} = \Phi - \sqrt{6}\beta\varphi$ it is possible to get rid of the argument of the Laplace operator in equation (3.49), and reduce the set of linear equations to the followings:

$$\begin{aligned} \delta'_\psi &= -\theta_\psi \,, \\ \theta'_\psi &= -\left(1 + \frac{\mathcal{H}'}{\mathcal{H}} - \sqrt{6}\beta\right)\theta_\psi - \mathcal{H}^{-2}\Delta\hat{\Phi} \,, \\ \Delta\hat{\Phi} &= \frac{3}{2}\mathcal{H}^2(Y\Omega_\psi\delta_\psi + \Omega_r\delta_r + \Omega_\phi\delta_\phi) \,, \end{aligned} \tag{3.53}$$

where $Y = 1 + 2\beta^2$. The last equation can be regarded as a *modified* Poisson equation; it shows that, already at the linear level, the fifth force acts on the ψ matter field as a gravitational-like interaction but $2\beta^2$ times more intense than standard gravity. This is a key feature of this model because it affects significantly the over-densities evolution. Notice that this result resembles the Newtonian picture already pointed out in (2.10). In the same fashion we showed for the uncoupled case, the three equations above can be compacted in a single one that describes the evolution of the ψ-matter density contrast:

$$\delta''_\psi + \left(1 + \frac{\mathcal{H}'}{\mathcal{H}} - \frac{\beta\phi'}{M_P}\right)\delta'_\psi - \frac{3}{2}(Y\Omega_\psi\delta_\psi + \Omega_r\delta_r + \Omega_\phi\delta_\phi) = 0. \tag{3.54}$$

Remind that we have set the scalar field to have a light mass, such that the fifth interaction is long range and all the matter inside the Hubble horizon experiences it. This implies that the speed sound of the scalar density approaches to unit and consequently, as pointed out in section 3.2, any ϕ fluid over-density cannot grow inside the horizon. We will therefore neglect it as like as the radiation fluid. The amplitude of both remains at the level inherited from inflation even in our modified gravity model.

The coupling $\beta(\phi)$ is a free parameter of the theory and, once fixed, it specifies completely the model and the mass of the perturbation. For large values, the additional attractive coupling widely overwhelm the contribute of standard gravity and boost the gravitational potential experienced by the matter fluid. Notice that a new

term proportional to δ'_ψ also pops up; it shows that, in dependence of the evolution of ϕ, the fifth-force acts damping or anti-damping the growth of matter density contrast. Even if the ψ fluid were not coupled nor in equilibrium with radiation fluid in the past, its density fluctuations are triggered by the very tiny post-inflationary radiation perturbation δ_r. This density contrast appears indeed as a source term in the modified Poisson equation and transfers the fluctuations via usual gravity. Thus, we can safely regard the initial amplitude for δ_ψ to be of the same order of the post-inflationary radiation inhomogeneities $\delta_r^{in} \simeq 10^{-7}$.

If the system has already reached the scaling solutions (2.33) when the perturbations re-enter the horizon scale, we can employ the set of density parameters (2.33), and the relation (2.34) to rearrange the previous equation as

$$\delta''_\psi - \delta'_\psi - \left(1 + \frac{1}{4\beta^2}\right)\delta_\psi = 0\,, \tag{3.55}$$

where we have substituted $\mathcal{H}' = -\mathcal{H}$ that specifies a radiation background. It is worth to point out that the anti-damping term in this equation enhances the growth of the density contrast, an effect due to the presence of the fifth force. In addition, the last term inside the brackets can be safely approximated to 1, as the coupling is naturally rather large, and in consequence the differential equation develops a β independence and becomes

$$\delta''_\psi - \delta'_\psi - \delta_\psi = 0\,. \tag{3.56}$$

Let us state the ansatz $\delta_\psi \simeq (a/a_{\rm in})^c$ to find an analytical solution; when substituted inside the differential equation it returns back two viable values for c that represent a decaying and a growing perturbation mode. The former becomes rapidly negligible and it is not interesting for our purposes, while the latter yields to

$$\delta_\psi = \delta_{\psi,{\rm in}}\,(a/a_{\rm in})^p\ , \qquad p = (1+\sqrt{5})/2 \approx 1.62\,, \tag{3.57}$$

where $a_{\rm in} \equiv a(t_{\rm in})$ is the scale factor at the onset of the scaling regime, or, if we suppose the system already lays on it, it is the moment perturbations re-enter the horizon. This solution predicts that at some N `the density contrast` δ_ψ `does`

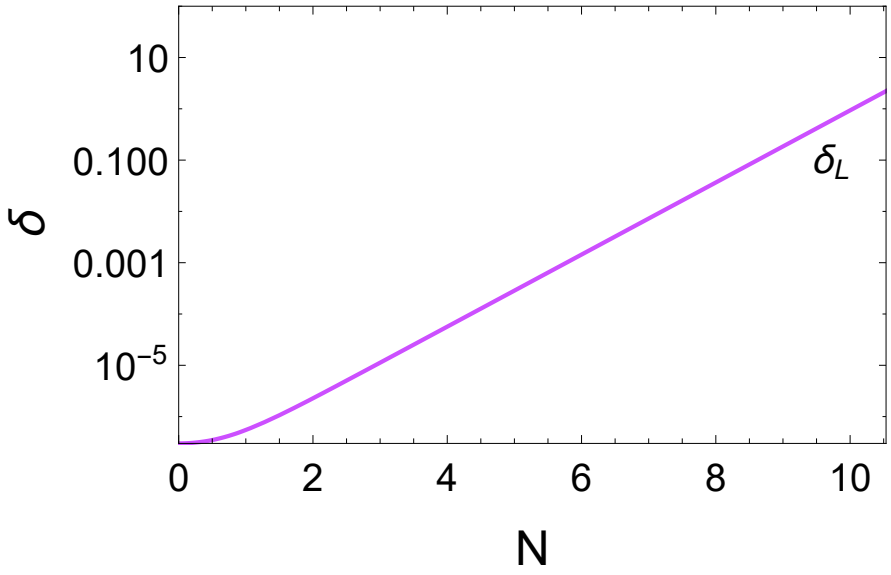

Figure 3.3. Linear growth of matter fluctuations enhanced by fifth-force during the radiation dominated era. This solution is worked out assuming $\beta = 100$, $\delta_{\rm in} = 10^{-6}$ and $\dot{\delta}_{\rm in} = 0$.

`enter in the non-linear regime`, a key difference with respect to non-relativistic matter without the fifth force. This is mainly due to the term $Y\Omega_\psi\delta_\psi$ in equation (3.55), which was negligible in the non-coupled case, while now is of unit order and sources its growth: the larger δ_ψ the more is enhanced.

Let us briefly discuss the case when at the horizon re-entering the cosmological dynamical system has not yet reached the scaling solution, that means Ω_ψ can be larger or smaller than the scaling value $1/(3\beta^2)$. This affects the pre-factor of the δ_ψ term in equation (3.55), leading, respectively, to a faster or a slower growth. Nonetheless, also the pre-factor of the anti-damping term $\dot{\delta}_\psi$ changes depending on the behaviour of ϕ', which is not yet constrained by the scaling behaviour. In particular, an initial Ω_ψ much smaller than $1/(3\beta^2)$ yields a factor $3Y\Omega_\psi/2$ rather lower than unit, with a subsequent small growth of the density contrast until the matter background density reaches the scaling value at t_{in}. Thereafter, the situation previously discussed is restored, and $t_{\rm in}$, can be considered as the effective point in time when perturbations starts to grow, even if they has re-entered at earlier time.

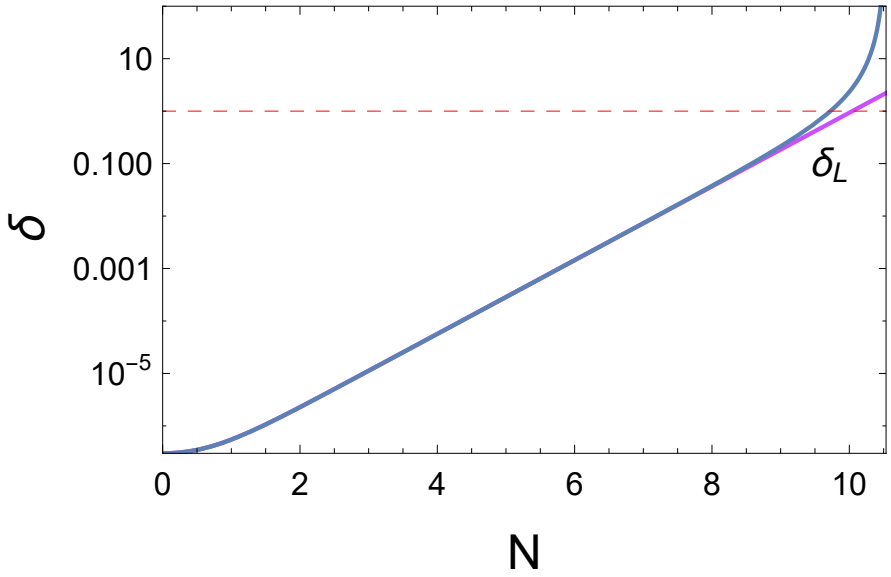

Figure 3.4. Non-linear and linear growth of matter fluctuations enhanced by fifth-force during the radiation dominated era. The dashed line in red indicates the non-linear regime threshold $\delta_\psi \sim 1$. To compute the plot we adopt $\beta = 100$, $\delta_{\rm in} = 3 \odot 10^{-7}$ and $\dot{\delta}_{\rm in} = 0$.

3.5.2 Non-linear treatment

Since the non-linear regime is actually achievable, in order to properly describe it, we shall extend the results of standard perturbation theory. This has been worked out in Ref. [24] for the Newtonian non-relativistic regime in the case of coupled quintessence cosmologies. We can adapt this result to our model such that the set of equations in (3.53), generalised at the full non-linear orders, reads as

$$\delta'_\psi = -\nabla_i(1+\delta_m)v^i_\psi\,, \tag{3.58}$$

$$v^{i\prime}_\psi = -\left(1+\frac{\mathcal{H}'}{\mathcal{H}}-\sqrt{6}\beta\right)v^i_\psi - v^j_\psi\nabla_j v^i_\psi - \mathcal{H}^{-2}\nabla^i\hat{\Phi}\,, \tag{3.59}$$

$$\Delta\hat{\Phi} = \frac{3}{2}\mathcal{H}^2(Y\Omega_\psi\delta_\psi + \Omega_r\delta_r + \Omega_\phi\delta_\phi)\,, \tag{3.60}$$

Again, we can compact them in to a single differential equation that describes the non-linear growth of matter density fluctuations:

$$\delta''_\psi + \left(1 + \frac{\mathcal{H}'}{\mathcal{H}} - \frac{\beta\phi'}{M_p}\right)\delta'_\psi - \frac{3}{2}(Y\delta_\psi\Omega_\psi + \Omega_R\delta_R)(1+\delta_\psi) - \frac{4}{3}\frac{\delta'^2_\psi}{(1+\delta_\psi)} = 0\,, \quad (3.61)$$

where we have already assumed $\delta_\phi \simeq 0$. In comparison with the linear case, the key features brought by presence of the fifth-force remain, but non-linearity shows up in the third and in the last terms of the equation. Following the previous considerations, we engage the scaling regime, neglect the scalar and the matter field fluctuations, to recast the previous equation as

$$\delta''_\psi - \delta'_\psi - \left(1 + \frac{1}{2\beta^2}\right)\delta_\psi(1+\delta_\psi) - \frac{4}{3}\frac{\delta'^2_\psi}{(1+\delta_\psi)} = 0\,, \quad (3.62)$$

The analytical solution in not trivial at all - if any exists - and it is much more efficient to proceed via a numerical approach adopting $\beta = 100$ in accordance with the relation in (3.45). The resulting curve is displayed in Figure 3.4 together with the linear case, which can eventually provide some reference values. The two solution do agree identically up to $N \simeq 9.5$ e-fold while, afterwards, the linear approximation loose its predictive power because non-linear contribution becomes important. The code we worked out found the density contrast δ_ψ to diverge at $N_c = 11.2$ e-fold; we will discuss in the next section about the physical interpretation of this point.

As depicted before, the coupling β specifies the mass of the first perturbation re-entering the horizon, and one could wonder how the evolution scenario depends on it, or rather whether different couplings lead to different evolution pictures. To figure it out, we can select a reference value, say the linear density contrast at N_c, $\delta_c \equiv \delta_L(N_c)$, and examine how it changes varying the value of β. The result of this analysis are displayed in Figure 3.5, and the outcoming picture reveals that from $\beta \sim 30$ upwards `the various growth scenarios are truly independent from the strength of the coupling`. The reader should not be surprises by this statement, indeed β appears in equation (3.62) only in the term $1 + 1/2\beta^2$, whose deviation from unit can be approximately discarded from $\beta \sim 10$ upwards as well. Therefore, the numerical solution recovered so far fixing $\beta = 600$, is valid equally for all this wide spectrum of couplings, or say for all the mass we want to investigate.

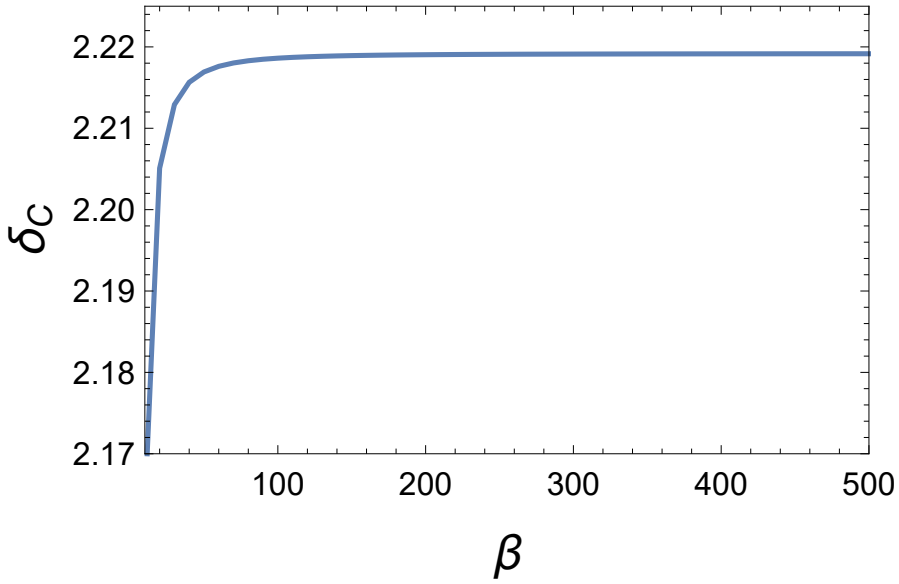

Figure 3.5. Comparison of the δ_c values as the coupling β of the theory varies but keeping the same initial conditions. The physical picture appears to be mildly dependent from it.

As a consequence, if we focus on other mass range rather than the solar mass and we adopt the same initial conditions, the solution of the perturbations equation wouldn't practically differ from the one depicted in Figure 3.4.

3.5.3 Spherical top-hat collapse

To understand what physically takes place when the density contrast raises to infinitely large values, we need to model somehow the density fluctuations averaged on a certain region [25]. To this end, consider a spherical region having radius R and imagine its density contrast to be described by its mean value $\hat{\delta}_\psi(t)$ in each point therein, that is by a *top-hat* function

$$\delta_\psi(t, \mathbf{x}) = \hat{\delta}_\psi(t)\Theta(R - x)\,. \tag{3.63}$$

Here $\mathbf{x}$ are the three-dimensional physical coordinates with the origin at the center of the shell and Θ is the Heaviside step function. If not further specified, we will always use hereafter $\delta_\psi(t)$ as the hat value $\hat{\delta}_\psi(t)$ to intend the average value of fluctuations inside a certain region. This model was proposed by Gunn and Gott in

1972 in Ref. [26] and probably is the most simple and intuitive approach to study *gravitational collapse* of over-dense regions. It assumes the existence of a spherically symmetric region, embedded in an Einstein-de Sitter background universe, with a density distribution higher than the mean density of the background. The Birkhoff's theorem of general relativity states that the evolution of such a region is affected only by the matter it contains, therefore the over-dense region will be independent of the surrounding background matter and can be regarded as a separate sub-universe with its own evolution.

The spatial mean value $\delta_\psi(a)$ evolves in time according to the non-linear equation (3.62) and, in particular, to its time dependence concur both the numerator and denominator of the ratio

$$\delta_\psi(a) = \frac{\rho_\psi(a) - \bar{\rho}_\psi(a)}{\bar{\rho}_\psi(a)} = \frac{\rho_\psi(a)}{\bar{\rho}_\psi(a)} - 1\,, \tag{3.64}$$

where the bar specified the background fluid quantities. The function $\bar{\rho}_\psi(a)$ represents the background density of the matter fluid and, as shown in section 2.2.3, when the system lays on the scaling solution it scales as radiation. Because of the universe expansion this value decreases with time, the background fluid dilutes, and one aspects the same effect to apply also to its over-densities. In spite of that, these are lead to increase enhanced by the fifth-force intense attraction among the ψ-particles which tends to bound them, counteracting the effect of the fast expansion. Accordingly, if the intense gravity-like force overwhelms the universe expansion effect, the matter shall collapse.

The reader may notice that not only the over-dense region associated to the first scale re-entering the horizon is on the way to collapse, but the same holds true for all the scales re-entering at later times. Moreover, as the time goes by, the over-densities spread over the spacetime could enter in mutual causal connection and merge together in increasingly bigger over-dense regions, potentially as large as the size of the horizon at that time. This picture drops when the screening condition is met and the fifth force effects fades off; from that moment the growth of re-entering scales is inhibited, and the already existing merged over-densities can eventually get stabilised via usual gravity. This is a very tough physical process to model. For this reason, it is necessary to adopt a simplified picture and distinguish between the

possible extremal outcoming scenarios.

Foremost, we decide to follow only the evolution of the particles within the first spherical shell re-entering the horizon and to disregard the interaction with its similes spread in the surrounding spacetime; we shall refer it as **scenario** $\mathcal{A}$.

The system of ψ-particles contained in a certain spherical region is not closed because of their interaction with the background scalar field, therefore the masses of particles change over time. In fact, the energy density of the matter fluid can be thought as the sum of contributions from n_ψ particles mass m_ψ, that is

$$\rho_\psi = \bar{n}_\psi m_\psi \,, \tag{3.65}$$

where the bar specifies the background value. In an expanding universe the background particle density scale as $\bar{n}_\psi \propto a^{-3}$, that means, in accordance with the scaling solution, the single particle mass scales as

$$m_\psi \propto a^{-1} \,. \tag{3.66}$$

We shall trace the spherical shell that encloses the same amount of particles contained by the initial horizon. A generic shell of radius R contains a number of particles $N = n_\psi R^3$, where n_ψ is the particle density within it. Prescribing the conservation of the total number of particles inside the shell we infer the evolution of its radius, indeed

$$\begin{aligned} n_\psi R^3 &= n_{\psi,\mathrm{in}} R_{\mathrm{in}}^3 \qquad (3.67) \\ \bar{n}_\psi (1+\delta_\psi) R^3 &= \bar{n}_{\psi,\mathrm{in}} (1+\delta_{\psi,\mathrm{in}}) R_{\mathrm{in}}^3 \\ \bar{n}_{\psi,\mathrm{in}} \left(\frac{a_{\mathrm{in}}}{a}\right)^3 (1+\delta_\psi) R^3 &= \bar{n}_{\psi,\mathrm{in}} (1+\delta_{\psi,\mathrm{in}}) R_{\mathrm{in}}^3 \,, \end{aligned}$$

where $R_{\mathrm{in}} = H_{\mathrm{in}}^{-1}$. The last equation describe the evolution of $R(a)$ and can be recast in a more compact form as

$$1 + \delta_\psi = (1 + \delta_{\psi,\mathrm{in}}) \left(\frac{a}{a_{\mathrm{in}}}\right)^3 \left(\frac{R_{\mathrm{in}}}{R}\right)^3 \,, \tag{3.68}$$

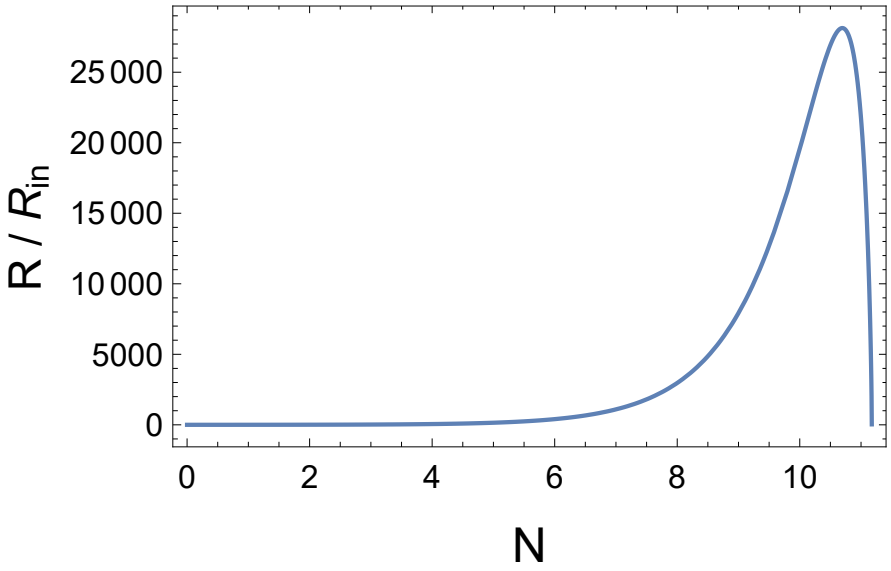

Figure 3.6. The curve describes the evolution of lumps growth factor as a funtion of the e-folding parameter N.

or, equivalently,

$$R(N) = R_{\rm in}\left(\frac{1+\delta_{\psi,\rm in}}{1+\delta_{\psi}}\right)^{1/3} e^{N}\,, \tag{3.69}$$

where we have used the definition of e-fold number $N = \ln(a/a_{\rm in})$. The evolution of the growth factor $r(N) \equiv R(N)/R_{\rm in}$ can be computed numerically thanks to the non-linear solution $\delta_{\psi}(N)$ we have previously obtained; the results are displayed in Figure 3.6. At initial times, when the effect of expansion of the universe stems the additional gravitational attraction between ψ-particles, the radius of the shell remains close to its starting value. Once the non-linear contribution becomes important, it quickly raises up to a maximum value that identifies the so-called *turn-around* point. In this stage the kinetic energy of the particles, which are dragged by the background universe expansion, overcomes the fifth interaction and maximise the size of the over-dense region, till the equilibrium between the two contributes is restored at the turn around. Here the function $r'(N)$ cross the zero and switches it sign: the shell begins to shrink. Then, the radius has a rapid fall towards a singular point when the density contrast solution diverges at N_c.

3.5.4 Virialization stage

On general grounds, velocity perturbations are expected to modify the above picture, leading in some cases to *virialized* objects and preventing the singularity. For this to happen, the fifth-force must vanish at some point, otherwise the very intense attraction would not allow a a stable state. On the other hand, before getting screened, the over-dense region must, at least, pass the turn around point, when the huge velocity of matter recontraction and the non-linear regime could allow the collapse also via standard gravity. Perhaps, this seems a very natural requirement since we expect the screening mechanism to be triggered when very large density fluctuations are met. Hereafter we will assume it to happen precisely at the virialization stage, when the perturbations reach the highest density. Let us just point out that a earlier screening would lead to a bigger, therefore less dense, structures because standard gravity would not shrink them as in the fifth force case. It will be clear within the next chapter that to the aim of our discussion this would strengthened our results.

Already in the early papers using the spherical top-hat by Press & Schechter [27], it was outlined that minimal deviations from sphericity, scarcely mattering during expansion, become determinant during recontraction, so leading the system to virialization. The particles inside the shell acquire a non zero component in the velocity field that deviates from the purely radial assumption and confers to the object the needed kinetic energy to counteract the collapse and stabilise. The standard works using top-hat gravitational collapse, namely via standard gravity, engage the conservation of energy in the matter particles system to predict a virialization radius that is half the one at turn around point. Clearly this cannot be applied to our case because, as we pointed out in Section 2.2.3, during the scaling regime there is a continuous leakage of energy between the ψ and ϕ fluids. Alternatively, this is also supported by the non conservation of the individual energy-momentum tensors in equation (2.7). That means, to get the viralization condition, we have to rely on the most general expression of the *virial theorem* for a dynamical set of particles, which

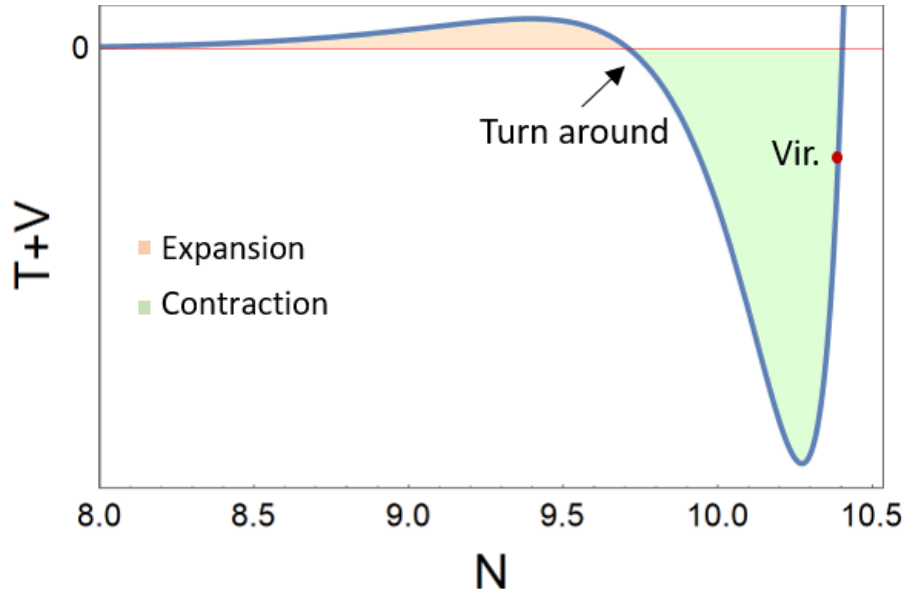

Figure 3.7. Total energy of the system of ψ-particle enclosed in the spherical shell.

states that the virial[3] equilibrium is reached once

$$2K + U = 0\,, \tag{3.70}$$

where K and U are respectively the time averaged kinetic and the potential energy describing the ψ-particles system enclosed in the spherical over-dense region. The potential energy U experienced by the collapsing shell can be regarded as made of different contributions. First, the potential sourced by the over dense spherical region, which can be split in a part provided by background density, that couples only via gravity, and another part provided by the over-density, that couples also via fifth-force. Second, the potential sourced by the other backgrounds fluid contained in the shell. The backgrounds gravitational potentials are computed according to standard Poisson equation, while the term coming from the over-density is described

[3]**Pill:** the word *virial* derives from "vis", the Latin word for "force" or "energy", therefore with "virial equilibrium" is intended the statistical equilibrium among the forces acting on the system of particles.

by its modified version in equation (3.53). This translates into

$$\frac{U(R)}{M} = -\frac{3}{5}G\frac{[\bar{M}+Y\delta M]}{R} - \frac{4\pi}{5}G(\rho_r+\rho_\phi) \tag{3.71}$$

$$= -\frac{3}{5}YG\frac{\delta M}{R} - \frac{4\pi}{5}G\rho_{cr}R^2 \tag{3.72}$$

where $\rho_{cr} = 3H^2/8\pi G$ with $H^2 = e^{-4N}/4$ for a radiation dominated universe, while M_b and δM are, respectively, the contributions to the mass of the shell given by the background of the density field and its deviation. In particular,

$$\delta M = M - \bar{M} = \frac{4\pi}{3}\rho_{cr}\Omega_\psi\delta_\psi R^3\,. \tag{3.73}$$

Joining this expression with the one for the average kinetic energy of the system

$$K = \frac{3}{10}M\,(\dot{R})^2 = \frac{3}{10}M\,e^{-4N}(R')^2\,, \tag{3.74}$$

we arrive at the virialization condition for the radius of the collapsed structures

$$2\,(R')_V^2 - [\Omega_\psi\delta_\psi(N)+1]\,R_V^2 = 0. \tag{3.75}$$

The numerical solution to this differential equation yields the e-fold number N_V associeted to the viralization stange and the corresponding value of the growth factor, namely

$$R_V = 2.1\cdot 10^4 R_{in}\,, \quad \text{with} \quad N_V = 11.07\,. \tag{3.76}$$

Notice that whatever be the initial radius, in a radiation dominated era the horizon grown as $\sim e^{2N}$, thus it is more than 10^9 times bigger than the horizon at the initial time, that means the over-dense region is always in the sub-horizon regime during the collapse stage.

The size of the horizon at formation time has been already estimated in section 3.4. It represents the moment when the formation process ends up in stable structures, namely the instant when these virialize. In order to complete the analysis, we need only to compute the initial radius of the over-dense regions, that is the value of the horizon at re-enter of perturbations $R_{\rm in} \equiv H_{\rm in}^{-1}$. The latter is obtained re-scaling

the mass and the horizon in equation (3.46) by N_V e-fold in the past. In agreement with equations (3.40) and (3.41), the re-scaling laws are

$$M_F = e^{2N_V} M_{\rm in}\,, \quad H_F^{-1} = e^{2N_V} H_{\rm in}^{-1}\,. \tag{3.77}$$

Thus, the resulting initial radius of the shell as a function of the mass therein is

$$R_{\rm in} \equiv H_{\rm in}^{-1} = 2.77 \cdot 10^7 \cdot e^{-2N_V/3} \left(\frac{M_{\rm in}}{M_\odot}\right)^{2/3} {\rm km} \tag{3.78}$$

According to (3.76), the viralization radius immediately follows

$$R_V = 5.9 \cdot 10^{11} e^{-2N_V/3} \left(\frac{M_{\rm in}}{M_\odot}\right)^{2/3} {\rm km}\,. \tag{3.79}$$

The re-scaling of the horizon mass modifies also the equation (3.45) which relates the coupling and the mass of the structures as

$$\beta_c \simeq 36 \left(\frac{M_{\rm in}}{M_\odot}\right)^{-1/6}\,. \tag{3.80}$$

Now, we need to work out one step more, let us explain why. As pointed out in equation (3.66), a certain amount of mass made out of ψ-particles decreases over time. This means that the mass $M_{\rm in}$ within the initial horizon is partially decayed up to the time of viralization time into $M_V = M_{\rm in} e^{-N_V}$. Therefore, the true mass-radius relation that characterises these lumps of matter is

$$R_{\mathcal{A}} \equiv R_V = 5.9 \cdot 10^{11} \left(\frac{M}{M_\odot}\right)^{2/3} {\rm km}\,, \tag{3.81}$$

where we got rid of the subscript and used M_V as M. Moreover, with respect to the virialized mass the critical value of the coupling reads as

$$\beta_c \simeq 7.5 \left(\frac{M_V}{M_\odot}\right)^{-1/6}\,. \tag{3.82}$$

In order to pass nucleosynthesis constraints discussed in section 3.4 on $\Omega_\phi + \Omega_\psi$, we shall require $\beta > 3$. In view of the previous relation, `the mass of the lumps`

must be $M_V < 60 M_\odot$. Note: this result does not constraints the model to provide only objects within this mass range since it depends on the initial density seed, thus it is valid only around the solar mass scales.

So far, we have presented the most simplified picture - to whom we have referred as **scenario** $\mathcal{A}$ - for the collapse process that represents the extreme limit when over-dense spherical regions spread the spacetime do not interact or merge during the matter lumps formation stage.

As already outlined, this is not what realistically happen; the over-dense regions to get apart for the expansion of the universe, but the causality horizon around them grow faster and eventually enclose ψ-particles belonging to other shell spread in the spacetime. Those starts to attract each other and merge in more massive ones having the size of the horizon at that time. When this process stops is not clear and depends also on the action of the screening mechanism, but another extreme limit would be to consider the matter halos resulting from merging sized and massive as the horizon at virialization; we shall refer it as **scenario** $\mathcal{B}$. Hence, in this last case the mass-radius relation of lumps would just be the one in equation (3.46), that is

$$R_{\mathcal{B}} = 2.7 \cdot 10^7 \left(\frac{M}{M_\odot} \right)^{2/3} \text{km} \,. \tag{3.83}$$

The attentive reader may wonder whether these structures virialize, as within the scenario $\mathcal{A}$, at the formation time. This is indeed the case because the viralization equation (3.75) does not depend on any mass, but just on the average over-density, and whatever region we consider collapsing, it will virializes at formation time.

Final remarks. The formation of PDMHs does not alter the standard cosmological evolution on large scales. In fact, those re-entering the horizon after halos formation remain freeze to the level of inhomogeneities inherited by the inflationary era since the action of the fifth-force is inhibited by the screening mechanism. Of course, even if on small scales dark matter is in the form of primordial dark matter halos, the mean value of over-densities on bigger scale remains unchanged and the growth of dark matter in this domain keeps being ruled by the Meszaros effect. Only the small picture is altered, not the big one: zooming out, our screened objects can be just regarded and behaves as particles of the cold dark matter fluid that drives the

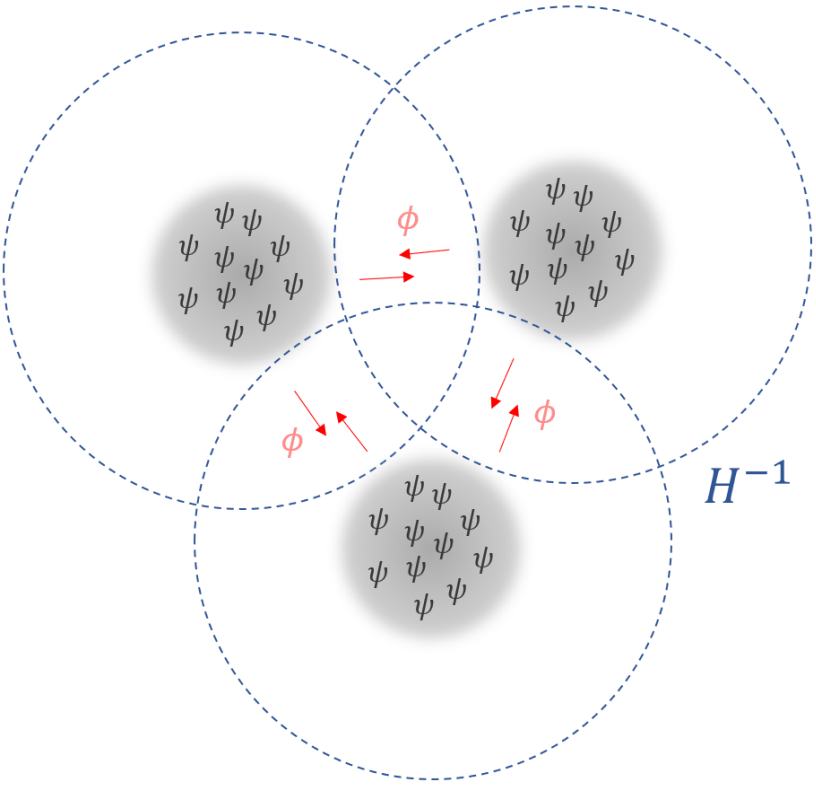

Figure 3.8. Realistic picture of the formation process. The dark matter lumps mutually interact and merge while they collapse.

formation of baryonic non-linear structures.

Chapter 4

Constraints analysis

The primordial fifth-force mechanism we have employed in this work provides the formation of dark matter lumps which might account for the missing matter of the universe, if not ruled out by experimental constraints. The question on whether this structures can be or not black holes naturally arises. To this concern, we evaluate the mass range where the viralization radius of the lumps turns to be smaller than the Schwarzshild radius. For the scenario $\mathcal{A}$, the condition

$$R_{\mathcal{A}} < 2GM = 2GM_{\odot}\frac{M}{M_{\odot}} \simeq 3\frac{M}{M_{\odot}}\mathrm{km}\,. \tag{4.1}$$

implies black holes are realised in the mass range

$$M > 10^{33}\, M_{\odot}\,, \tag{4.2}$$

that is only for very massive initial scale at the horizon re-enter after inflation. As aforementioned, the outstanding LIGO/VIRGO detection of gravitational waves [28] has renewed the interest to investigate possible sources belonging to the solar mass window; to explore this mass range has therefore a great appeal. The previous relation suggests clearly that `the dark lumps are not primordial black holes` within this range, but rather larger and less dense screened compact objects of non-interacting matter. Regarding the scenario $\mathcal{B}$, the numerical term above lowers by $\sim 10^{10}$ orders but black holes production seems unlikely as well. As a consequence, we cannot compare directly our results to the experimental constraints

on the abundance of primordial black holes in the universe, and a careful analysis must be worked out in order to adapt them. Since the lumps results to see much less compact and dense than PBHs in any case, we shall name them hereafter as `Primordial Dark Matter Halos` (PDMH).

In this chapter we carry out this analysis in order to figure out whether the prospective of providing the dark matter in the universe within our model is viable or not for solar mass halos. We will discuss it for both scenarios $\mathcal{A}, \mathcal{B}$ outlined in previous section.

4.1 PBHs: State of the Art

The idea that highly over-dense regions in the primordial universe can undergo gravitational collapse to form black holes dates back to Hawking proposal in 1971 [29], which was strongly influenced by former works of Zel'dovich & Novikov (1967). This field of study is very active nowadays because the presence of these screened objects around the universe could solve the problem of the missing (dark) matter in the observations.

Formation threshold

In Carr's early papers on PBHs [30] was pointed out that in order to realise such objects in a primordial era, the post-inflationary density contrast must exceed the threshold $\delta_c = 1/3$. Since then, this argument has been very widely debated in the literature, but further analytical and numerical analysis confirmed and improved the former prediction. This threshold is very large if compared to post-inflationary power spectrum inhomogeneities, and the possibility to provide all dark matter within the tail of the probability curve having these level of fluctuations is very low. Thus, the proposals on the table of PBHs models often rely on particular features of the power spectrum, such a sudden rise and peaks at suitable scales - see Figure 4.1. With this regard, our formation framework is very unique and naive since it does not stray from the nearly scale assumption and from CMB observations to provide compact dark structures. Here below, we take a digression from the main discussion and show how this formation threshold level crops up. Following Ref.

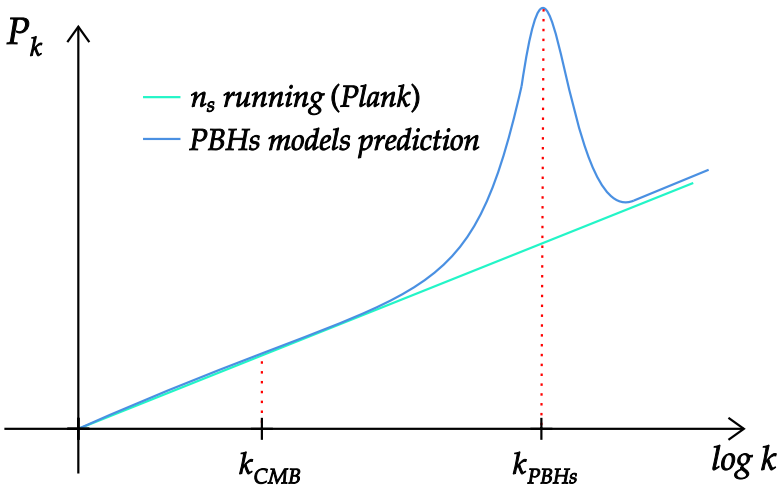

Figure 4.1. Comparison between the post-inflationary primordial power spectrum predicted by PBHs models and the nearly scale invariance assumption.

[31], we consider a locally spherical symmetric perturbed region embedded in the flat FLRW universe, whose metric is given by the usual

$$\mathrm{d}s^2 = -\mathrm{d}\tau^2 + R^2(\tau)\left[\frac{\mathrm{d}r^2}{1-kr^2} + r^2\left(\mathrm{d}\theta^2 + sin^2\theta\mathrm{d}\phi^2\right)\right], \tag{4.3}$$

where τ is the standard time parameter, $R^2(\tau)$ is the scale factor of the sub-universe region, or equivalently the radius. The second Friedmann equation describes the evolution of the latter, and reads as

$$H^2(\tau) \equiv \left(\frac{\dot{R}(\tau)}{R(\tau)}\right)^2 = \frac{8\pi G}{3}\rho(\tau) - \frac{k}{R^2(\tau)}, \tag{4.4}$$

the dot specifying the derivative with respect to τ - only in this section. If one selects a coordinate system where the initial rate of expansion is the same for both the perturbed and the background universe, the density contrast at the initial times t_{in},τ_{in} can be express as

$$\delta_{\mathrm{in}} = \frac{\rho_{\mathrm{in}} - \bar{\rho}_{\mathrm{in}}}{\bar{\rho}_{\mathrm{in}}} = \frac{k}{\bar{H}_{\mathrm{in}}^2 R_{\mathrm{in}}^2}, \quad \text{with} \quad \bar{H}_{\mathrm{in}} \equiv \bar{H}(t_{\mathrm{in}}) = H(\tau_{\mathrm{in}}) \equiv H_{\mathrm{in}}, \tag{4.5}$$

with the bar quantities being related to the background. The over-dense perturbed region will reach it is maximum radius R_c at a time τ_* when $\dot{R}(\tau_*) = 0$ or, equivalently,

$$H^2(\tau_*) = \frac{8\pi G}{3}\rho(\tau_*) - \frac{k}{R^2(\tau_*)} \tag{4.6}$$

$$= \frac{8\pi G}{3}\bar{\rho}_{\rm in}(1+\delta_{\rm in})\left(\frac{R_{\rm in}}{R_c}\right)^4 - \frac{k}{R_c^2} \tag{4.7}$$

$$= \bar{H}^2_{\rm in}(1+\delta_{\rm in})\left(\frac{R_{\rm in}}{R_c}\right)^4 - \frac{R^2_{\rm in}\bar{H}^2_{\rm in}}{R_c^2}\delta_{\rm in} = 0\,. \tag{4.8}$$

The last equality implies:

$$R_c = \sqrt{\frac{1+\delta_{\rm in}}{\delta_{\rm in}}}R_{\rm in} \simeq \delta_{\rm in}^{-1/2}R_{\rm in}\,, \tag{4.9}$$

and since in the background radiation dominated universe $t \sim a^2$, then

$$t_c \simeq \frac{t_{\rm in}}{\delta_{\rm in}} \tag{4.10}$$

If we want to allow the growth of density contrast δ rather than its damping, we must require this region to be larger than the Jeans scale (3.22), that is

$$R_J \simeq c_s t_c < R_c, \quad \text{or} \quad c_s < \frac{R_{\rm in}}{t_{\rm in}}\,\delta_{\rm in}^{1/2}\,. \tag{4.11}$$

Finally, taking into account the radiation sound velocity, we recover the threshold level mentioned above:

$$\frac{1}{3} < \delta(t_{\rm in}). \tag{4.12}$$

Its worth to emphasise that the latter is a necessary but not a sufficient condition for the over-dense regions to collapse in PHBs.

Constraints on abundance

In the last almost 50 years there has been an intense effort by the scientific community to constrain or prove the presence of black holes having a primordial origin,

and many physical process has been investigated to understand the consequence of several scenarios. Over the last 50 years, thanks to achievements of many different types of cosmological and astrophysical observations , stringent upper limit on the PBH abundance has been obtained for a vast PBH mass range [32]. Indeed, depending on the mass, PBHs trigger different observational signals and several mass window can be constrained. Due to *Hawking radiation* PBHs lighter than $\simeq 10^{15}$ g do not exist nowadays because they would have been already evaporated by the age of the universe. Nonetheless, the viability of the mass range above this level has been strongly explored and only a tiny window around and below $10^{-11}\, M_\odot$ seems to be a viable way to provide the dark matter content of the universe [33]. On the other hand, the solar mass window, even if pretty closed to viability, has gained a renewed interest since PBHs could account for the gravitational wave signals observed by LIGO. The up to date constraints on $f_{\rm PBH} = \Omega_{\rm PBH}/\Omega_{\rm DM}$ in this region are shown in Figure 4.2 - note that these are valid assuming PBHs mass function to be monochromatic. This picture displays the physical processes giving rise to constraints for PHBs with a mass from 10^{-5} up to 10^3 solar masses, which are listed here below.

- ◇ Detection in the CMB of PBHs accretion effects.
- ◇ Observation of stars microlensing by EROS/MACHO collaboration.
- ◇ Change in galaxy lensing magnification due to caustic crossing.

Further constraints have been proposed and can be found in the literature on the topic [35, 36], but these are rather controversial and usually disregarded; here, we shall adopt the same choice. The last two classes of constraints, which both rely on *gravitational lensing* effects, will be focused throughout the rest of this chapter. Before that, let us briefly describe how accretion effects can set an upper limit on the PBHs abundance.

The very intense black holes gravity induces the infall of the surrounding Baryonic gas during primordial era. In this stage the gas is compressed, its density and temperature increase, and it can be fully ionized either by the internal collisions of gas particles or by the outgoing radiation. The closer the gas to the horizon,

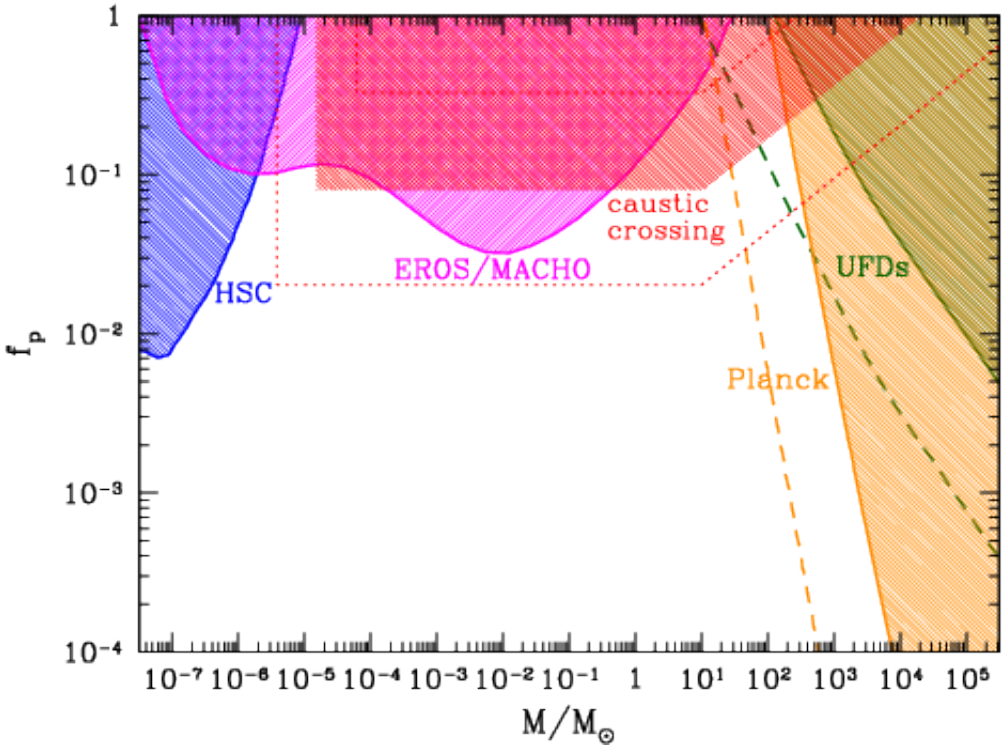

Figure 4.2. Constraints on the mass abundance of primordial black holes f_p. Shaded regions show excluded regions from caustic crossing - with different parametrization, EROS/MACHO microlensing, ultra-faint dwarf galaxies, and Planck cosmic microwave background observations. For UFDs and Planck, conservative limits are shown by solid lines, whereas more stringent limits are shown by dashed lines. Picture from Ref. [34]

the more remarkable become these feature, such that near the black hole horizon, the gas temperature is enormous and the ionized gas results in an intense radiation emanates outward, characterised by a certain luminosity parameter. This radiation, in turn, interacts with the radiative gas filling the Universe and modifies the spectrum of the CMB photons from the Planckian distribution, the decoupling time of the CMB photons, and the ionization history. Thus PBHs might leave a signature in the CMB observables. Its non-detection is translated into the upper limit on the PBHs abundance. However, the models of the accretion process is nowadays not completely understood due to it is complexity and relies, in some cases, on observationally established empirical rules - as the one for luminosity. Indeed, the constraints depicted in Figure 4.2 can be stronger or weaker in dependence of several

assumptions.

In both scenarios $\mathcal{A}$ and $\mathcal{B}$, our dark halos have a monochromatic mass function. However, within the solar mass range, these are not PBHs and cannot be ruled out by these constraints directly. The CMB constrains just depicted above can be indeed easily escaped by our structures in both scenarios. In fact, the luminosity of primordial black holes is mostly due to the Bremsstrahlung radiation emitted in the vicinity of the Schwarzschild radius, since it is there where the accreated gas acquires relativistic velocities. As far as our dark halos are significantly larger than their Schwarzschild radius and do not provide such an intense gravitational coupling, we can foresee that the CMB constraints on them are doomed to disappear. That statement can be rigorously evinced adapting to our radius the guideline in Ref. [37]. Anyway, this affect only a part of the outlined mass window, namely $10^1 M_\odot < M < 10^4 M_\odot$, and for sake of brevity we will not go through deeper details. Perhaps, the constraints comparison of the authors has focused on the analysis of *lensing* constraints.

4.2 Gravitational lensing

In this section we stray a little from the discussion on constraints to briefly introduce the theory of gravitational lensing, remanding for further details to Ref. [38, 39, 40]. The effect of light rays bending due to a source of gravitational field is predicted by general relativity and can be studied in the framework of scalar perturbation theory.

Consider a congruence of null geodesics on the spacetime manifold that models light rays travelling in the universe according to geometrical optics in general relativity. To track their path and features we can choose among them a *fiducial ray* and parameterise it with an affine parameter - see Fig. 4.3. In curved spacetime the path followed by the light rays from a source to an observer is specified by the extension of *Fermat's principle* in curved spacetimes.

Fermat's principle: "Be given a space-time manifold, with S the event of the light source and l the time-like world line of the observer, then a null curve γ from S to l is a light ray if, and only if, it minimises the arrival time parameter by whom

is described."

It is worth to stress that it does not refer to the time light rays need to travel between the two extremes, since a proper time cannot be defined and has no meaning, but rather it states a stationary property of the time of arrival measured by the observer.

If $u_{\rm obs}$ is the velocity of a free falling observer, we can choose to normalize the tangent vector $\tilde{k}$ to the fiducial ray such that $\langle \tilde{k}, u_{\rm obs} \rangle = 1$. The wave vector k is also a tangent vector to the fiducial ray, and its projection on the observer four velocity yields the *observed* frequency of the wave $\omega_{\rm obs}$. Therefore, the normalization condition of $\tilde{k}$ implies $\tilde{k} = k/\omega_{\rm obs}$.

We imagine this bundle of light rays to be connected by a curve $\gamma(\sigma)$ with tangent vector $\partial_\sigma \gamma = v$, which encodes the deviations among the rays as the affine parameter varies. According to the equation of geodesic deviation

$$\nabla^2_{\tilde{k}} v = R(\tilde{k}, v)\tilde{k}\,. \tag{4.13}$$

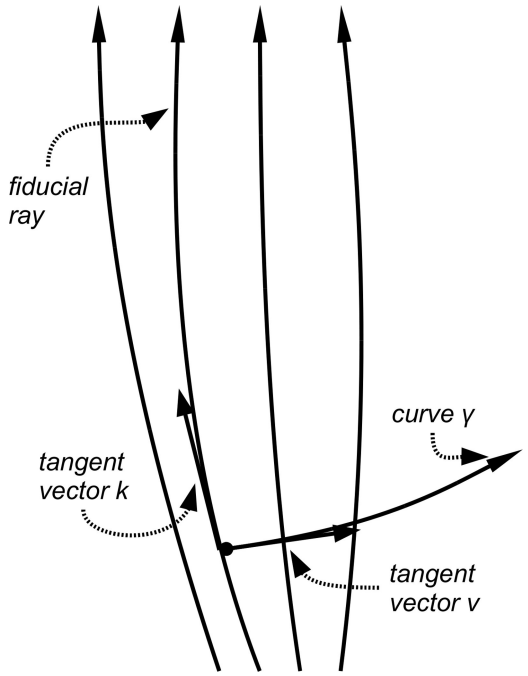

Figure 4.3. Bundle of light rays travelling trough the spacetime manifold.

To elaborate further this relation we need to specify a system of coordinates. To this end, we select a screen in the 3-space of the observer spanned by the vectors $E_{1,2}$ and perpendicular to the tangent vector $\tilde{k}$. The basis vectors can be parallel-transported along the fiducial ray and serve, together with $\tilde{k}$, as system of spatial coordinates along the congruence. Accordingly, the geodesic equation can be recast

$$\nabla^2_{\tilde{k}} \begin{pmatrix} v^1 \\ v^2 \end{pmatrix} = \mathcal{T} \begin{pmatrix} v^1 \\ v^2 \end{pmatrix} , \tag{4.14}$$

where we have decomposed v in the new basis $E_{1,2}$ and $\mathcal{T}$ is the *optical matrix*

$$\mathcal{T} = \begin{pmatrix} \mathcal{R} + \Re(\mathcal{F}) & \Im(\mathcal{F}) \\ \Im(\mathcal{F}) & \mathcal{R} - \Re(\mathcal{F}) \end{pmatrix} \tag{4.15}$$

with the components

$$\begin{aligned} \mathcal{R} &= -\frac{1}{2} R_{\alpha\beta} \tilde{k}^\alpha \tilde{k}^\beta + \frac{1}{2} C_{\alpha\beta\gamma\delta} \epsilon^\alpha \tilde{k}^\beta \tilde{k}^\gamma \epsilon^{*\delta} , \\ \mathcal{F} &= \frac{1}{2} C_{\alpha\beta\gamma\delta} \epsilon^\alpha \tilde{k}^\beta \tilde{k}^\gamma \epsilon^\delta . \end{aligned} \tag{4.16}$$

Here we made use of the complex vector $\epsilon = E_1 + \mathrm{i}E_2$ and of the Weyl curvature, that is the Riemann tensor deprived of all its possible contractions. In case of small peculiar velocities inhomogeneities in the universe, and considering the weak field limit, we can assume that is always possible to split the tidal matrix in two contributes

$$\mathcal{T} = \mathcal{T}_{\mathrm{bg}} + \mathcal{T}_{\mathrm{cl}} , \tag{4.17}$$

The first specifies a background contribution and the second encodes the presence of its local inhomogeneities.

The background is a homogeneous and isotropic spacetime equipped with a flat Friedmann-Lemaître-Robertson-Walker metric, that is

$$\mathrm{d}s^2 = a^2(\eta) \left[-\mathrm{d}\eta^2 + \mathrm{d}w^2 + \mathrm{d}\Omega^2 \right] , \tag{4.18}$$

where η is the conformal time related to cosmic time t by $a\mathrm{d}\eta = c\mathrm{d}t$, and w is the co-moving radial distance, alternatively called the *line of sight*. Closed and

opened universes are considered is in [38, 39]. For a homogeneous metric, the Weyl contribute vanishes, the tidal matrix become purely diagonal, and by means of Einstein equations we gather

$$R_{\alpha\beta}\tilde{k}^{\alpha}\tilde{k}^{\beta} = G_{\alpha\beta}\tilde{k}^{\alpha}\tilde{k}^{\beta} = \frac{8\pi G}{c^4}T_{\alpha\beta}\tilde{k}^{\alpha}\tilde{k}^{\beta} \ . \tag{4.19}$$

These relation turn to be very useful because in equation (4.16) , thanks to the index exchange symmetry of Ricci tensor, we can substitute $R_{\alpha\beta}\tilde{k}^{\alpha}\tilde{k}^{\beta} = G_{\alpha\beta}\tilde{k}^{\alpha}\tilde{k}^{\beta}$. Since the projection of k on u is the frequency of the light as measured by an observer co-moving with the fluid, from the normalization of $\tilde{k}$ it follows

$$|\langle\tilde{k}, u\rangle| = \frac{|\langle k, u\rangle|}{\omega_{\rm obs}} = \frac{\omega}{\omega_{\rm obs}} = 1 + z \, . \tag{4.20}$$

Accordingly, the optical tidal matrix for the background contribution becomes

$$\mathcal{R} = -\frac{4\pi G}{c^2}\rho_0(1+z)^5 \, , \quad \text{with} \quad \mathcal{T}_{\rm bg} = -\mathcal{R}\mathbb{I}_2 \, , \tag{4.21}$$

where we have assumed the universe to be filled with a pressureless fluid. This allow us to recast equation (4.14) for the homogeneous background and, after some straightforward manipulations and making use of Friedmann equation [38] , it read as

$$\frac{\mathrm{d}^2}{\mathrm{d}w^2}\frac{v^i}{a} = 0 \ , \tag{4.22}$$

where we have parameterised the curves by means of the co-moving radial distance w of FLRW metric.

Now, we have to infer the contribution due to inhomogeneities and combine it with the result just obtained. It can be modelled by means of scalar perturbations theory, adopting the weak field limit, and using the perturbed FLRW metric we have derived in Chapter 3, that is

$$\mathrm{d}s^2 = a^2(\eta)\left[-(1+2\phi)\mathrm{d}\eta^2 + (1-2\phi)\left(\mathrm{d}w^2 + \mathrm{d}\Omega^2\right)\right] \tag{4.23}$$

Since the components of the metric are fixed, we can work out Riemann, Weyl, Ricci tensors and Ricci scalar. In addition, the Einstein tensor turns to be

$$G_{\alpha\beta} = \vec{\nabla}^2\phi \, \delta^0_\alpha\delta^0_\beta \ , \tag{4.24}$$

where $\vec{\nabla}^2$ is the spatial Laplace operator. In analogy to the background case, substituting the above relations, we can write down the clump contribution to the tidal matrix, that is

$$\mathcal{T}_{\rm cl} = -2 \begin{pmatrix} \phi_{,11} & \phi_{,12} \\ \phi_{,12} & \phi_{,22} \end{pmatrix} , \tag{4.25}$$

the derivatives being taken with respect to the co-moving spatial coordinates x_i of the perturbed FLRW metric in (4.23), defined as $\mathrm{d}x_i = (1-\phi)\mathrm{d}\omega_i$. Notice that the components of v are related to the latter simply as $v_i = a_i x_i$ with i = 1,2, namely these are their correspondents in the physical coordinate frame. The fiducial ray experiences a gravitational potential $\phi^{(0)}$ due to the FLRW background; a deviation $\delta\phi = \left(\phi - \phi^{(0)}\right)$ from the background value encodes the potential due to due to the inhomogeneities. Expanding the relation

$$\partial_i \left(\phi - \phi^{(0)}\right) = \partial_i \delta\phi = \partial_j \partial_i \phi \Big|_0 x^j = -\frac{1}{2} \left(\mathcal{T}_{\rm cl}\right)_{ij} x^j , \tag{4.26}$$

we can state the following geodesics equation for the clumps contribution

$$\frac{\mathrm{d}^2 x^i}{\mathrm{d}w^2} = -2\partial^i \delta\phi , \tag{4.27}$$

The complete propagation equation describing the light rays bundle, and that takes into account both the homogeneous and inhomogeneous contributions, is obtained combining (4.22) and (4.27)

$$\frac{\mathrm{d}^2 x^i}{\mathrm{d}w^2} = -2\partial^i \phi , \tag{4.28}$$

where we renamed $\delta\phi$ as ϕ because only deviations from the background are physically meaningful. This equations tell us how the light rays deforms in each point of their path with respect to the fiducial under the influence of the gravitational field originated by deviation from a FLRW background. It is a second order equation and, as a consequence, we have to declare two initial conditions: firstly, at $\omega = 0$, that is at the observer point, x_i =0 by assumption, and secondly, when $\omega = 0$ $\mathrm{d}x_i/\mathrm{d}\omega = \theta_i$. Loosely speaking, these θ_i are the angles from where the light rays

originates according to the observer. Thus, the solution to equation (4.28) reads as

$$x^i(w) = w\theta^i - 2\int_0^w \mathrm{d}w(w - w')\partial^i\phi\left(w'\theta_i, w'\right) \ . \tag{4.29}$$

Here we have employed an approximation; indeed the gravitational potential was evaluated at $w'\theta_i$, that is not the path taken by the light ray, which is described by the null geodesics $x(\omega')$ of the perturbed FLRW metric (4.18). Anyway, if we try to expand $x(\omega')$ about the unperturbed path, we discover that the deviations are proportional to a second order term in the Newtonian potential ϕ and can be discarded since we work in the weak fields limit. This is called *Born approximation*. Evaluating this solution at the position of the light source, specified by the co-moving distance ω_s, it yields

$$\beta^i = \theta^i - 2\alpha^i(\theta^j)\,, \tag{4.30}$$

with $\beta^i = x^i(w_\mathrm{s})/f_K(w_\mathrm{s})$ the true angular position of the source seen by the observer and $\alpha^i(\theta^j)$ being defined by

$$\alpha^i(\theta^j) \equiv 2\int_0^{w_\mathrm{s}} \mathrm{d}w' \frac{(w_\mathrm{s} - w')}{w_\mathrm{s}} \partial^i\phi\left(w'\theta^j, w'\right) \tag{4.31}$$

The previous equation is the so-called *lens equation* and it plays a crucial role for gravitational lensing. It relates the true position of a source with the apparent one, which differs by the final deflection angle the light rays experience through their path. Thought at first glance it seems a very simple equations, it hides some tricky features because the deflection 2-d angle $\vec{\alpha}$ depends on the observed 2-d angle $\vec{\theta}$. For a certain initial direction (β^1, β^2) the solutions (θ^1, θ^2) can be several, that is several possible angles at which the observers reveal the light coming from the source.

Since $\partial_i = \partial_{\theta_i}/\omega$, we can also recast the deviation angle (4.30) as the gradient (in angular coordinates) of an effective lensing potential

$$\psi(\theta^j) = 2\int_0^{w_\mathrm{s}} \mathrm{d}w' \frac{w_\mathrm{s} - w'}{w' w_\mathrm{s}} \phi\left(w'\theta^j, w'\right) \ . \tag{4.32}$$

This reduces the lensing to the following schematic picture. The potential ψ assigns a number at each point on the two-sphere which represents the observer's sky, while its gradient defines a vector field on it. The lens equation, therefore, set a map

ϕ between the angular vectors of the observer's sky and the two-sphere describing true initial angular direction at the source location. Its differential $D\phi$ measures the deformation induced by gravitational lensing on light images. Indeed, the lens equation predicts that the soling angle formed by source light rays is eventually different from the emission to the arrival positions and, as a consequence, the observer can experience a different flux of photons. The determinant of $D\phi$ measures the deviation of the initial solid angle with respect to the observed one, thus its inverse tell us how much an image is *magnified* or demagnified by gravitational lensing. Accordingly, we define the *magnification* as

$$\mu = \frac{1}{|\det(D\phi)|} \tag{4.33}$$

The trivial case in (4.30) is the no-deflection angle, that is $\alpha = 0$ and consequently $\det(D\phi) = 1$. The image turns up not to be magnified nor de-magnified and light rays are not affected by lensing. On the other hand, the points where the leasing map is singular and not invertible, i.e $\det(D\phi) = 0$, identify the so-called *caustics* curves and lead to a infinitely magnified source.

Since (4.30) define the lens mapping, then $(D\varphi)^i_j = \delta^i_j - \psi^i_j$ or equivalently we can take out the trace-less contribution as

$$(D\varphi)^i_j = \begin{pmatrix} 1-\kappa & 0 \\ 0 & 1-\kappa \end{pmatrix} - \frac{1}{2}\begin{pmatrix} (\partial^1\partial_1\psi - \partial^2\partial_2\psi) & 2\partial^1\partial_2\psi \\ \partial^1\partial_2\psi & -(\partial^1\partial_1\psi - \partial^2\partial_2\psi) \end{pmatrix} , \tag{4.34}$$

where the have introduced the *convergence* $\kappa = \partial^i\partial_i\psi/2$, which is responsible for the isotropic stretching of source images under the lens mapping. The second matrix encodes rather the distortion of images by the so-called *shear* terms. According to the definition of the lensing potential (4.32), the convergence is

$$\kappa\left(x^j\right) = \int_0^{w_\mathrm{s}} \mathrm{d}w' \, \frac{w'(w_\mathrm{s} - w')}{w_\mathrm{s}} \, \partial_i\partial^i\phi\left(x^j, w'\right) \ , \tag{4.35}$$

where the index i stands for the spatial co-moving coordinates x^i perpendicular to the line of sight. Within Born approximation, at the source and observer positions the unperturbed background is restored and the derivative of the gravitational potential with respect to the line of sight direction must vanish. Thus Poisson equation

$\delta\phi = 4\pi/c^2\rho$ entails

$$\kappa(\theta^i) = \frac{4\pi G}{c^2}\int \mathrm{d}w' \frac{(w_\mathrm{s} - w_\mathrm{d})w_\mathrm{d}}{w_\mathrm{s}}\rho\left(w'\theta^i, w'\right) \ . \tag{4.36}$$

Loosely speaking, the convergence $\kappa(\vec{\theta})$ satisfies a Poisson equation in the transverse space, and perhaps its role is similar to a 2-d density originating the lensing potential ψ. As a consequence, by means of the Green function of the Laplacian operator in two dimensions, it yields

$$\psi(\vec{\theta}) = \frac{1}{\pi}\int \mathrm{d}^2\vec{\theta'}\,\kappa(\vec{\theta'})\ln\left|\vec{\theta} - \vec{\theta'}\right| \ . \tag{4.37}$$

4.2.1 Thin lens approximation

For most of the cosmological scenarios, the distance between the observer and the source is much larger then the typical extension of the over-dense region (hereafter the *lens* or the *deflector*) that perturbs the FLRW background along the line of sight of the observer. Therefore, its extension along the line of sight of the observer can be neglected and just the deviation due to the transverse direction to the line of sight must be taken into account. it means we will sum up all the contribution to the potential along the line of sight, that is

$$\phi(w\theta^i, w) = \delta(w - w_\mathrm{d})\int \mathrm{d}w'\phi(w_\mathrm{d}\theta^i) = \delta(w - w_\mathrm{d})\phi_\perp(w_\mathrm{d}\theta^i) \ , \tag{4.38}$$

$\phi^\perp$ being implicitly defined by last equality. Then, the lensing potential in equation (4.32) reduces as

$$\psi(\theta^i) = 2\frac{w_\mathrm{s} - w_\mathrm{d}}{w_\mathrm{d}w_\mathrm{s}}\phi_\perp \ . \tag{4.39}$$

It follows that, directly from its definition, also the convergence simplifies:

$$\kappa(\theta^i) = \frac{4\pi G}{c^2}\frac{(w_\mathrm{s} - w_\mathrm{d})w_\mathrm{d}}{w_\mathrm{s}}\int \mathrm{d}w'\rho\left(w'\theta^i, w'\right) = \frac{\Sigma(\theta^i)}{\Sigma_\mathrm{cr}} \ , \tag{4.40}$$

where we have introduced the *surface mass density* $\Sigma(\theta^i)$ and the *critical surface mass density* Σ_cr as

$$\Sigma(\theta^i) = \int \mathrm{d}w'\rho\left(w'\theta^i, w'\right) \ , \qquad \Sigma_\mathrm{cr}^{-1} := \frac{4\pi G}{c^2}.\frac{(w_\mathrm{s} - w_\mathrm{d})w_\mathrm{d}}{w_\mathrm{s}} \ . \tag{4.41}$$

A corollary to Fermat's principle, the so-called *odd-number theorem* regulates the number of formed images: non-singular thin lenses produce an odd number of images. Notice that it does not mean that for any position of the source we have always the same amount of images, but just that their number must be odd.

Axially symmetric systems: the point-like lens

If we deal with a lens that exhibits an axial surface mass density, the above equations simplifies even more. In facts, the lens equation reduces to one angular dimension θ, since all light rays travelling from the source to the observe must lie on the 3-dimensional plane spanned by the source, the lens and the observer [39]. Moreover, if this plane degenerates into a straight line, this plane acquires a degeneracy since it can have any inclination with respect to the latter. That means light rays are deviated with the same α at every angular position on the transverse surface and circular images can form. with an axially symmetric density mass surface, the equation (4.37) reads as

$$\psi(\theta) = 2\left[\ln\theta\int_0^\theta \theta' \mathrm{d}\theta'\,\kappa(\theta') + \int_\theta^\infty \theta'\mathrm{d}\theta'\,\ln\theta'\kappa(\theta')\right] . \tag{4.42}$$

The derivative of this expression with respect of θ entails the deviation angle appearing in the lens equation

$$\alpha(\theta) = \frac{m(\theta)}{\theta}, \qquad m(\theta) = 2\int_0^\theta \theta'\mathrm{d}\theta'\,\kappa(\theta') \ . \tag{4.43}$$

With very straightforward calculations, one can also compute the determinant of the lens map in (4.34), that is

$$\det(D\varphi) = \left(1 - \frac{\mathrm{d}}{\mathrm{d}\theta}\frac{m(\theta)}{\theta}\right)\left(1 - \frac{m(\theta)}{\theta^2}\right) , \tag{4.44}$$

its inverse being the magnification of the image. Therefore, if one it is interested in recovering the magnification associated to the source signal, it would be first necessary find the solutions $\theta(\beta)$ to the lens equation, that gives the relation between the observed an the real angular position, and substitute it in the previous equation to know each image magnification.

In order to introduce commonly employed lensing quantities, we briefly discuss the case of a point mass M. With this regard, the density of the lens is a Dirac delta in the position space $\rho(\vec{x}) = M\delta(\vec{x})$., and from equation (4.40) the convergence is

$$\kappa(\vec{\theta}) = \frac{4\pi GM}{c^2}\frac{(w_\mathrm{s} - w_\mathrm{d})w_\mathrm{d}}{w_\mathrm{s}}\delta(w_\mathrm{d}\vec{\theta}) \ , \tag{4.45}$$

Equation (4.43) returns the deflection angle, and it is possible to readily write down the lens equation

$$\beta = \theta - \frac{4GM}{c^2\theta}\frac{w_\mathrm{s} - w_\mathrm{d}}{w_\mathrm{d}w_\mathrm{s}} \ , \tag{4.46}$$

This is always a second order equation in the variable θ and, as a consequence, it admits two solutions. The only exception is when $\beta = 0$, that is when the source and the lens are aligned. In this case the equation becomes first order, that means the image seen by the observer is a ring with angular size

$$\theta_\mathrm{E} = \left(\frac{4GM}{c^2}\frac{w_\mathrm{s} - w_\mathrm{d}}{w_\mathrm{d}w_\mathrm{s}}\right)^{1/2} \ , \tag{4.47}$$

which is referred as *Einstein radius*, which can be also recast in terms of physical length in the deflector plane

$$R_E = \theta_\mathrm{E}w_\mathrm{d} = \left(\frac{4GM}{c^2}\frac{(w_\mathrm{s} - w_\mathrm{d})w_\mathrm{d}}{w_\mathrm{s}}\right)^{1/2} \ . \tag{4.48}$$

. Notice that it is very common to re-scale the angles in the lens equation as $x = \theta/\theta_\mathrm{E}$ and $y = \beta/\theta_\mathrm{E}$. Once the solutions to this system are computed, it is handily to prove that the total magnification is given by

$$\mu = \frac{y^2 + 2}{y\sqrt{y^2 + 4}} \ . \tag{4.49}$$

If a point-like object - such as a primordial black hole - lens the light from a point-like source, the magnification of the observed image can be very huge and, in the case the source and the object are co-linear, it raises up to an infinite value: it forms a caustic. Let us point out that when *beta* is very larger than θ_E, that is $y \gg 1$ the magnification effect is negligible and the lens mapping reduces to the identity. It means that the Einstein radius identifies the typical scale for the source distance at which lensing effects becomes considerable.

4.2.2 Microlensing

We have mentioned that the lensing phenomenon can result in a splitting of the source light rays that produce more than a unique image in the observer's sky. Weather this happen or not depends on the strength of lens, or rather on the density of the object that provide inhomogeneities in the gravitational field. Therefore, *strong* lensing or *weak lensing* phenomena both produce multiple images and differ basically by the magnitude of the convergence parameter κ associated to the lens; the first are capable to produce separated, multiple and highly magnified images, while the second observe just a distortion, nor a deflection, in the weakly lensed image. A further possibility is achieved when the angular separations of the images lensed and deflected by a compact object is so small that the individual ones cannot be resolved by observations, but only their total magnification can be inferred. This possibility was originally referred as *microlensing* in view of angular deviations of the unresolved images at the 10^{-6} arcsecond level. However, in modern times, this term has obtained a broader meaning, indicating all the phenomena that produce single or multiple indistinguishable images presenting a transient in the observed magnification function . We will elaborate this point in a while but, for the sake of completeness, we mention that fainter limits are also observable, and in the literature are referred as the *millilensing* and *femtolensing* regimes [40, 33, 41].

As pointed out in equation (4.49) the magnification due to a point-like object depends on the distance between the lens and the source projected in the deflection plane, or eventually their angular distance. it means that if we consider a source and a lens which have a non zero relative velocity, the flux of light the observer detect will depends on time. The shape of the typical magnification curve of a microlensing phenomenon is depicted in Figure 4.2.2; the rise and fall of the detected flux describes manifestly the approach of the source to the point of minimum distance from the lens and its following departure. The closer it gets to the compact object, the higher the peak of the magnification curve. Moreover, if the observer detects the source crossing the centre of the lens, that is at $y = 0$, it is possible to have an infinitely magnified image.

This discussion directly applies to primordial black holes, which are very compact

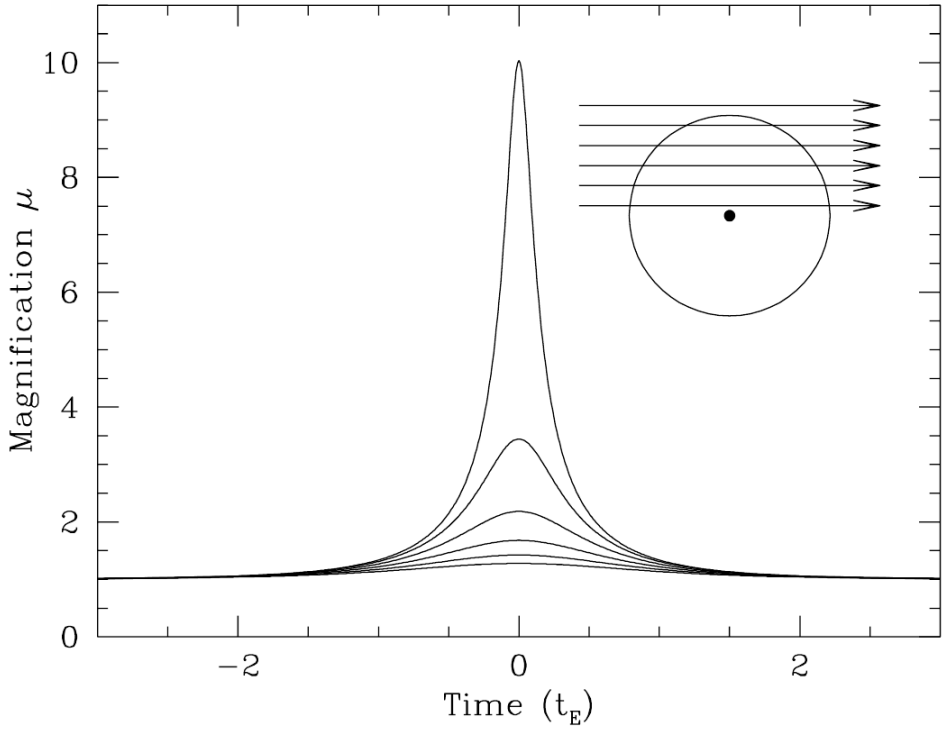

Figure 4.4. Typical curves of a microlensing transient phenomenon as the minimum approach distance of the source from lens varies. Picture from Ref. [41]

objects and as such can be regarded as point-like sources with mass M. Indeed, for in MACHO/EROS experiments the sources are stars of the Large Magellanic Cloud whose distance is approximately $\sim 50\,\mathrm{Kpc}$. Therefore for this lensing configuration, according to Ref. [42], the Einstein radius is

$$R_E = 3.16 \cdot 10^9 \cdot \left(\frac{M}{M_\odot}\right)^{1/2} [x(1-x)]^{1/2}\ \mathrm{km}\,, \tag{4.50}$$

where $x = w_\mathrm{d}/w_\mathrm{s}$, $0 < x < 1$, M is the mass of the lens and $M_\odot$ is the solar mass. The value $x = 1/2$ corresponds to a lens equally distant from the source and the observer, with an Einstein radius $R_E \simeq 1.6 \cdot 10^9 \cdot M/M_\odot\,\mathrm{km}$. A solar mass black hole has a typical Schwarzschild radius $R_S \simeq 3\,\mathrm{km}$, that means it can be safely regarded as a point like.

4.2.3 Lensing signature of PDMHs

In 1986, Paczyński figured out that it is possible to test the hypothesis that some fraction of dark matter is in the form of compact object by monitoring a few million stars in the Magellanic Clouds [43]. The discussion on how the microlensing constraints translates to our dark halos context naturally arise, in this section we will discuss it separately for the two formation scenarios.

Scenario $\mathcal{A}$

In this case, the radius of the dark halos was estimated in (3.81) to be

$$R_{\mathcal{A}} = 5.9 \cdot 10^{11} \left(\frac{M}{M_\odot} \right)^{2/3} \text{km} \,. \tag{4.51}$$

Whenever we consider a mass $M > M_\odot^{-16}$, the Einstein radius is larger then the viralization one. That means the point-like lens approximation breaks down in this window and we shall regard the halos as *extended lenses*. These might be still able to produce detectable lensing signals and their identification by the MACHO/EROS collaborations cannot be excluded. To this end we assume the dark halos density distribution to be described by a non-singular isothermal profile

$$\rho = \frac{A}{(r^2 + R_{\mathcal{A}}^2)} \,, \tag{4.52}$$

where r denotes the radial distance from the centre of the sphere and A is a normalization constant obtained by equating the mass of the lump to the integration of the distribution over the volume enclosed by the *core* or virialization radius. It is worth to stress that the realistic profile that model the distribution of matter particles inside the lump is unknown, but the isothermal naturally arise requiring the hydrostatical equilibrium condition for a collisionless particles system [44]. It is the most employed in the literature to model dark matter halos but, nonetheless, other options are possibles. Anyway, the alternatives are not expected to largely deviate from it because the virialization phase has to be allowed as well. Hence, our conclusion will be almost independent from this choice.

The virialization radius is significantly smaller than the distance to standard microlensing sources, which include, for instance, stars in the Large Magellanic Cloud at around 50 Kpc. This hierarchy allows us to describe the halos as thin lenses with respect to the line of sight. We can additionally benefit from the axial symmetry of the problem to describe the lensing effects in terms of a single deflection angle α on the plane spanned by the positions of the source, the observer and the lens. This assumption simplifies the analysis and, as shown in Section 4.2, it is very straightforward to derive the lens equation

$$\beta(\theta) = \theta - \alpha(\theta) = \theta - \frac{1}{\theta}\frac{2\theta_E^2\pi}{(4-\pi)\theta_{\mathcal{A}}}\left[\sqrt{\theta^2+\theta_{\mathcal{A}}^2} - \theta_{\mathcal{A}}\right] \tag{4.53}$$

$$= \theta - \frac{\theta_0}{\theta}\left[\sqrt{\theta^2+\theta_{\mathcal{A}}^2} - \theta_{\mathcal{A}}\right]. \tag{4.54}$$

where all the distances on the lens plane have been expressed as angular distance, e.g. $\theta_{\mathcal{A}} = R_{\mathcal{A}}/w_{\rm d}$, and we have implicitly defined $\theta_0 = \frac{2\theta_E^2\pi}{(4-\pi)\theta_{\mathcal{A}}}$. Since we must take into account the total magnification produced by the lens, that is the sum of the magnification of each single image in the observer's sky, we can reduce the problem to study the number of the lens mapping solutions. This map is non-singular and is subjected to the odd-number theorem, thus we expect one or three images to form - an higher number is already unlikely because of the weak lensing regime. The function $\beta(\theta)$ goes to $\pm\infty$ as θ goes to $\pm\infty$, therefore in order to have more than one zero, it must have two extrema, namely a maximum and a minimum. Whether this to happen or not it is inferred studying the zero points of its derivative

$$\frac{{\rm d}\beta}{{\rm d}\theta} = \left(1 - \frac{\theta_0\theta_{\mathcal{A}}}{\theta^2}\right) + \frac{\theta_0\theta_{\mathcal{A}}^2}{\theta^2\sqrt{\theta^2+\theta_{\mathcal{A}}^2}} = 0\,. \tag{4.55}$$

The sum of these two term can be null only if the first one is negative, that requires

$$|\theta| < \sqrt{\theta_0\theta_{\mathcal{A}}}\,. \tag{4.56}$$

Bearing in mind this constraint,the two solution to the quadratic equation reads as

$$\left(\frac{\theta^2}{\theta_0\theta_{\mathcal{A}}}\right)^2 = 1 + \frac{\theta_{\mathcal{A}}}{2\theta_0}\left[\pm\sqrt{1+\frac{4\theta_0}{\theta_{\mathcal{A}}}} - 1\right]. \tag{4.57}$$

According to the previous condition the right hand side must be smaller than one, thus the only relevant solution is the one with the minus sign, which lead to the two extrema

$$\theta_{\pm} = \pm\sqrt{\theta_0\theta_{\mathcal{A}}}\left[1 - \frac{\theta_{\mathcal{A}}}{2\theta_0}\left(\sqrt{1+\frac{4\theta_0}{\theta_{\mathcal{A}}}}+1\right)\right]^{1/2} . \tag{4.58}$$

In addition, these exist only if the therm in parentheses is positive, so the condition to produce multiple images is

$$\theta_{\mathcal{A}} < \frac{\theta_0}{2} \simeq 3\theta_E \tag{4.59}$$

The viralization radius within the scenario $\mathcal{A}$ does not fulfil this condition, and in consequence, `the halos lensing produces only one image`. This means we do not have to sum up different contributes to evaluate the total magnification, and neither to solve the lens equation for the only one produced. Following the prescriptions at the end of Section 4.2, the magnification with respect to the observed image angular position reads as

$$\begin{aligned} \mu^{-1}(\theta) &= \left(1 - \frac{d}{d\theta}\frac{m(\theta)}{\theta}\right)\left(1 - \frac{m(\theta)}{\theta^2}\right) \qquad (4.60)\\ &= \left[\left(1 - \frac{\theta_0}{2\sqrt{\theta^2+\theta_{\mathcal{A}}^2}}\right)^2 - \frac{\theta_0^2\left(2\theta_{\mathcal{A}}\sqrt{\theta^2+\theta_{\mathcal{A}}^2} - 2\theta_{\mathcal{A}}^2 - \theta^2\right)^2}{4\theta^4\left(\theta^2+\theta_{\mathcal{A}}\right)}\right] . \end{aligned}$$

When the source is far from the object $\mu(\theta \to \pm\infty) \to 1$, the image is nor deflected nor magnified. Since the radius of the halos depends on the mass, also the magnification they produce exhibits this dependence. In Figure 4.5 the magnification function and its maxima are depicted with respect to different halos masses. Comparing this with the MACHO collaboration identification threshold $\mu > \mu_{\text{detect}} \simeq 1.30$ [45], we can select a mass window from $10^{-11}M_{\odot}$ upwards, where `the dark halos cannot be detected`. Note that the according to the expression (4.51) the density of halos goes as M^{-1}, therefore the more massive is a lump, the lower its density. This reflects in in a lack of an upper bound for detectable mass window. In light of these results, together with the nucleosynthesis constraints pointed out in section 3.5.4, we identify a `mass window from` 10^{-11} `to` 60 `solar`

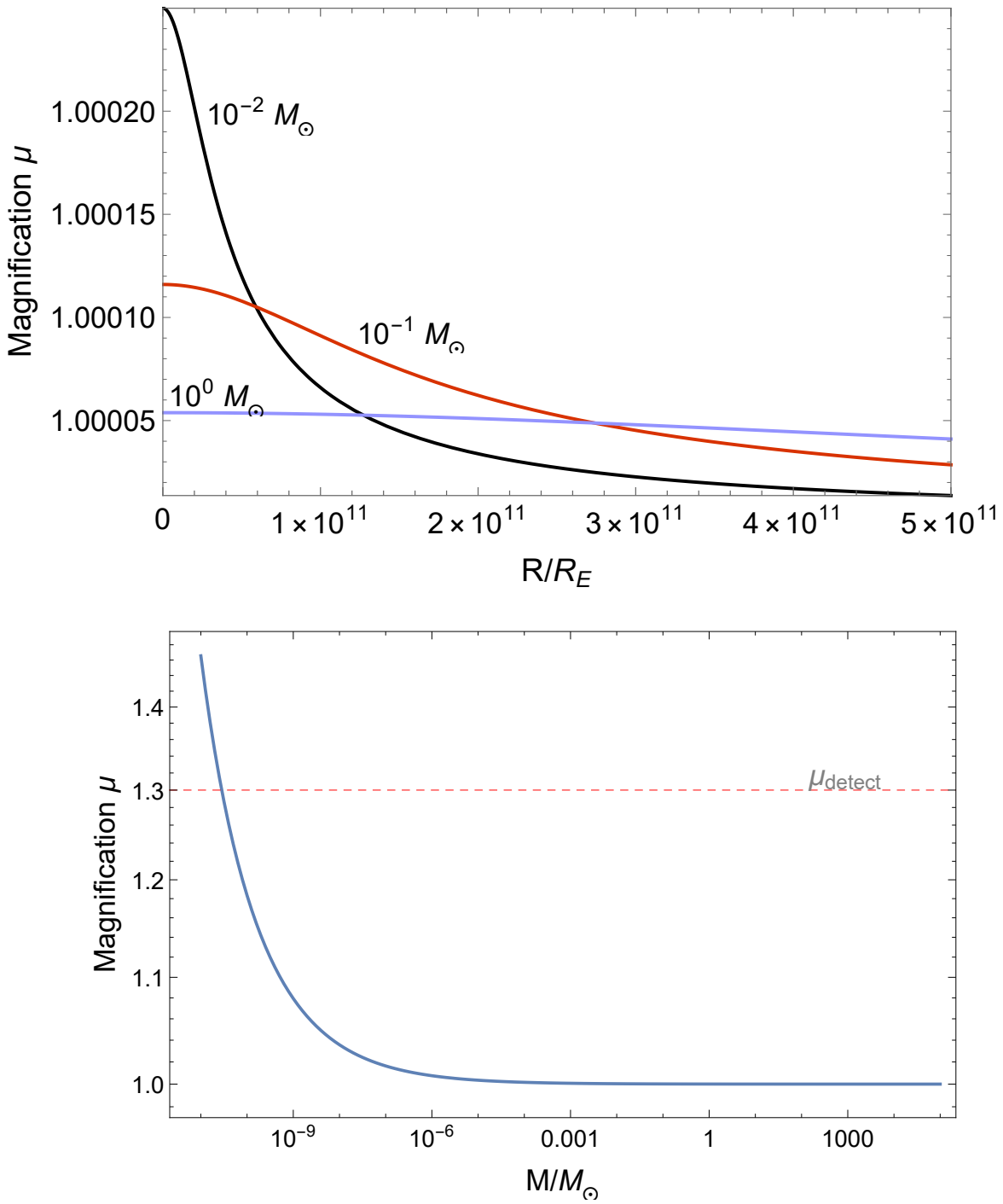

Figure 4.5. Top panel: the magnification produced by dark halos barely perturb the light rays flux. Bottom panel: maximum magnification produced by a dark halo as a function of its mass.

`mass unit where this scenario is viable` for providing the entire dark matter content of the universe.

Scenario $\mathcal{B}$

The numerical factor in the expression

$$R_{\mathcal{B}} = 2.7 \cdot 10^7 \left(\frac{M}{M_\odot}\right)^{2/3} \text{km}\,, \tag{4.61}$$

is too small to escape the point-like lens approximation within the solar mass range. Therefore, the scenario $\mathcal{B}$ describes halos which are seen just like primordial black holes by microlensing experiments.

Caustic crossing

In this section we will follow the discussion carried out in Ref. [33]. The Hubble Space Telescope detected an event (MACS J1149 Lensed Star 1) of a star meeting the caustic line of a galaxy cluster lens and providing a fast magnification transient - estimated magnification $\mu > 2000$; this is called a caustic-crossing event. A natural explanation for the presence of the caustic is a cumulative contribution from several point mass lens in the same galaxy cluster. The expected magnification from this set up was $\mu \sim 6000$: much higher than the observed one. Anyway, caustic are significantly distorted even by the presence of tiny point masses and this distortion results in a reduction of the predicted infinitely large magnification - in reality it never diverges due to the finite size of the source. The observed magnification curve requires a certain amount of point masses to be explained, since the more the point masses, the more the reduction of the magnification. This does not translates directly into a lower and upper bound for f_{PBH} because there are stars, known as Intra-Cluster Stars (ICS), that produce the same effect on the caustic. Nonetheless, the uncertainty on the abundance of these stars, can result in the upper limit on f_{PBH} [34] in Figure 4.2.

As in the case of stellar microlensing, also these constraints rely on point-like lens approximation for compact dark matter. The sourcing star in MACS J1149 Lensed

Star 1 is much further $\sim 10^6$ Kpc than stars in the Large Magellanic Cloud ~ 50 Kpc, thus according to (4.48) we expect a lower Einstein radius for this set up

$$R_E \simeq 5 \cdot 10^6 \left(\frac{M}{M_\odot}\right)^{1/2} . \tag{4.62}$$

This means that either in this case, but within both scenarios, dark halos must be regarded as extended lens and, in principle, should be able to escape these constraints too. Anyway, we remand a deeper analysis to a future work.

Final remark. In this chapter we pointed out the possibility to escape lensing constraints within the fifth-force modified gravity framework, but it is worth to remark that it has a very general validity and appliance, besides our model. In principle, the solar mass windows could be completely unconstrained for any screened compact object that breaks the point-like approximation. In this view, in Figure 4.6 presented here below we explored the magnification maxima for a wide range of radii and masses for MACHO/EROS microlensing phenomena.

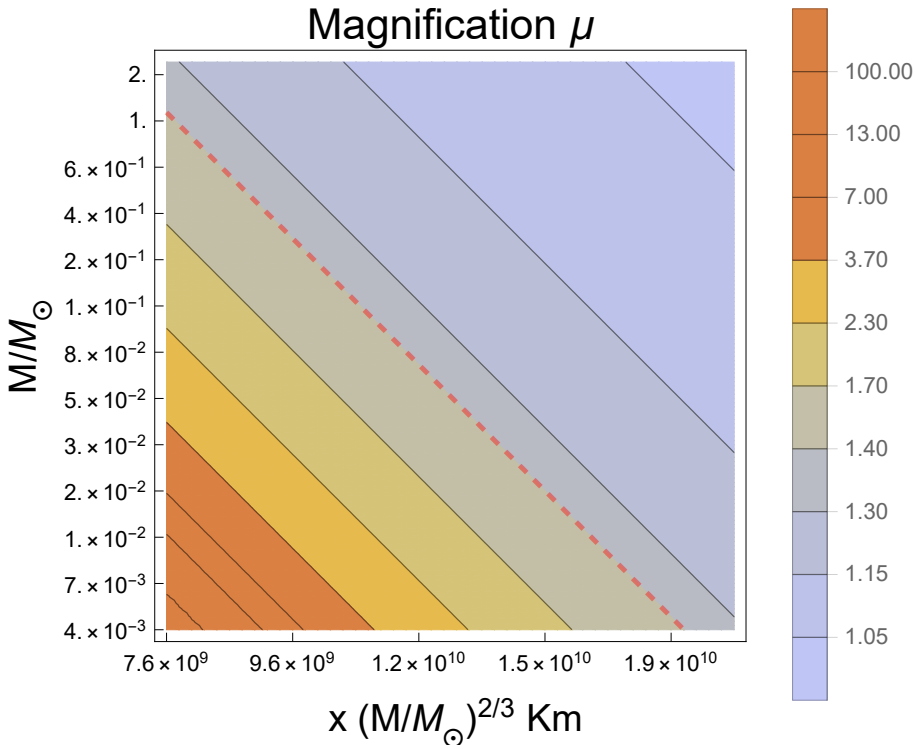

Figure 4.6. Magnification maxima for a wide range of radii and masses. The red line identifies the (blue) region where dark compact objects become undetectable.

Conclusions

In this thesis work we have presented an alternative scenario that might provide the missing dark matter of the universe. We have shown that a primordial modified gravity set-up, in particular a more intense gravity-like interaction, enhances the growth of the post-inflationary density perturbations during the radiation dominated era. These eventually collapse in structures we have named Primordial Dark Matter Halos (PDMHs). The latter do not aim to explain the intrinsic nature of dark matter, but rather, if really existing, could point out that the missing matter is in form of screened objects made out of clustered non-interacting particles. Indeed, what is really the nature of the non-interacting ψ-matter field is not clear but many proposals in the literature suggest its existence. It's worth to remark that, if this picture was proved to be true, no experiments could ever detect directly the dark matter.

The results we have presented in the end of Chapter 3 and the whole Chapter 4 are completely original. There we claimed the formation of PDMHs within two extremal scenario. The first predicts the existence of primordial halos which seems to be able to escape the lensing constraints in the mass window from 10^{-11} to 10^{2} solar mass unit. On the other hand, the second scenario seems to be not viable to provide all the dark matter as it is killed by PBHs constraints. Our conclusions do not allow to tell which of these two is the closest to the true physical picture, and future works must involve N-body simulations in order to adequately follow the merging processes and the screening mechanism that lead to the formation of the

halos. Furthermore, a more accurate treatment of the other possible constraints in the solar mass window shall be taken into account too.

Even if providing dark matter in form of PDMHs were ruled out by numerical simulations resulting in halos which are not able to pass the lensing constraints, this work has pointed out that provide dark matter in the solar mass window might still be possible. All we need, rather that PBHs, are screened compact objects which are not seen by constraints as point-like lens and must be treated as extended ones.

Bibliography

[1] F. Zwicky. "On the Masses of Nebulae and of Clusters of Nebulae". In: 86 (Oct. 1937), p. 217. DOI: 10.1086/143864.

[2] P. A. R. Ade et al. "Planck 2015 results. XX. Constraints on inflation". In: *Astron. Astrophys.* 594 (2016), A20. DOI: 10.1051/0004-6361/201525898. arXiv: 1502.02114 [astro-ph.CO].

[3] C. Wetterich. "Cosmology and the Fate of Dilatation Symmetry". In: *Nucl. Phys.* B302 (1988), pp. 668–696. DOI: 10.1016/0550-3213(88)90193-9. arXiv: 1711.03844 [hep-th].

[4] Bharat Ratra and P. J. E. Peebles. "Cosmological consequences of a rolling homogeneous scalar field". In: *Phys. Rev. D* 37 (12 June 1988), pp. 3406–3427. DOI: 10.1103/PhysRevD.37.3406. URL: https://link.aps.org/doi/10.1103/PhysRevD.37.3406.

[5] Austin Joyce et al. "Beyond the Cosmological Standard Model". In: *Phys. Rept.* 568 (2015), pp. 1–98. DOI: 10.1016/j.physrep.2014.12.002. arXiv: 1407.0059 [astro-ph.CO].

[6] Timothy Clifton et al. "Modified Gravity and Cosmology". In: *Phys. Rept.* 513 (2012), pp. 1–189. DOI: 10.1016/j.physrep.2012.01.001. arXiv: 1106.2476 [astro-ph.CO].

[7] Luca Amendola and Shinji Tsujikawa. *Dark Energy: Theory and Observations*. Cambridge University Press, 2010. DOI: 10.1017/CBO9780511750823.

[8] Luca Amendola, Javier Rubio, and Christof Wetterich. "Primordial black holes from fifth forces". In: *Phys. Rev.* D97.8 (2018), p. 081302. DOI: 10.1103/PhysRevD.97.081302. arXiv: 1711.09915 [astro-ph.CO].

[9] Luca Amendola. "Coupled quintessence". In: *Phys. Rev.* D62 (2000), p. 043511. DOI: 10.1103/PhysRevD.62.043511. arXiv: astro-ph/9908023 [astro-ph].

[10] C. B. Collins and J. M. Stewart. "Qualitative Cosmology". In: *Monthly Notices of the Royal Astronomical Society* 153.4 (Sept. 1971), pp. 419–434. ISSN: 0035-8711. DOI: 10.1093/mnras/153.4.419. eprint: http://oup.prod.sis.lan/mnras/article-pdf/153/4/419/8079221/mnras153-0419.pdf. URL: https://dx.doi.org/10.1093/mnras/153.4.419.

[11] Sebastian Bahamonde et al. "Dynamical systems applied to cosmology: dark energy and modified gravity". In: *Phys. Rept.* 775-777 (2018), pp. 1–122. DOI: 10.1016/j.physrep.2018.09.001. arXiv: 1712.03107 [gr-qc].

[12] Edmund J. Copeland, M. Sami, and Shinji Tsujikawa. "Dynamics of dark energy". In: *Int. J. Mod. Phys.* D15 (2006), pp. 1753–1936. DOI: 10.1142/S021827180600942X. arXiv: hep-th/0603057 [hep-th].

[13] Andrei D. Linde. "A New Inflationary Universe Scenario: A Possible Solution of the Horizon, Flatness, Homogeneity, Isotropy and Primordial Monopole Problems". In: *Phys. Lett.* 108B (1982). [Adv. Ser. Astrophys. Cosmol.3,149(1987)], pp. 389–393. DOI: 10.1016/0370-2693(82)91219-9.

[14] Luca Amendola. "Scaling solutions in general nonminimal coupling theories". In: *Phys. Rev.* D60 (1999), p. 043501. DOI: 10.1103/PhysRevD.60.043501. arXiv: astro-ph/9904120 [astro-ph].

[15] Javier Rubio and Christof Wetterich. "Emergent scale symmetry: Connecting inflation and dark energy". In: *Phys. Rev.* D96.6 (2017), p. 063509. DOI: 10.1103/PhysRevD.96.063509. arXiv: 1705.00552 [gr-qc].

[16] Clare Burrage and Jeremy Sakstein. "Tests of Chameleon Gravity". In: *Living Rev. Rel.* 21.1 (2018), p. 1. DOI: 10.1007/s41114-018-0011-x. arXiv: 1709.09071 [astro-ph.CO].

[17] Justin Khoury and Amanda Weltman. "Chameleon cosmology". In: *Phys. Rev.* D69 (2004), p. 044026. DOI: 10.1103/PhysRevD.69.044026. arXiv: astro-ph/0309411 [astro-ph].

[18] Chung-Pei Ma and Edmund Bertschinger. "Cosmological perturbation theory in the synchronous and conformal Newtonian gauges". In: *Astrophys. J.* 455 (1995), pp. 7–25. DOI: 10.1086/176550. arXiv: astro-ph/9506072 [astro-ph].

[19] E. Lifshitz. "Republication of: On the gravitational stability of the expanding universe". In: *J. Phys.(USSR)* 10 (1946). [Gen. Rel. Grav.49,no.2,18(2017)], p. 116. DOI: 10.1007/s10714-016-2165-8.

[20] James M. Bardeen. "Gauge Invariant Cosmological Perturbations". In: *Phys. Rev.* D22 (1980), pp. 1882–1905. DOI: 10.1103/PhysRevD.22.1882.

[21] P. Meszaros. "The behaviour of point masses in an expanding cosmological substratum". In: *Astron. Astrophys.* 37 (1974), pp. 225–228.

[22] A. Riotto. "Inflation and the Theory of Cosmological Perturbations". In: (2018). URL: http://webtheory.sns.it/ggilectures2018/riotto/riotto.pdf.

[23] Y. Akrami et al. "Planck 2018 results. X. Constraints on inflation". In: (2018). arXiv: 1807.06211 [astro-ph.CO].

[24] Luca Amendola. "Linear and non-linear perturbations in dark energy models". In: *Phys. Rev.* D69 (2004), p. 103524. DOI: 10.1103/PhysRevD.69.103524. arXiv: astro-ph/0311175 [astro-ph].

[25] Nico Wintergerst and Valeria Pettorino. "Clarifying spherical collapse in coupled dark energy cosmologies". In: *Phys. Rev.* D82 (2010), p. 103516. DOI: 10.1103/PhysRevD.82.103516. arXiv: 1005.1278 [astro-ph.CO].

[26] James E. Gunn and J. Richard Gott III. "On the Infall of Matter into Clusters of Galaxies and Some Effects on Their Evolution". In: *Astrophys. J.* 176 (1972), pp. 1–19. DOI: 10.1086/151605.

[27] William H. Press and Paul Schechter. "Formation of galaxies and clusters of galaxies by selfsimilar gravitational condensation". In: *Astrophys. J.* 187 (1974), pp. 425–438. DOI: 10.1086/152650.

[28] B. P. Abbott et al. "Observation of Gravitational Waves from a Binary Black Hole Merger". In: *Phys. Rev. Lett.* 116.6 (2016), p. 061102. DOI: 10.1103/PhysRevLett.116.061102. arXiv: 1602.03837 [gr-qc].

[29] B. J. Carr and S. W. Hawking. "Black holes in the early Universe". In: 168 (Aug. 1974), pp. 399–416. DOI: 10.1093/mnras/168.2.399.

[30] B. J. Carr. "The primordial black hole mass spectrum". In: 201 (Oct. 1975), pp. 1–19. DOI: 10.1086/153853.

[31] Junichi Yokoyama. "Formation of MACHO primordial black holes in inflationary cosmology". In: *Astron. Astrophys.* 318 (1997), p. 673. arXiv: astro-ph/9509027 [astro-ph].

[32] Bernard Carr, Florian Kuhnel, and Marit Sandstad. "Primordial Black Holes as Dark Matter". In: *Phys. Rev.* D94.8 (2016), p. 083504. DOI: 10.1103/PhysRevD.94.083504. arXiv: 1607.06077 [astro-ph.CO].

[33] Misao Sasaki et al. "Primordial black holes—perspectives in gravitational wave astronomy". In: *Class. Quant. Grav.* 35.6 (2018), p. 063001. DOI: 10.1088/1361-6382/aaa7b4. arXiv: 1801.05235 [astro-ph.CO].

[34] Masamune Oguri et al. "Understanding caustic crossings in giant arcs: characteristic scales, event rates, and constraints on compact dark matter". In: *Phys. Rev.* D97.2 (2018), p. 023518. DOI: 10.1103/PhysRevD.97.023518. arXiv: 1710.00148 [astro-ph.CO].

[35] Miguel Zumalacarregui and Uros Seljak. "Limits on stellar-mass compact objects as dark matter from gravitational lensing of type Ia supernovae". In: *Phys. Rev. Lett.* 121.14 (2018), p. 141101. DOI: 10.1103/PhysRevLett.121.141101. arXiv: 1712.02240 [astro-ph.CO].

[36] Jaiyul Yoo, Julio Chaname, and Andrew Gould. "The end of the MACHO era: limits on halo dark matter from stellar halo wide binaries". In: *Astrophys. J.* 601 (2004), pp. 311–318. DOI: 10.1086/380562. arXiv: astro-ph/0307437 [astro-ph].

[37] Yacine Ali-Haïmoud and Marc Kamionkowski. "Cosmic microwave background limits on accreting primordial black holes". In: *Phys. Rev.* D95.4 (2017), p. 043534. DOI: 10.1103/PhysRevD.95.043534. arXiv: 1612.05644 [astro-ph.CO].

[38] Matthias Bartelmann. "Gravitational Lensing". In: *Class. Quant. Grav.* 27 (2010), p. 233001. DOI: 10.1088/0264-9381/27/23/233001. arXiv: 1010.3829 [astro-ph.CO].

[39] P. Schneider, J. Ehlers, and E. E. Falco. *Gravitational Lenses*. 1992, p. 112. DOI: 10.1007/978-3-662-03758-4.

[40] Scott Dodelson. *Gravitational Lensing*. Cambridge University Press, 2017. DOI: 10.1017/9781316424254.

[41] Joachim Wambsganss. "Gravitational Microlensing". In: (2006), pp. 453–540. DOI: 10.1007/978-3-540-30310-7_4. arXiv: astro-ph/0604278 [astro-ph].

[42] H. J. Witt and S. Mao. "Can lensed stars be regarded as pointlike for microlensing by MACHOs?" In: 430 (Aug. 1994), pp. 505–510. DOI: 10.1086/174426.

[43] B. Paczynski. "Gravitational microlensing by the galactic halo". In: 304 (May 1986), pp. 1–5. DOI: 10.1086/164140.

[44] J. Binney and S. Tremaine. *Galactic Dynamics*. Princeton series in astrophysics. Princeton University Press, 1987. ISBN: 9780691084459. URL: https://books.google.de/books?id=01yNf7mipb0C.

[45] C. Alcock et al. "The MACHO project: Microlensing results from 5.7 years of LMC observations". In: *Astrophys. J.* 542 (2000), pp. 281–307. DOI: 10.1086/309512. arXiv: astro-ph/0001272 [astro-ph].